Ralph J. Roberts
CENTER FOR RESEARCH
IN
ECONOMIC GEOLOGY

ANNUAL RESEARCH MEETING-1998

Program and Reports

7-8 January 1999
Midby-Byron Building
Room 107-109
University of Nevada, Reno
Reno, NV 89557

STRUCTURAL GEOLOGY OF THE RAIN FAULT SYSTEM, RAIN SUB-DISTRICT, CARLIN TREND, NEVADA

Tommy B. Thompson
CREG, Director

Introduction

At the time of last year's Annual Research Meeting we documented that the Rain fault conjugate system had a major component of strike separation and that the Rain fault kinematic indicators pointed to dextral displacement. The N40-50°W Rain fault and its NE-striking conjugates played a major role in breccia development and in localizing gold. The purpose of this communication is to demonstrate that significant changes in strike along the Rain fault system equally are important in localizing and, actually enhancing breccia development and gold localization.

Strike Deviations Along The Rain Fault

To the northwest of the Rain open pit within the underground workings, the strike of the Rain fault and those sub-parallel to it deviates to nearly due west; dips change from 68-80°W to a range of 38-45°S (**Fig. 1**). That change in strike and dip in the dextral Rain system resulted in a local zone of transpression. Breccia development in that zone is much more extensive, and grade-thickness contours (**Fig. 2**) indicate a much wider zone of mineralized rock.

The zone of transpression (**Fig. 1**) generated a positive flower structure that has been documented with core drilling from underground drill stations. The Rain sub-parallel faults do not appear to extend back and intersect with the Rain fault; rather, the displacement on the eastern and western extremities of these faults appears to to be negligible while within the central portions they exhibit significant displacement. The nature of such displacements is typical of positive flower structures.

The structural features of the Rain fault system are detailed in the attached manuscript (Williams, Thompson, Powell and Dunbar, In Review: Economic Geology).

Mineralogical Changes Along the Rain Fault

The obvious change along strike of the Rain fault is the increase in gold grades to the northwest (**Fig. 3**). Other changes include a decrease in barite content from the open pit (>30% barite) to the Zone 4 (<5% barite). Preliminary data on fluid inclusions suggest that there is a corresponding increase northwestward in fluid temperatures from the pit area into Zone 4. Such changes allow an interpretation of increased fluid Po_2 with gold precipitation and a corresponding increase in sulfate from the northwest to the southeast.

FIGURE 1. Rain Fault.

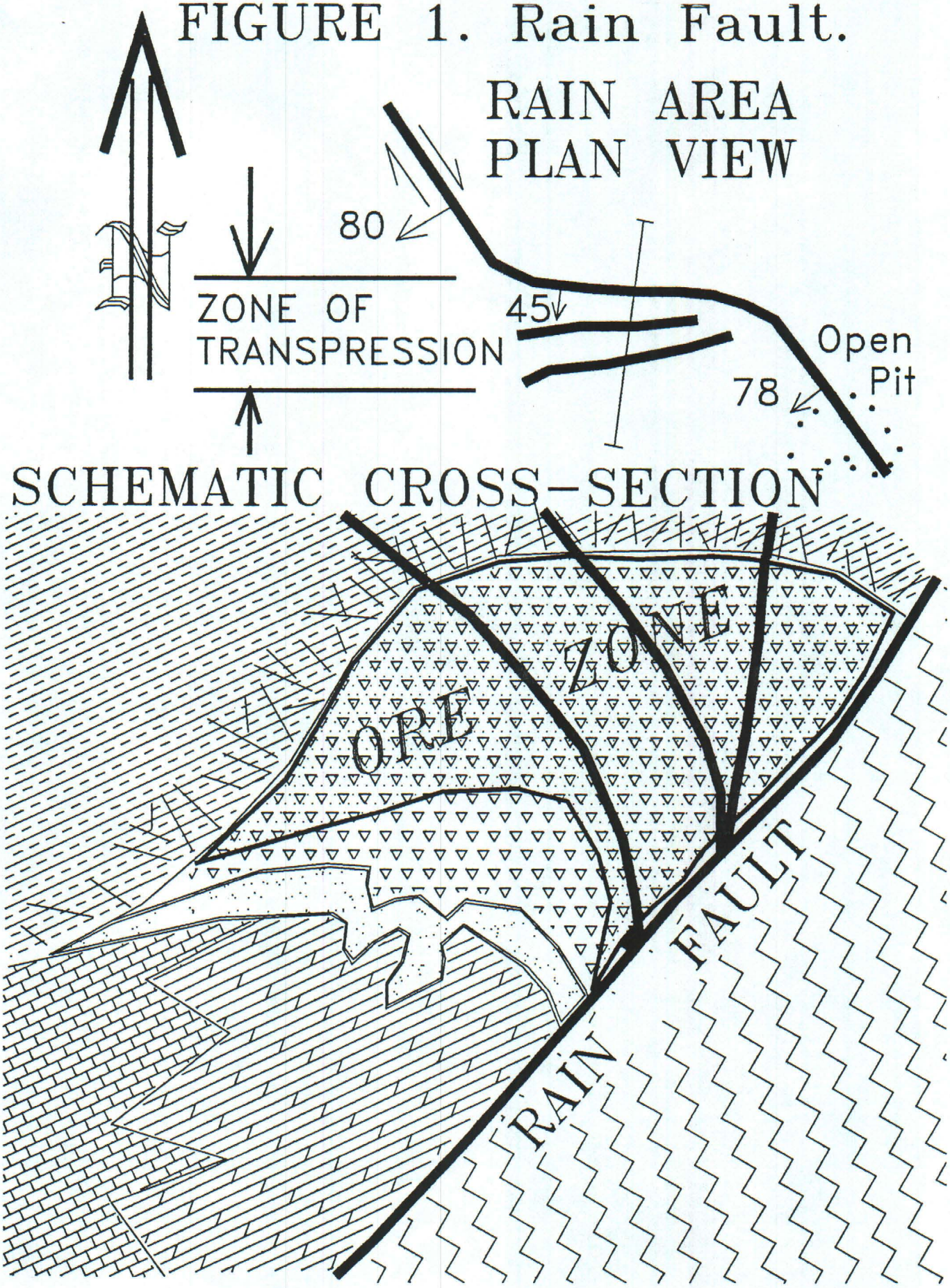

FIGURE 2. Grade-thickness along the Rain fault system.

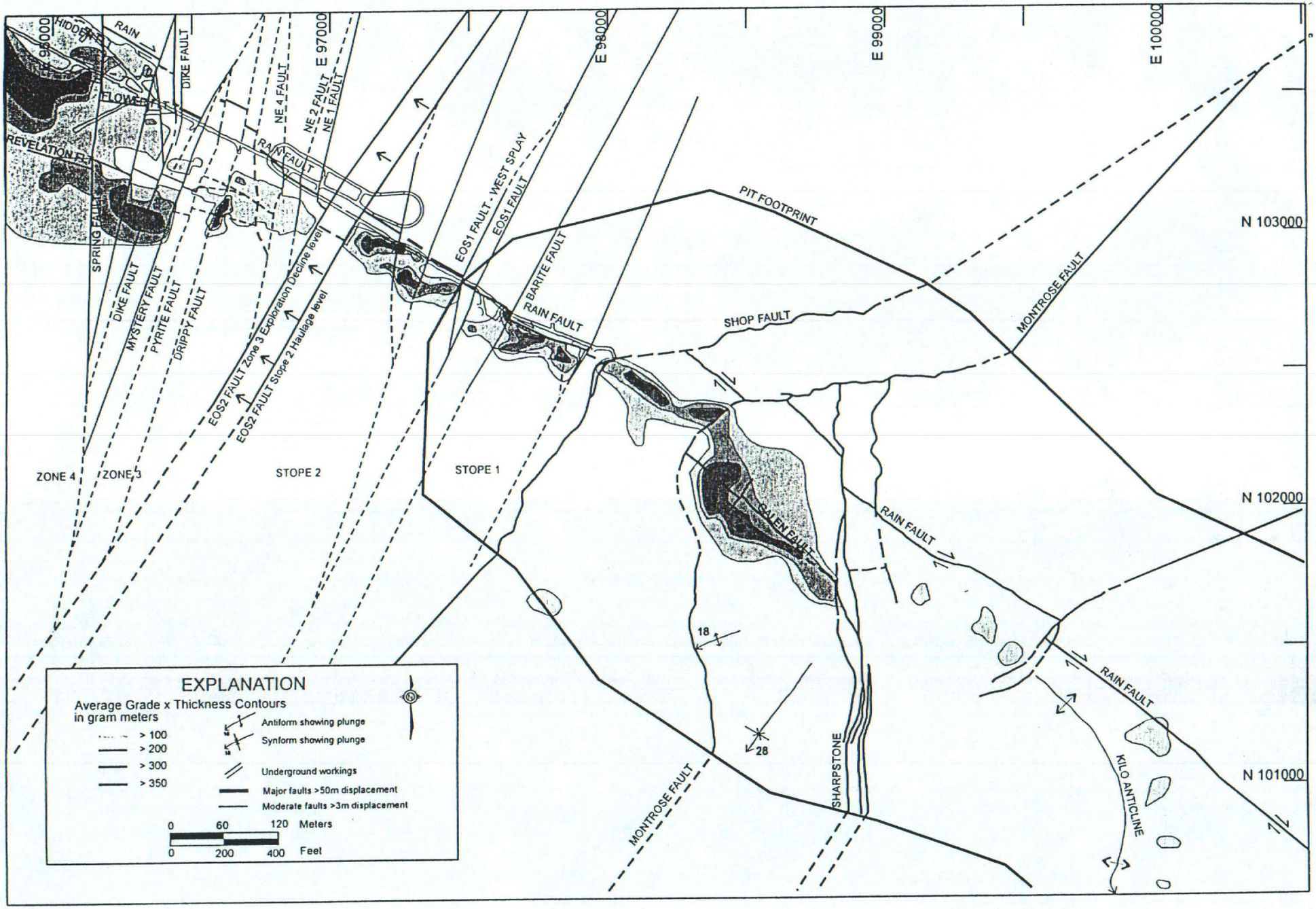

FIGURE 3. Average gold grade along the Rain fault system.

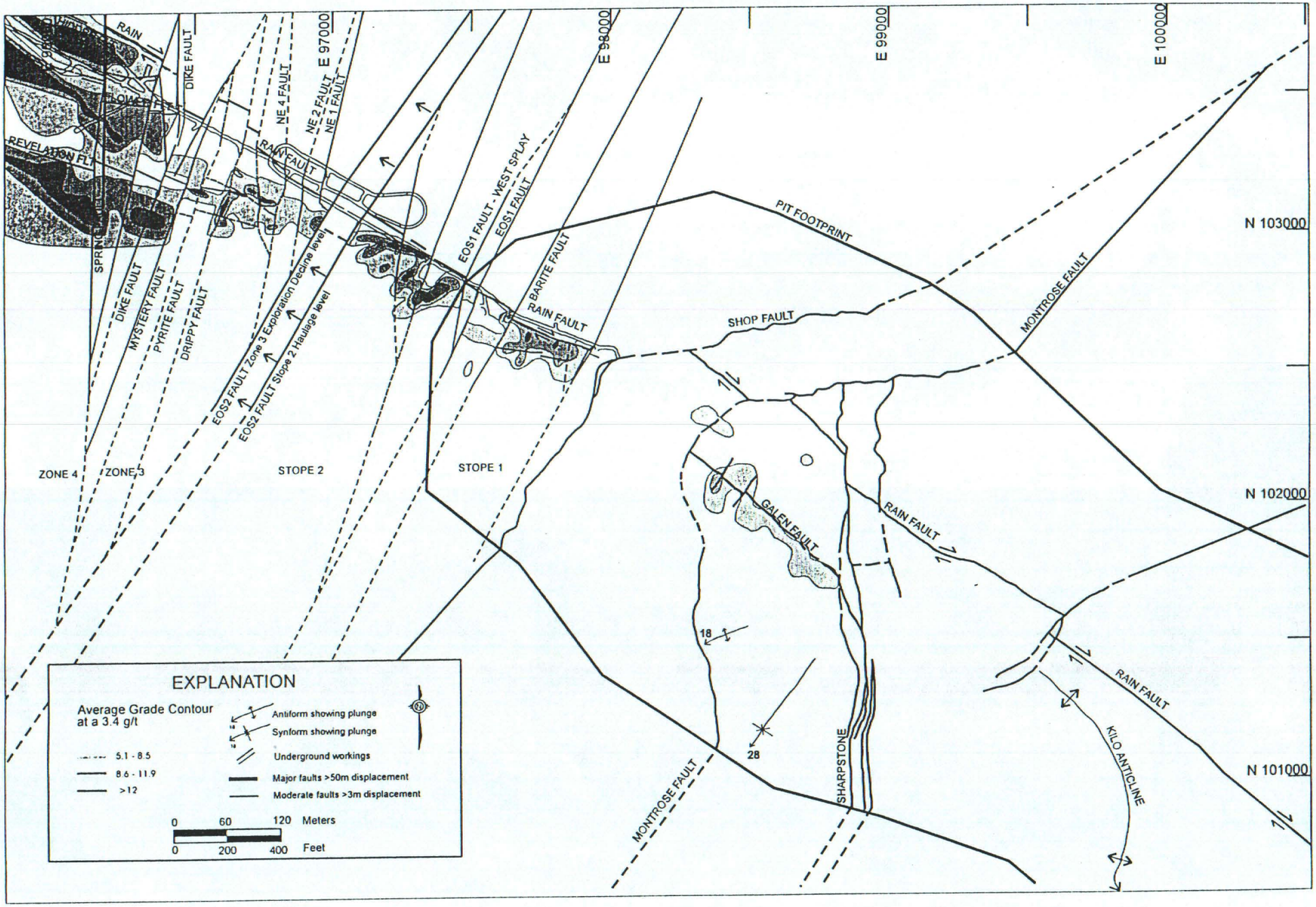

Structure, Alteration, and Geochemistry of the Rain Mine, Elko County, Nevada

Lori J. Shallow
Tommy B. Thompson
Ralph J. Roberts Center for Research in Economic Geology
Department of Geological Sciences, Mackay School of Mines, University of Nevada-Reno

Introduction

The Rain subdistrict is located at the southern tip of the Carlin trend approximately thirteen kilometers southeast of the town of Carlin, Nevada (Fig. 1). The Rain orebody is hosted in a wedge-shaped composite breccia body along the hanging wall of the Rain fault. The breccia body occurs within the siliciclastic rocks of the Mississippian Webb Formation at and above the unconformable contact with the Devonian Devils Gate Limestone (Fig. 2).

Irregular pods of refractory mineralized breccia were discovered by exploratory drilling at the Rain mine in 1996. All ore discovered up until this time had been oxide; however, the ratio of refractory breccia to oxide breccia appears to be increasing to the northwest. The purpose of this research is to reach an understanding of structure, alteration, and geochemistry of the refractory breccias at Rain in order to interpret their origin and to predict their occurrences. Specific goals include the following: 1) identifying the alteration types and distribution near the refractory breccia bodies, 2) examining the geochemistry of breccia types and fault zones, 3) determining the nature of the oxidation (hypogene versus supergene), and 4) determining the importance of carbon in the Rain orebody. A secondary goal of this research is to determine the mineral-gold association in the Rain ores.

Breccias

The development of the composite breccia body which hosts the Rain orebody is described by Williams (1992). The breccia body is composed of four types of breccias: crackle breccia, hydrothermal breccia, tuffisite, and collapse breccia (Fig. 3). The crackle breccia forms the upper periphery of the orebody, the hydrothermal breccia forms the interior and hosts the bulk of the ore, the tuffisite cross-cuts the crackle breccia and hydrothermal breccia along faults, and the collapse breccia forms the floor of the orebody. Alteration associated with the orebody includes quartz-pyrite-barite veining, silicification, dolomitization, and oxidation.

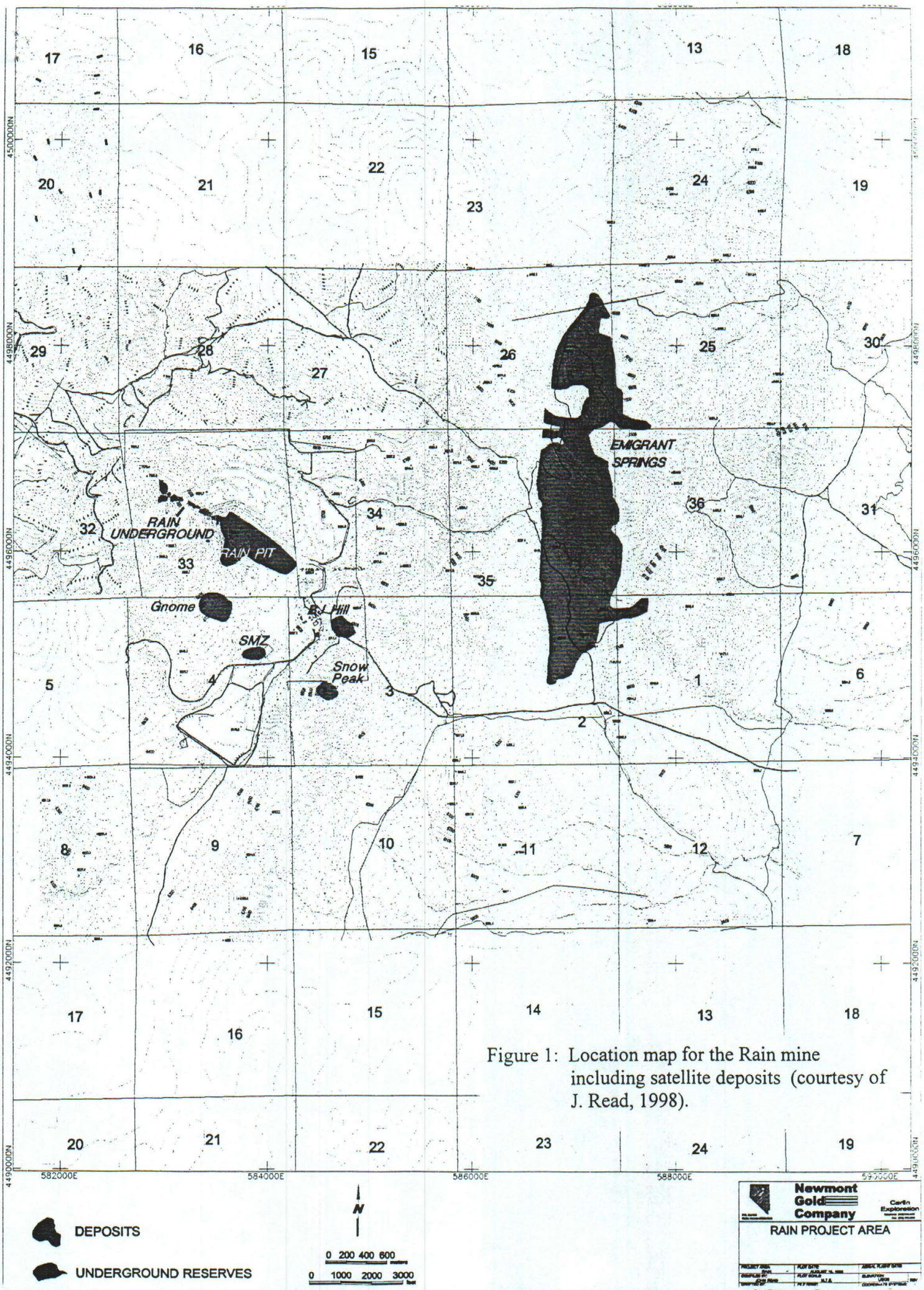

Figure 1: Location map for the Rain mine including satellite deposits (courtesy of J. Read, 1998).

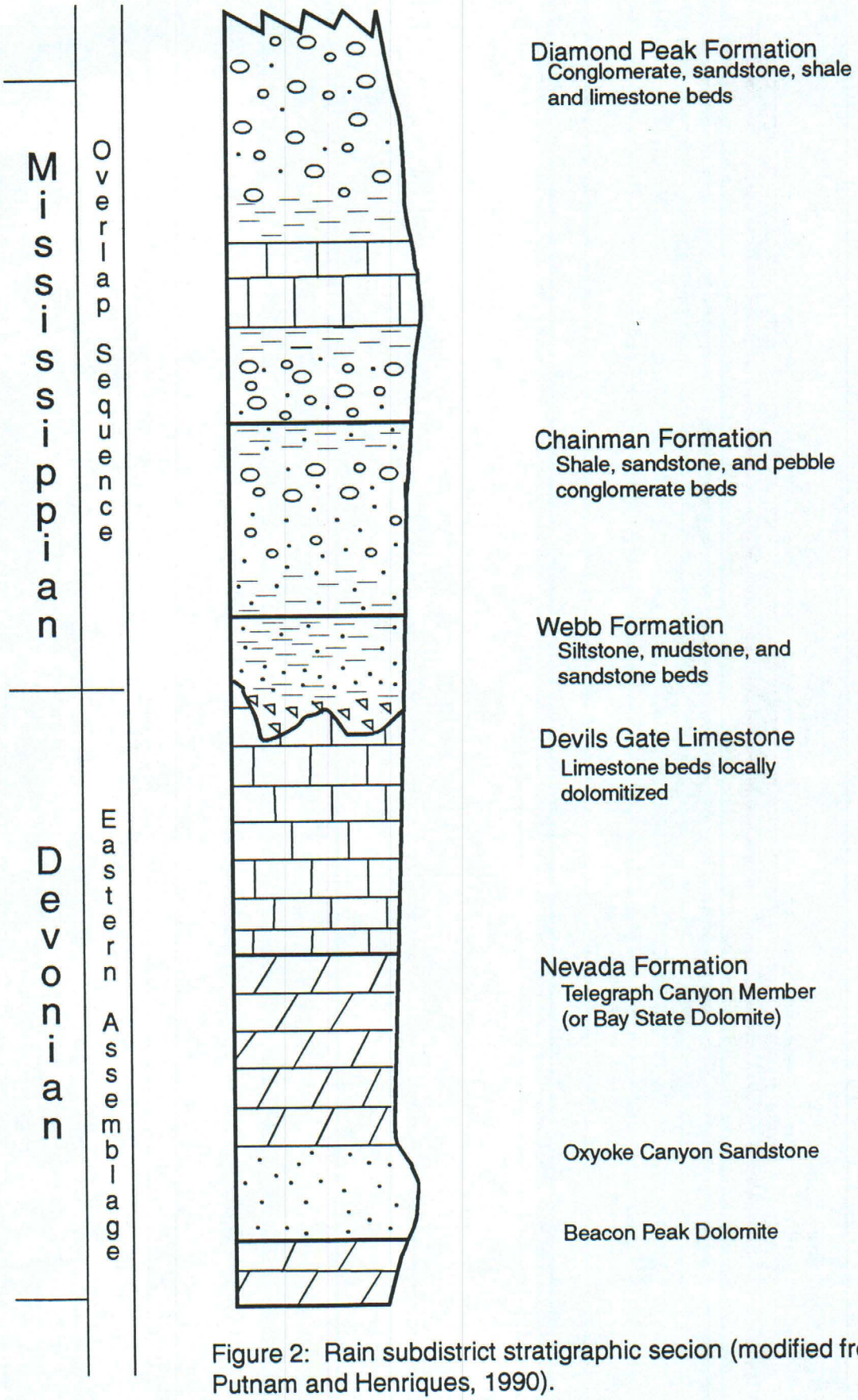

Figure 2: Rain subdistrict stratigraphic secion (modified from Putnam and Henriques, 1990).

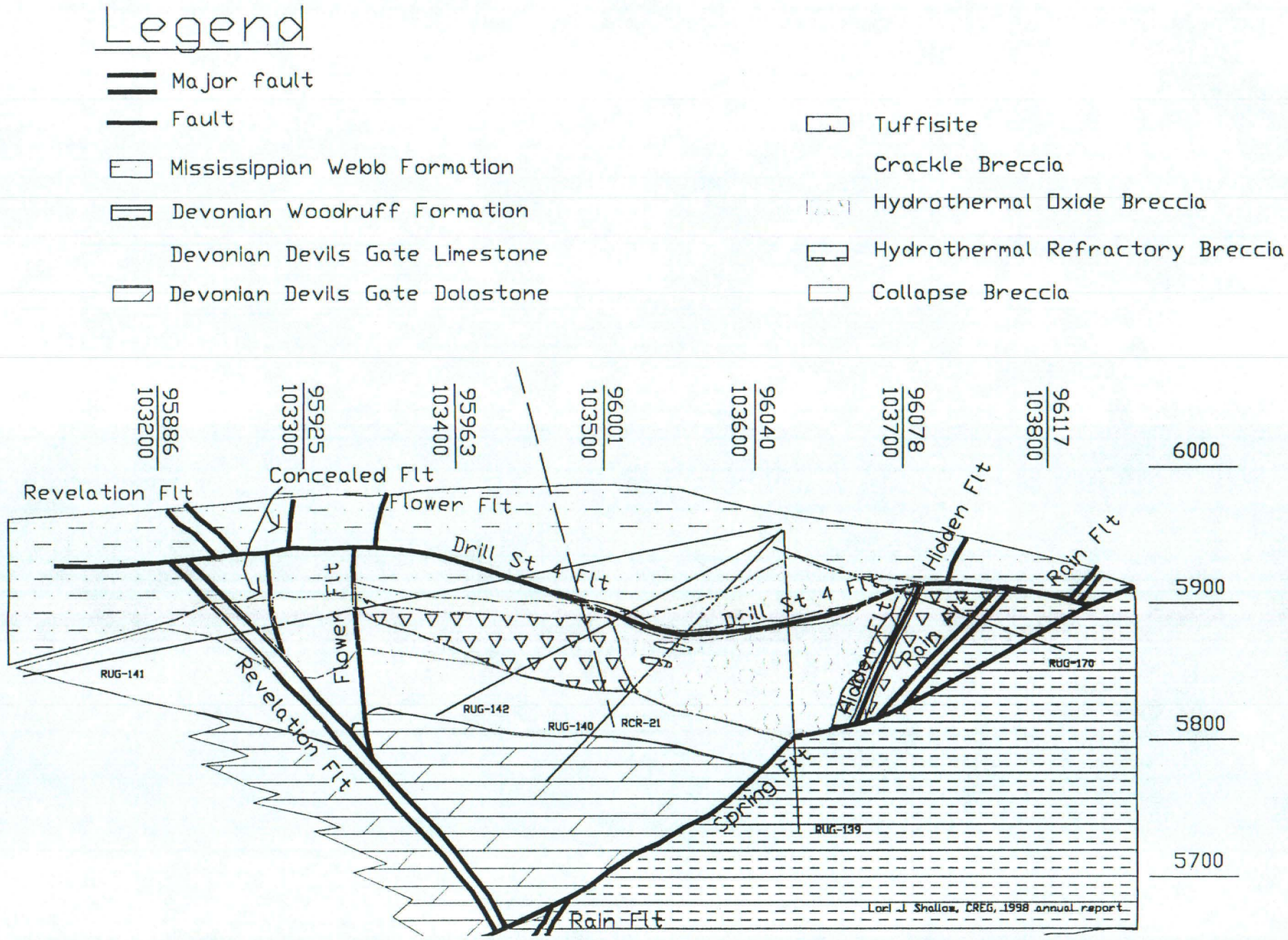

Figure 3: Cross section of the composite breccia body along the source of the geochemical samples of 1998.

Crackle breccia

Crackle breccia is defined by Williams (1992) as a breccia with minimal rotation and abrasion of fragments resulting in a jigsaw puzzle texture where fragments can be placed back together. The crackle breccia zone ranges from six to fifteen meters in thickness and has gradational contacts with both the unbrecciated Webb formation and the hydrothermal breccia. The fragments of the crackle breccia are monolithic angular Webb Formation and compose sixty five to ninety five percent of this unit.

Several types of alteration are present in the crackle breccia. Detrital quartz within the fragments commonly display quartz overgrowths, locally with rutile needles extending through the overgrowths. Pyrite crystals also have thin anisotropic porous rims slightly less reflectant than the cores adjacent to the hydrothermal breccia. Crackle breccia is locally silicified adjacent to the hydrothermal breccia. Both goethite and hematite can be observed as indigenous replacements of pyrite, as veinlets cutting the crackle breccia, as disseminations throughout the matrix, and as botryoidal or anhedral void fillings. Quartz-pyrite-barite-sphalerite veinlets are present throughout the crackle breccia.

Hydrothermal breccia

Hydrothermal breccia is composed of silicified and unsilicified fragments of Webb Formation, and Devils Gate Limestone in 15 to 20 percent matrix. Hydrothermal breccia can be either oxide or refractory. Typically, refractory breccias have slightly higher grades than oxide breccias. Refractory breccias in the oxide portion of the orebody are commonly situated adjacent to tuffisites. Hydrothermal minerals in both oxide and refractory breccias include quartz, barite, rutile, apatite, pyrite, marcasite, arsenian marcasite, and orpiment (possibly originally realgar).

Alteration in the hydrothermal breccia is dominantly silicic. The quartz typically occurs as replacements, overgrowths, and open-space fillings and contains abundant carbonate inclusions. Quartz and barite are euhedral to subhedral and contain inclusions of apatite, rutile, carbonate, pyrite, marcasite, and orpiment. Quartz and barite crystals commonly coat vugs present within the hydrothermal breccia. Both barite ± quartz veins and pyrite veins cut the hydrothermal breccia. Pyrite and marcasite crystals have up to two generations of overgrowths, one being barren and one being arsenic-bearing.

Tuffisite

Tuffisite is an argillized fluidized fragmental material that cuts both the hydrothermal and crackle breccias along structures, most notably the Rain parallel Revelation fault. Subangular to subround fragments compose ten to thirty percent of the tuffisite. These are surrounded by a fluidized matrix of quartz, pyrite, smectites, and rock flour. Subhedral to anhedral disseminated pyrite composes two to seven percent of the rock. The tuffisite is not mineralized except where it contains fragments of mineralized material.

Collapse Breccia

Collapse breccia extends down into the Devils Gate Limestone and forms the floor of the breccia body. This collapse breccia is composed of fragments of Webb Formation, crackle breccia, hydrothermal breccia, and Devils Gate Limestone. The collapse breccia can be two to thirty feet thick and is commonly associated with large voids. The matrix of the collapse breccia is dominantly a thick hematitic clay and this unit is invariably oxidized.

Paragenesis

Ore-forming events can be separated into three main categories: passive silicification, main ore stage, and supergene. Williams (1992) separated the main ore stage events into three episodes of brecciation and a void-filling stage; however, this study has not gone into such detail as the earlier study in this respect. Additionally, Williams (1992) recognized an early potassic alteration in the open pit for which no evidence has been found in this study. The paragenesis, detailed on figure 4, has been divided spatially into the hanging wall, which includes the Webb Formation and the crackle breccia, and the main orebody, which incudes the hydrothermal body and the tuffisites. Although the collapse breccia is not part of the orebody, it is represented in the main orebody (supergene) section of this diagram for simplicity's sake.

Passive Silicification Stage

The passive silicification stage was pre-ore and was preceded by structural preparation (Fig. 5a). Early fluids traveled up along structures and both dolomitized and silicified the Devils Gate Limestone. In the Webb Formation, passive silicification originated along the structures but spread secondarily along bedding planes. The Woodruff Formation shows only local silicification.

Quartz in this stage co-precipitated with marcasite and pyrite, and rutile. The quartz occurs as replacements and overgrowths on detrital grains. Commonly the quartz contained abundant

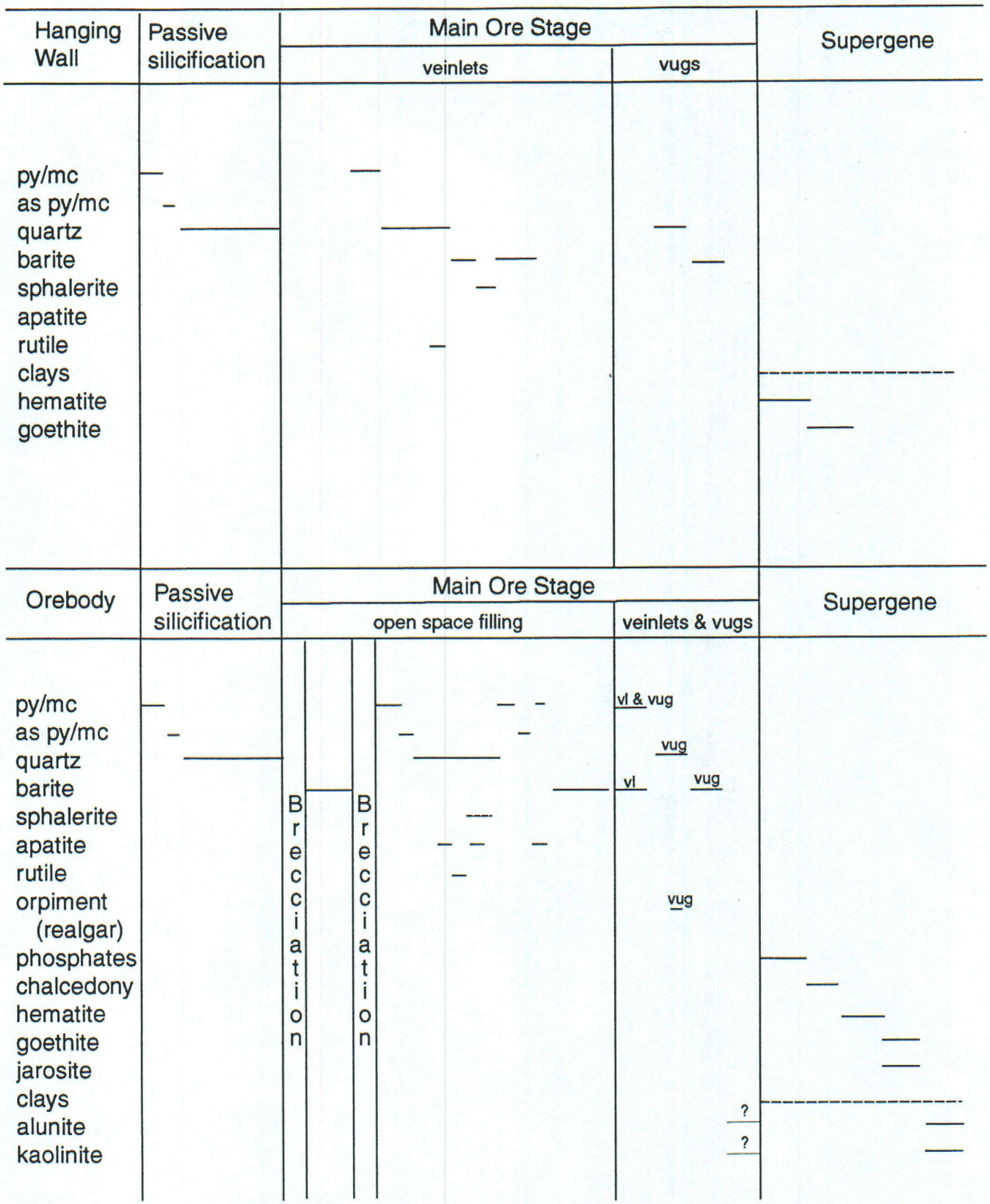

Figure 4: Paragenetic diagram from the Rain mine.

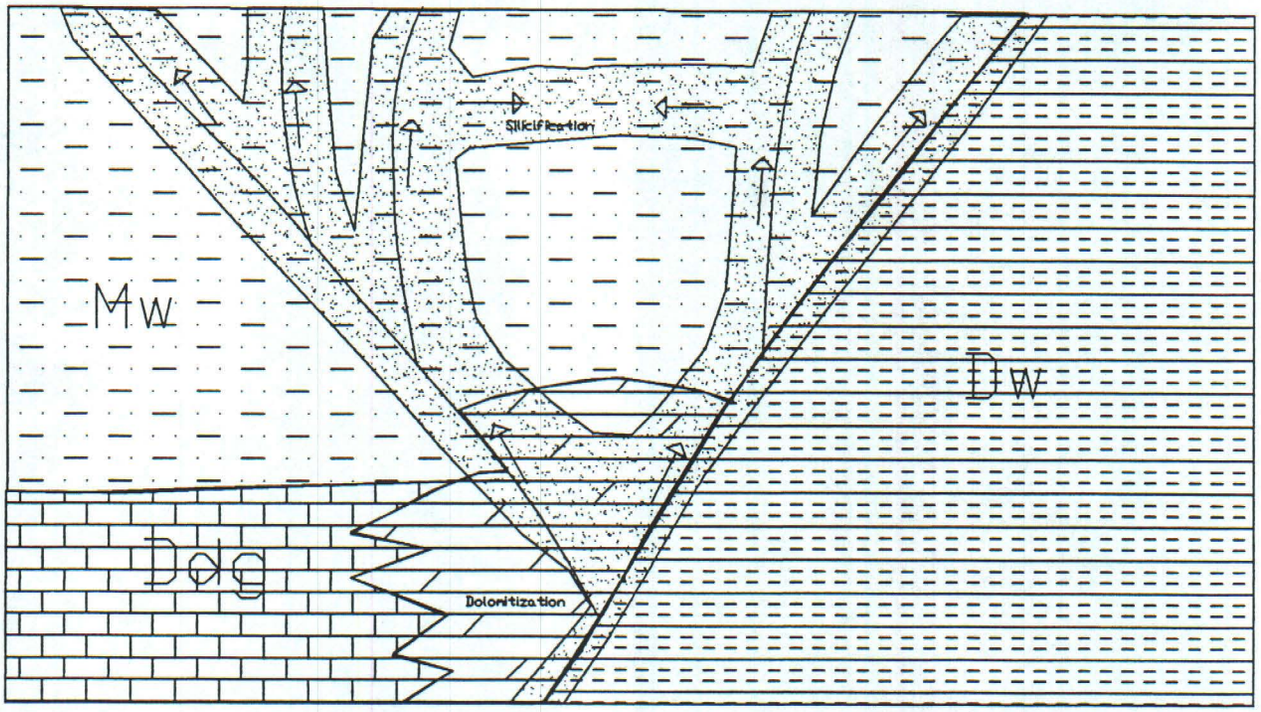

Figure 5a: Passive silicification along structures and bedding planes.

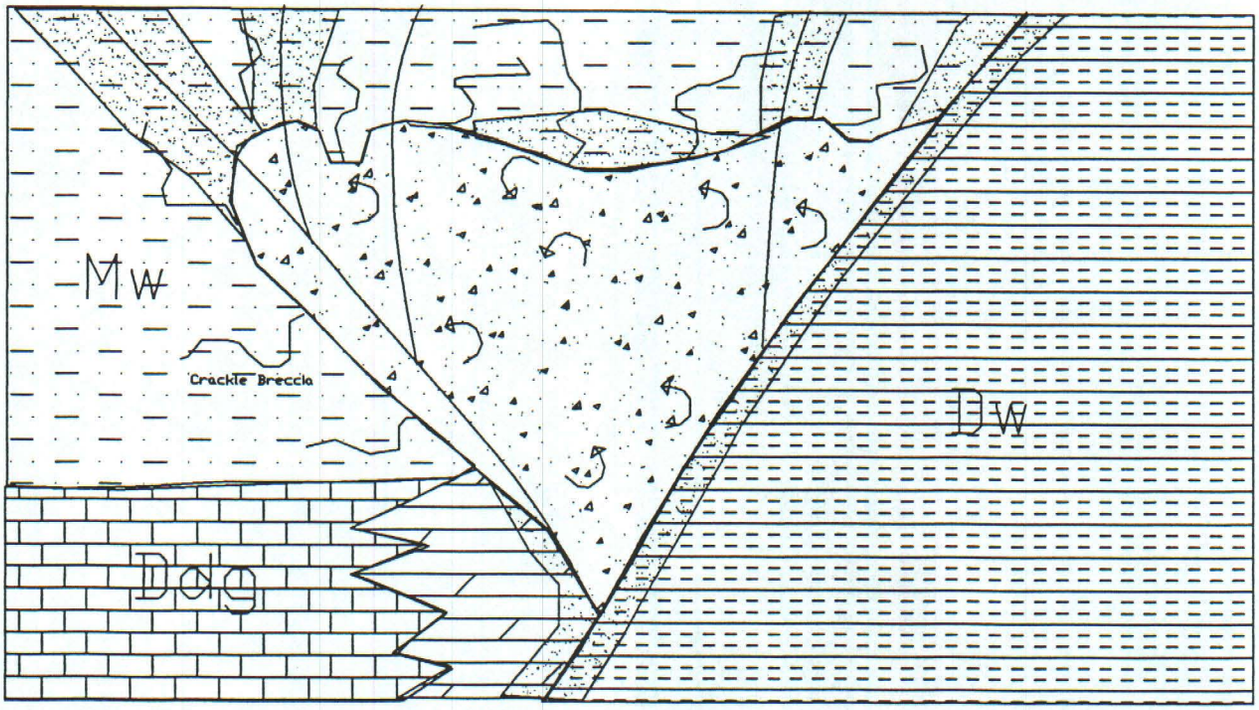

Figure 5b: Main ore stage multiple brecciation and open space filling.

carbonate inclusions along certain growth zones. Locally, the marcasite and pyrite have thin arsenian marcasite and pyrite rims. The end result of this passive silicification was a silica cap which allowed pressure to build up beneath it.

Main Ore Stage

The main ores stage began with a sudden release of pressure, possibly the failure of the silica cap, which caused boiling and brecciation (Fig. 5b). The boiling of these hydrothermal fluids caused fragments of silicified Webb Formation and unsilicified Webb formation along with Devils Gate Limestone to be mixed. Pore space was created from this brecciation, and the pore space was filled by pyrite, marcasite, quartz, and barite. Simultaneously, these main ore stage fluids formed veinlets into the much less porous Webb Formation. Therefore, the crackle breccia formed coincidently with the hydrothermal breccias. As the quartz filled the pore spaces in the hydrothermal breccias, it reformed the silica cap, allowing pressure to rebuild and the brecciation process to repeat. Upon the completion of boiling and brecciation, late fluids deposited vug-fillings and late veinlets which cut the orebody. Vug fillings include euhedral quartz and euhedral barite. Veinlets were composed of barite ± quartz and of pyrite.

The forms of quartz, barite, marcasite, and pyrite in these stages are mainly euhedral to subhedral. The quartz commonly contains growth zones with abundant carbonate inclusions. Apatite, rutile, and orpiment (presumably a replacement of realgar) are also common inclusions.

Pyrite and marcasite are either subhedral, euhedral, or framboidal, and they have up to two generations of pyrite/marcasite overgrowths. X-ray mapping of a pyrite framboid (fig. 6) and spectral analyses of several overgrowths (Fig. 7, Fig. 8, Appendix 1) show that one of these overgrowth stages is arsenic-bearing. Weight percentages of arsenic in these overgrowths range from 0.97 to 9.93. The cores are uniformly without arsenic. One of the overgrowth stages is also barren of arsenic.

Sphalerite is present within the main ore stage in both the crackle breccia and the hydrothermal breccia. In the crackle breccia, it is represented by euhedral crystals (1 to 3 millimeters in width) in veinlets along with barite and quartz (Fig 9). The sphalerite present in the veinlet is strongly zoned from iron rich (red) to iron poor (yellow). Twinning is common along planes not parallel to the zoning. Fluid inclusions are abundant along lineations parallel to these twin planes but not within the twin planes themselves. Euhedral sphalerite overgrowths encompass several smaller

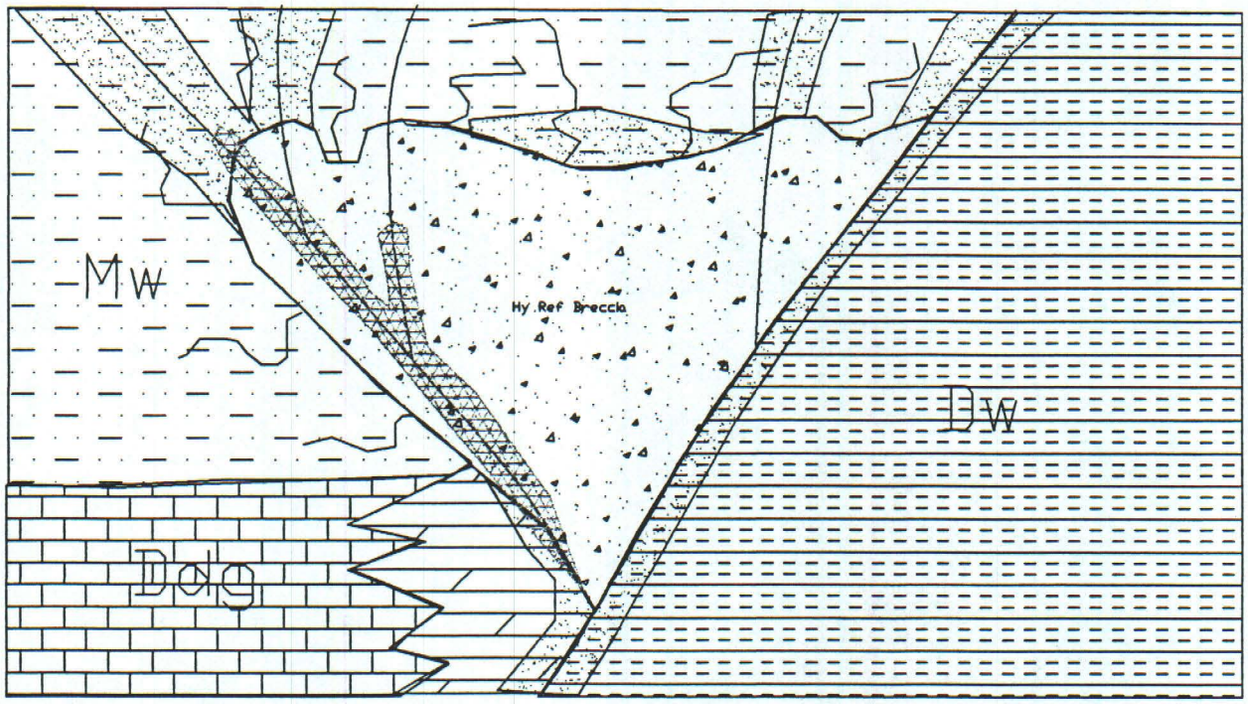

Figure 5c: Tuffisite emplacement.

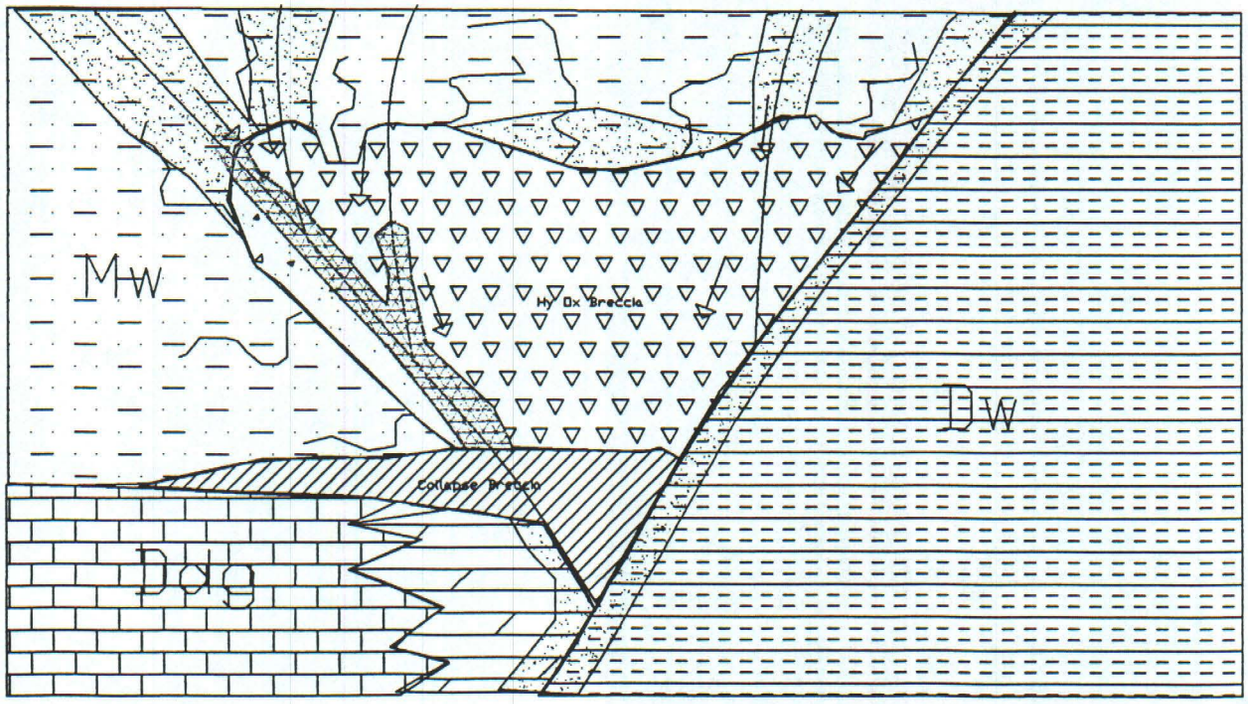

Figure 5d: Oxidation and karstification caused by supergene fluids.

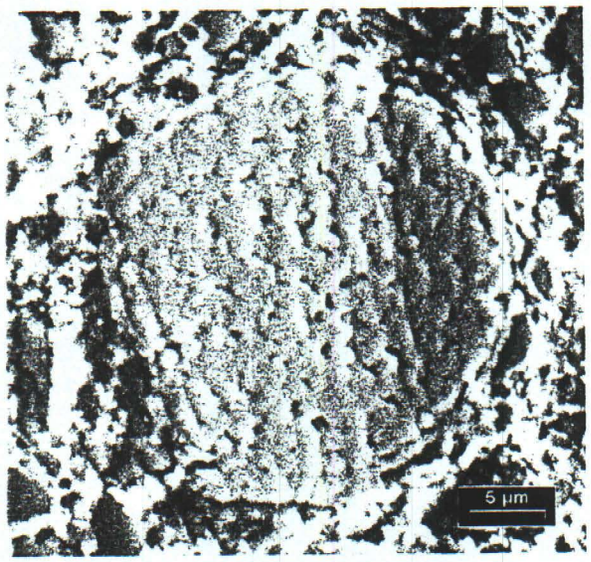

a

Figure 6: (a) SEM image of pyrite framboid from drill hole RUG 158 15-20' (b) x-ray map of iron content (c) x-ray map of arsenic content (d) x-ray map of sulfur content (e) x-ray map of silica content. Brighter colors indicate higher abundances of given element.

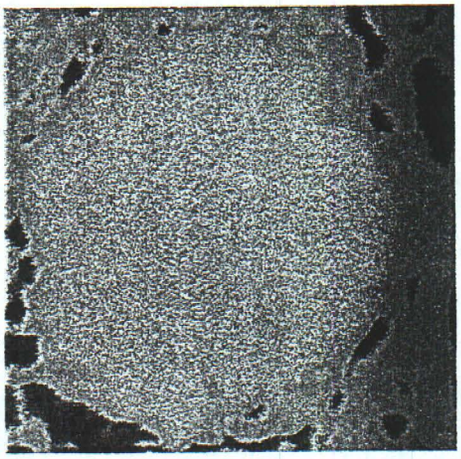

b

c

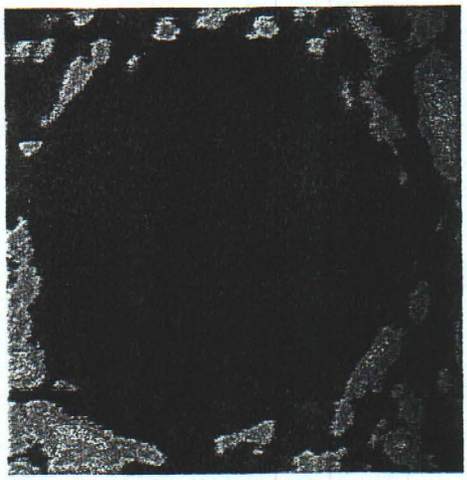

d

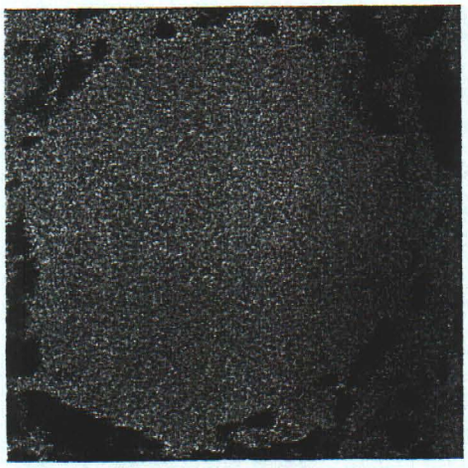

e

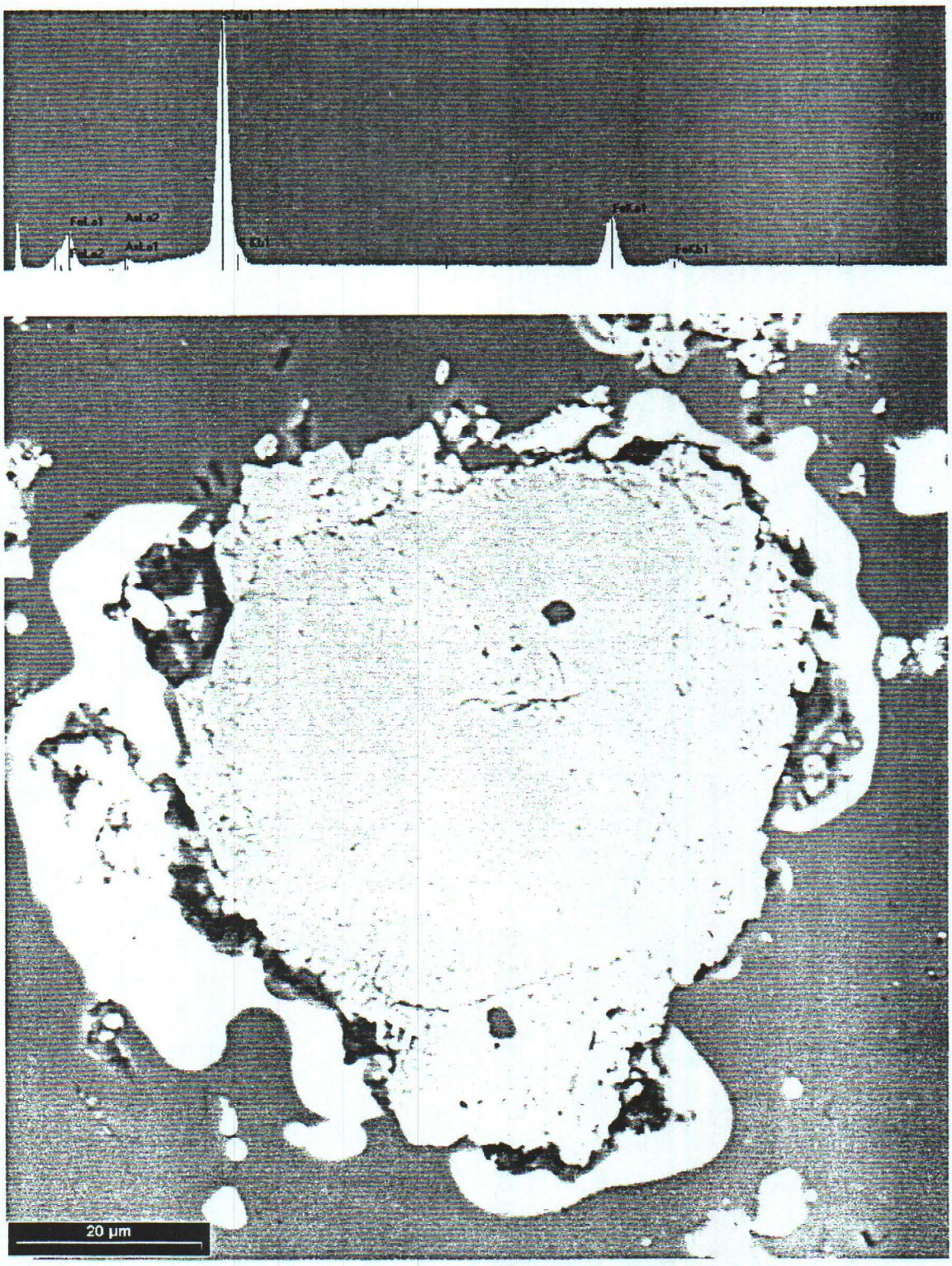

Figure 7: SEM image and spectral report from an overgrowth on pyrite from RCR 25.1 1434.5'.

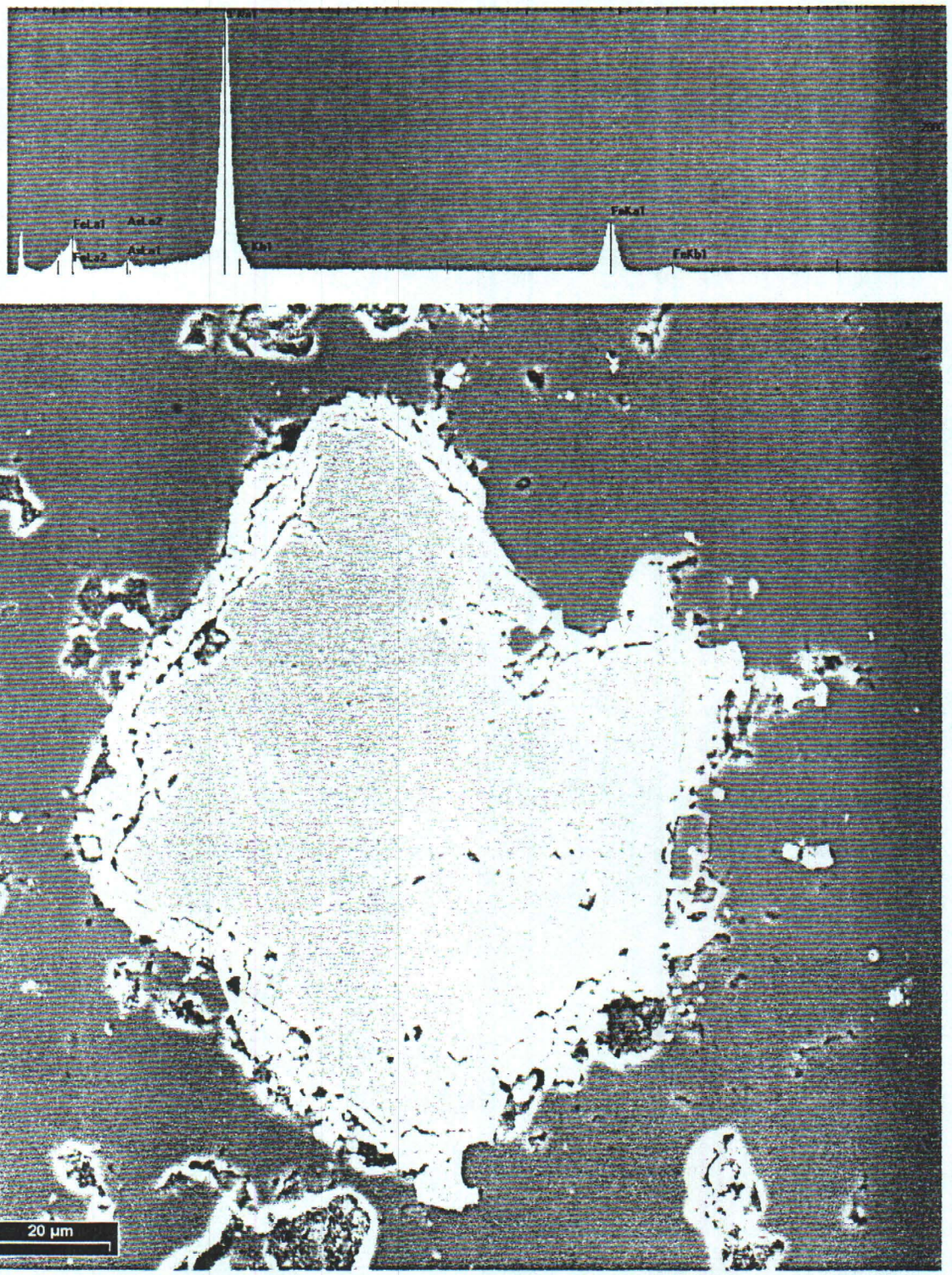

Figure 8: SEM image and spectral report from the overgrowth on pyrite from RCR 25.1 1434.5'.

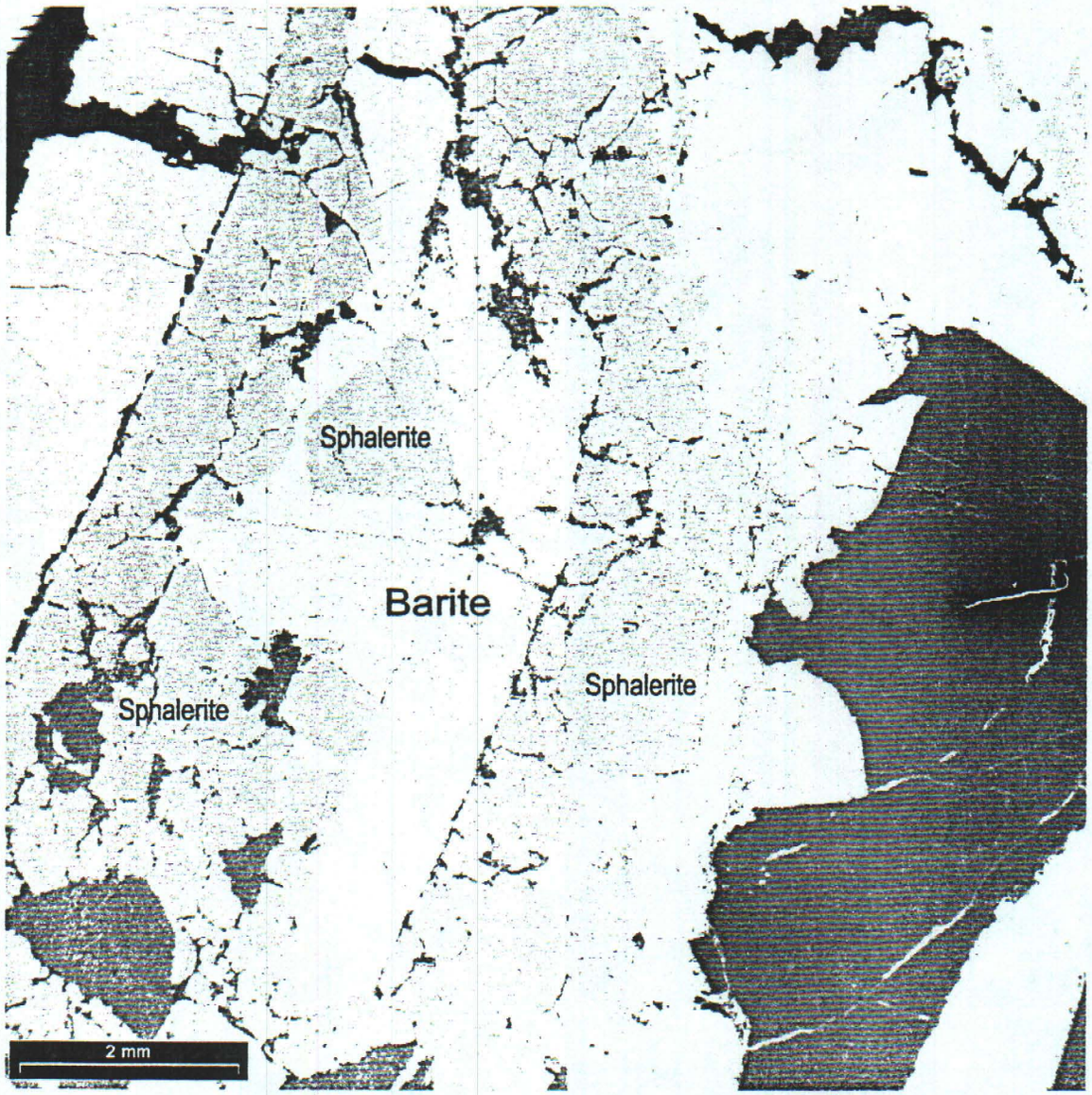

Figure 9: SEM image of sphalerite (zoning not visible) on a euhedral barite crystal in the crackle breccia of RCR 50 1915'.

sphalerite crystals. In the hydrothermal breccia, the sphalerite is much smaller (20 to 30 microns in width) and present as anhedral fragments (Fig 10). It does not display the spectacular zoning or twinning observed in the sphalerite in the crackle breccia. The grain margins of the sphalerite fragments in the hydrothermal breccia appear to be embayed. The timing for sphalerite emplacement in the main orebody is unclear and is presumed to be the same as in the crackle breccia.

At the end of the main stage is a period of tuffisite emplacement. The tuffisites consist of small subangular to subround fragments in a matrix of quartz and rock flour. Locally the tuffisites contain fragments of hydrothermal breccia or crackle breccia. Underlying collapse breccia locally contains fragments of tuffisite. Therefore, tuffisite emplacement is temporally constrained the end of hydrothermal brecciation and the beginning of collapse breccia formation.

Supergene

In the supergene stage, meteoric fluids percolated down structures and through the breccia body, causing oxidation and karstification at the Devils Gate Limestone-Webb Formation unconformity (Williams, 1992). The earliest deposition in the supergene stage consists of a botryoidal phosphate in precipitated in open spaces. Chalcedony was deposited over the phosphate in open spaces. Later hematite coated fractures and open spaces and pseudomorphed pyrite and marcasite. Goethite and jarosite formed next as fracture coatings, pseudomorphs, and veinlets. It was during the supergene stage that the collapse breccia formed from ponding of meteoric fluids below the orebody. Supergene kaolinite and alunite are present along faults in the open pit (Williams, 1992).

Geochemistry

The geochemistry of the Rain system was examined in order to determine differences among individual units, changes along strike, affiliations between elements and the orebody and structures, and gold-mineral associations. A geochemical database was compiled for this purpose from three separate groups of data (Fig. 11). The first set of data was collected by Newmont geologists from six vertical reverse circulation holes over the present day open pit in 1981 and 1982 (Appendix 2-a). The chips were prepared and analyzed at GSI Labs using a partial digestion-organic extraction/ICP method for ten elements. The second set of data consisted of grab samples from the Rain underground and open pit collected by the authors and Newmont geologists in the fall of 1997 (Appendix 2-b). The samples were prepared and analyzed for twenty four elements at Chemex Labs using either an ICP or AAS analytical method. The third set of data was collected in 1998 from a fan

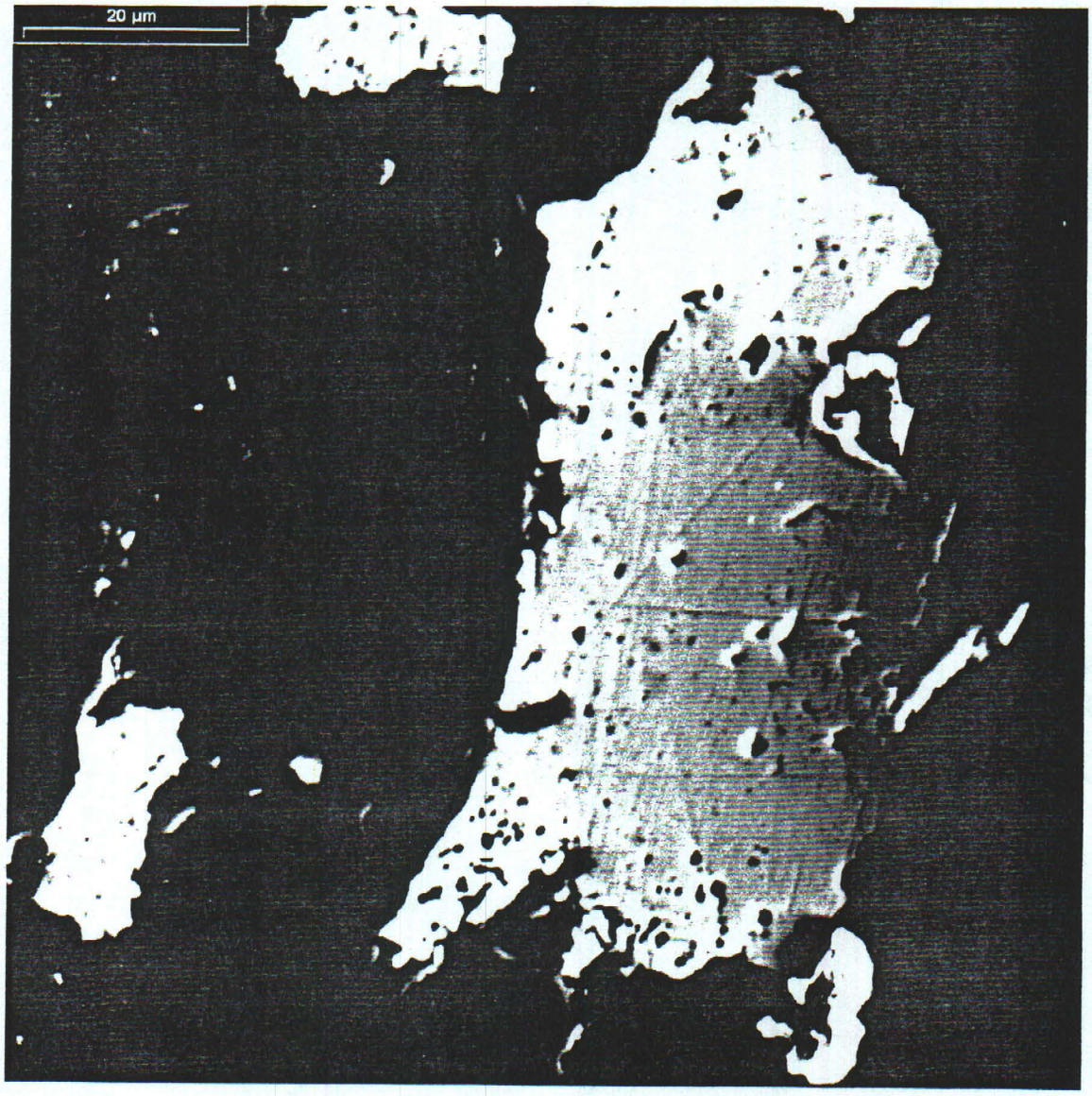

Figure 10: Sphalerite from hydrothermal breccia in RCR 25.1 1434.5'.

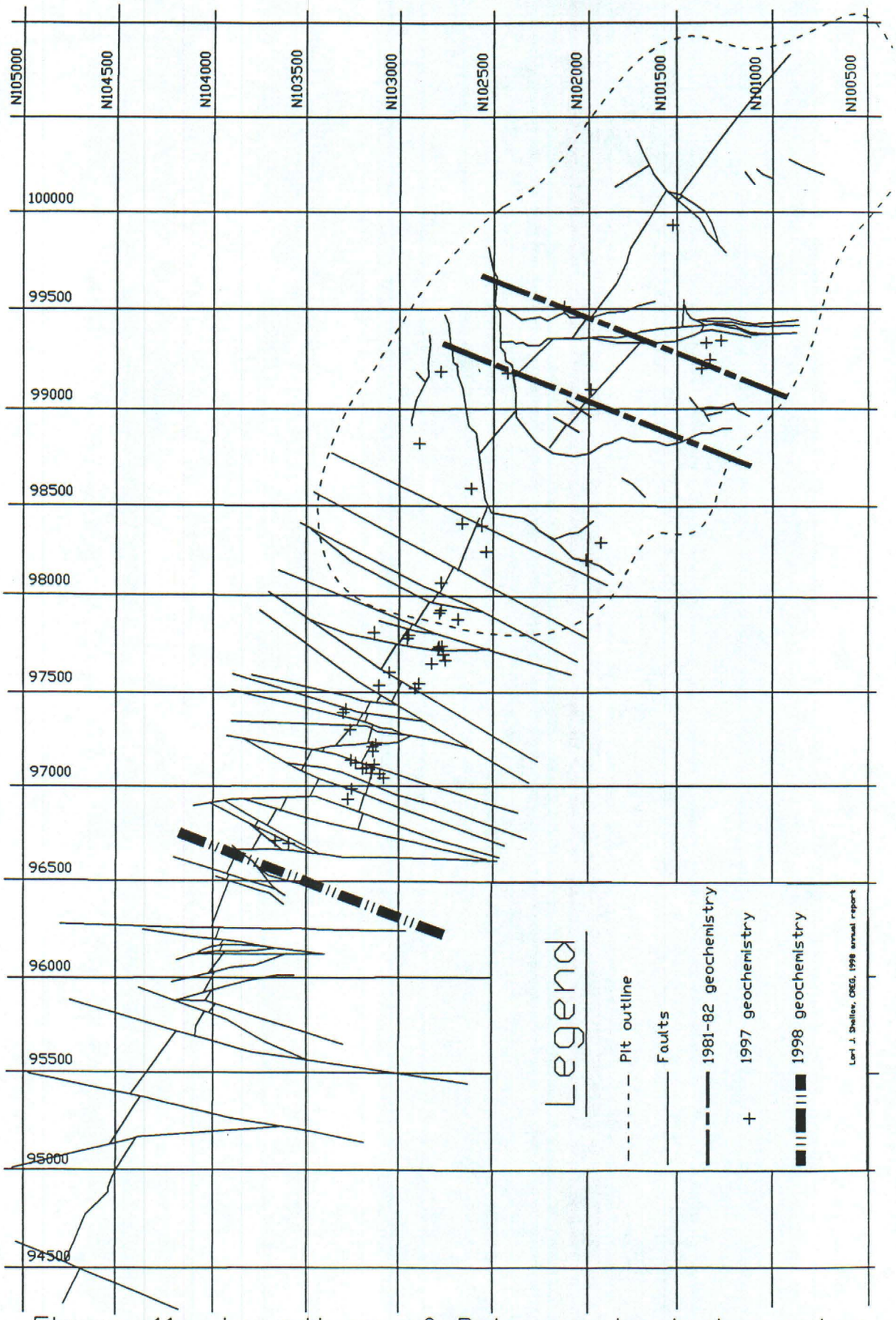

Figure 11: Locations of Rain geochemical samples projected to map level.

of core holes in the underground mine workings (Appendix 2-c). The samples were prepared and analyzed by Chemex Labs for thirty two elements using a ICP-AES analysis and for whole rock with XRF analyses.

The first set of data collected in 1981 and the third set of data collected in 1998 are largely compatible. Notable exceptions to this are the antimony and mercury analyses, for which GSI Labs reported inflated values at that time. Detections limits also differed for bismuth and cadmium. For these reasons, antimony, mercury, bismuth, and cadmium were not included in any comparisons made between these sets of data.

The second set of data collected in 1997 from grab samples appears incompatible with both of the other sets of data. Overall, values seem extremely high when compared with the other two sets. This may be due to contamination during collection of the samples or to the samples' close proximity to major structures. In any case, the second set of data was treated separately from the others and no comparisons were made with the other two sets of data.

Differences among units

The data obtained from the geochemistry collected in 1998 from six core holes in the Rain underground reveals significant variations in elemental abundances among the different units in the Rain mine. Averages from the Chainman and Webb Formations, crackle breccia, hydrothermal breccia (composite of both oxide and refractory), tuffisite, and the Devils Gate Limestone are listed in table 1. When the Chainman Formation, stratigraphically highest of these units, is compared with the underlying Webb Formation, several differences are accented. The Webb Formation shows local increases in gold, antimony, and thallium concentrations relative to the Chainman Formation. The Webb Formation also contains consistently elevated values of arsenic, calcium, iron, and phosphorous compared to the Chainman Formation. Concentrations of barium, chromium, and strontium are significantly lower in the Webb Formation.

Below the Webb Formation in the Rain mine is the crackle breccia. Concentrations of gold, arsenic, barium, cadmium, chromium, mercury, manganese, molybdenum, lead, antimony, strontium, thallium, and zinc all increase in the crackle breccia relative to the unbrecciated Webb Formation. The most significant increases in these elements are barium, antimony, mercury, and manganese (at twenty four, seven, three and almost three times greater concentrations, respectively). Elements which decrease in abundance in the crackle breccia relative to the Webb Formation include aluminum,

Unit	Au (ppm)	Ag (ppm)	Al (%)	As (ppm)	Ba (ppm)	Be (ppm)	Bi (ppm)	Ca (%)	Cd (ppm)	Co (ppm)
Chainman Fm.	0.001	0.200	0.631	232.857	168.571	0.500	2.000	0.050	0.643	9.286
Webb Fm.	1.863	0.200	0.747	462.075	35.500	0.500	2.100	0.223	0.525	8.825
Crackle Bx	2.063	0.200	0.410	549.200	858.000	0.500	2.000	0.054	2.800	4.000
Hydrothermal Bx	6.174	0.297	0.280	1020.366	947.105	0.500	2.000	0.139	0.767	3.718
Tuffisite	3.647	0.200	0.774	5137.200	412.000	0.500	2.000	0.168	0.500	23.200
Collapse Bx	2.066	0.244	0.609	1701.444	512.222	0.500	2.000	4.094	2.389	4.889
Devils Gate Ls	0.126	0.200	0.164	340.400	1052.000	0.500	2.000	11.506	0.700	5.000

Unit	Cr (ppm)	Cu (ppm)	Fe (%)	Ga (ppm)	Hg (ppm)	K (%)	La (ppm)	Mg (%)	Mn (ppm)	Mo (ppm)
Chainman Fm.	193.857	38.286	1.887	10.000	8.429	0.206	10.000	0.037	42.143	2.000
Webb Fm.	54.150	44.425	3.350	10.000	9.450	0.325	10.000	0.063	59.250	1.375
Crackle Bx	69.200	27.400	2.456	10.000	20.800	0.166	10.000	0.028	184.000	2.000
Hydrothermal Bx	134.226	10.174	2.989	10.000	23.916	0.065	10.000	0.021	49.697	6.953
Tuffisite	88.200	51.400	7.294	10.000	123.200	0.080	10.000	0.072	49.000	4.600
Collapse Bx	90.444	14.222	5.241	10.000	17.333	0.126	10.000	0.948	425.556	4.333
Devils Gate Ls	33.800	4.600	1.368	10.000	4.400	0.050	10.000	5.242	678.000	1.000

Unit	Na (%)	Ni (ppm)	P (ppm)	Pb (ppm)	Sb (ppm)	Sc (ppm)	Sr (ppm)	Ti (%)	Tl (ppm)	U (ppm)
Chainman Fm.	0.010	30.143	440.000	14.000	2.000	1.286	58.714	0.010	10.000	10.000
Webb Fm.	0.010	39.325	739.500	15.400	3.650	2.300	20.750	0.010	12.250	10.000
Crackle Bx	0.010	16.000	360.000	43.600	22.400	1.400	40.400	0.010	10.000	10.000
Hydrothermal Bx	0.010	26.271	1043.605	24.500	86.163	1.026	50.211	0.010	13.026	10.000
Tuffisite	0.010	67.800	1912.000	34.000	87.200	5.000	65.600	0.012	20.000	10.000
Collapse Bx	0.010	55.222	3692.222	22.222	219.111	1.556	68.000	0.010	42.222	10.000
Devils Gate Ls	0.010	31.000	496.000	17.200	74.400	1.000	109.400	0.010	12.000	10.000

Unit	V (ppm)	W (ppm)	Zn (ppm)
Chainman Fm.	57.571	10.000	93.714
Webb Fm.	41.975	10.000	112.700
Crackle Bx	30.800	10.000	181.600
Hydrothermal Bx	37.195	10.526	118.484
Tuffisite	48.400	10.000	130.800
Collapse Bx	48.111	12.222	387.222
Devils Gate Ls	11.200	10.000	292.800

Table 1: Averages from the Webb Formation, crackle breccia, hydrothermal breccia (composite), tuffisite, collapse breccia, and Devils Gate Limestone.

Lori J. Shallow, CREG, 1998 annual report

calcium, cobalt, copper, iron, potassium, magnesium, nickel, phosphorous, scandium, and vanadium.

Changes that take place in the hydrothermal breccia relative to the crackle breccia include increases in gold, silver, arsenic, barium, calcium, chromium, iron, mercury, molybdenum, nickel, phosphorous, lead, antimony, strontium, thallium, and vanadium. The most striking of these increases include gold, arsenic, chromium, molybdenum, phosphorous, and antimony. Aluminum, cadmium, cobalt, copper, potassium, manganese, scandium, and zinc all show decreases in the hydrothermal breccia compared to the crackle breccia. With the exception of manganese, lead, phosphorous, and thallium, the crackle breccia and the hydrothermal breccia change in the same way but with different intensities relative to the Webb Formation.

Tuffisite is present along structures cutting both hydrothermal breccia and crackle breccia. Relative to the averages of hydrothermal breccia, the tuffisite shows a decrease in gold, silver, barium, cadmium, copper, manganese, molybdenum, and antimony. Aluminum, arsenic, cobalt, copper, iron, mercury, nickel, phosphorous, scandium, thallium, and zinc are elevated in the tuffisite relative to the hydrothermal breccia. The elements arsenic, cobalt, copper, mercury, nickel, lead and zinc are significantly higher than any of the other units in the Rain system.

The collapse breccia is composed of fragments of Webb Formation, crackle breccia, hydrothermal breccia, tuffisite, and Devils Gate Limestone in a hematitic clay matrix. For this reason, it will not be compared to the other units. The Devils Gate Limestone has significantly different concentrations of elements relative to the other units exposed at the mine and seems to have clearly influenced only the collapse breccia.

Oxide versus refractory hydrothermal breccias

Oxide and refractory hydrothermal breccias are very similar geochemically; however, averages of oxide and refractory hydrothermal breccias show slight differences (Table 2). Refractory hydrothermal breccias have significantly higher arsenic and cobalt values and slightly elevated gold, copper, mercury, and thallium values relative to the oxide breccias. The oxide hydrothermal breccia has significantly higher concentrations of barium, manganese, phosphorous, lead, antimony, and zinc relative to the hydrothermal refractory breccia.

Changes along strike

Changes along the strike of the Rain fault were determined by using data collected from six vertical reverse circulation holes in 1981 and 1982 and from six core holes in a drill fan in the Rain

underground in 1998 (Fig. 3, Fig. 12). Because individual units could not be broken out in the reverse circulation holes, averages were taken from each entire group of holes with no regard to individual units. Mercury and antimony were disregarded due to unreliable values reported from that early data. Means, medians, and standard deviations were compared from each set of data; however, minimum and maximum concentrations were not compared due to differences in detection limits (Table 3) . All changes will be reported as comparing the southeast (open pit) to the northwest (underground).

All averages, including gold, silver, arsenic, copper, molybdenum, lead, and zinc increase to the northwest . Likewise, all standard deviations including gold, silver, arsenic, copper, molybdenum, lead, and zinc increase to the northwest. The medians of silver, arsenic, and molybdenum decrease to the northwest, whereas gold, copper, lead, and zinc increase.

Affiliations between elements and the breccias and structures

The data collected from the mine workings in 1997 and the data from the core drill fan collected in 1998 have been plotted and contoured. The grab samples from 1997 were projected to the level of the map (Fig. 13a-e). The data from 1998 were plotted along the drill holes at the footages indicated in appendix 2-C (Fig. 14a-e). Because values from these two data sets had consistently different ranges, they are compared to one another in only a qualitative sense.

Both the grab samples and the samples from the drill fan show a positive correlation between gold, arsenic, antimony, mercury, and barium. In the plan view, barium seems to be more closely related to the Rain and Revelation faults. This is supported by observations from the open pit. In cross section, arsenic, antimony, mercury, and barium are all more closely associated with northwest-striking faults and the breccia body with the highest of these values being present within the fault zones. Antimony and barium show higher values along the Revelation fault than along the Rain fault at this location.

Mineral associations

Correlation matrices have been computed for the geochemistry from 1997 and 1998 (Table 4a, Table 4b). Values of greater than positive 0.50 are arbitrarily considered as significant. In the case of both sets of data, gold is not correlative with any other element. Arsenic is slightly correlative to cobalt, mercury, and nickel in the 1998 data. This relationship is most likely due to the extremely high values of elements in the tuffisite relative to other units. In the 1997 data, arsenic shows a good

	Au (ppm)	Ag (ppm)	Al (%)	As (ppm)	Ba (ppm)	Be (ppm)
Hydrothermal oxide bx	4.83	0.29	0.26	833.63	1254.21	0.50
Hydrothermal refractory bx	7.52	0.30	0.30	1207.10	640.00	0.50

	Bi (ppm)	Ca (%)	Cd (ppm)	Co (ppm)	Cr (ppm)	Cu (ppm)
Hydrothermal oxide bx	2.00	0.14	0.68	1.74	150.05	7.95
Hydrothermal refractory bx	2.00	0.14	0.85	5.70	118.40	12.40

	Fe (%)	Ga (ppm)	Hg (ppm)	K (%)	La (ppm)	Mg (%)
Hydrothermal oxide bx	3.76	10.00	19.63	0.06	10.00	0.03
Hydrothermal refractory bx	2.21	10.00	28.20	0.07	10.00	0.01

	Mn (ppm)	Mo (ppm)	Na (%)	Ni (ppm)	P (ppm)	Pb (ppm)
Hydrothermal oxide bx	72.89	7.11	0.01	26.84	1144.21	37.00
Hydrothermal refractory bx	26.50	6.80	0.01	25.70	943.00	12.00

	Sb (ppm)	Sc (ppm)	Sr (ppm)	Ti (%)	Tl (ppm)	U (ppm)
Hydrothermal oxide bx	118.53	1.05	56.42	0.01	11.05	10.00
Hydrothermal refractory bx	53.80	1.00	44.00	0.01	15.00	10.00

	V (ppm)	W (ppm)	Zn (ppm)
Hydrothermal oxide bx	37.79	11.05	141.37
Hydrothermal refractory bx	36.60	10.00	95.60

Table 2: Averages for hydrothermal oxide and refractory breccias.
n=30

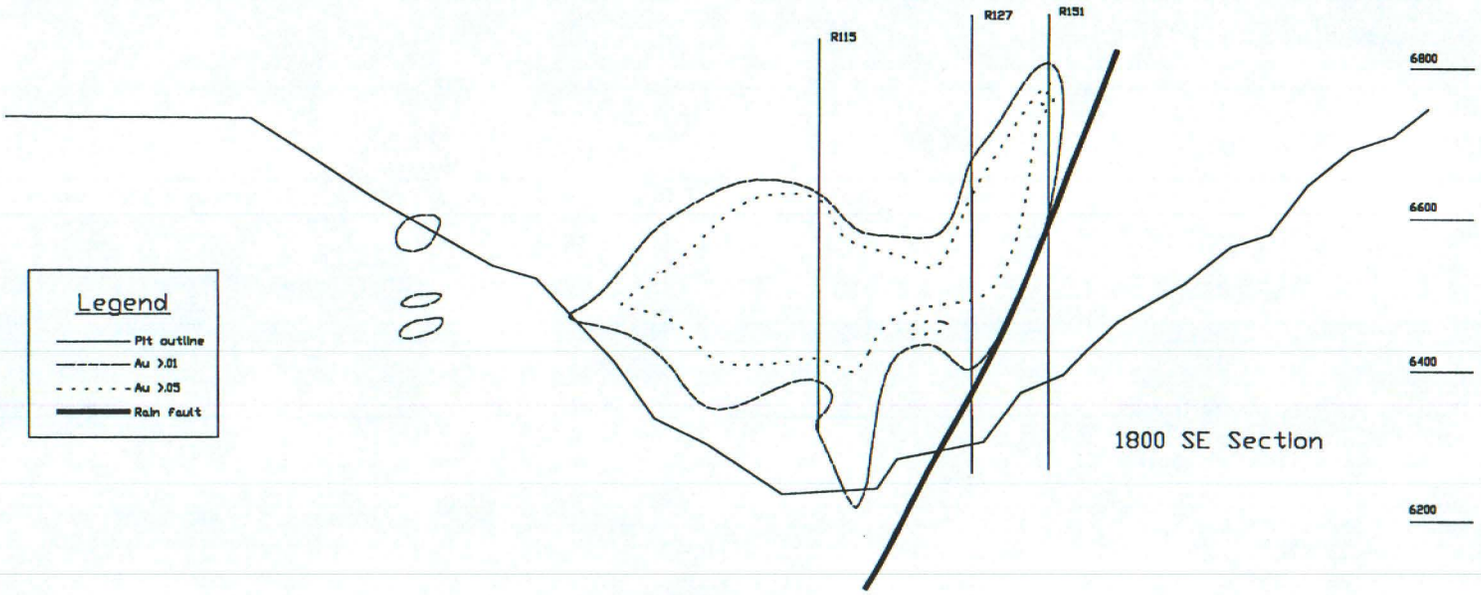

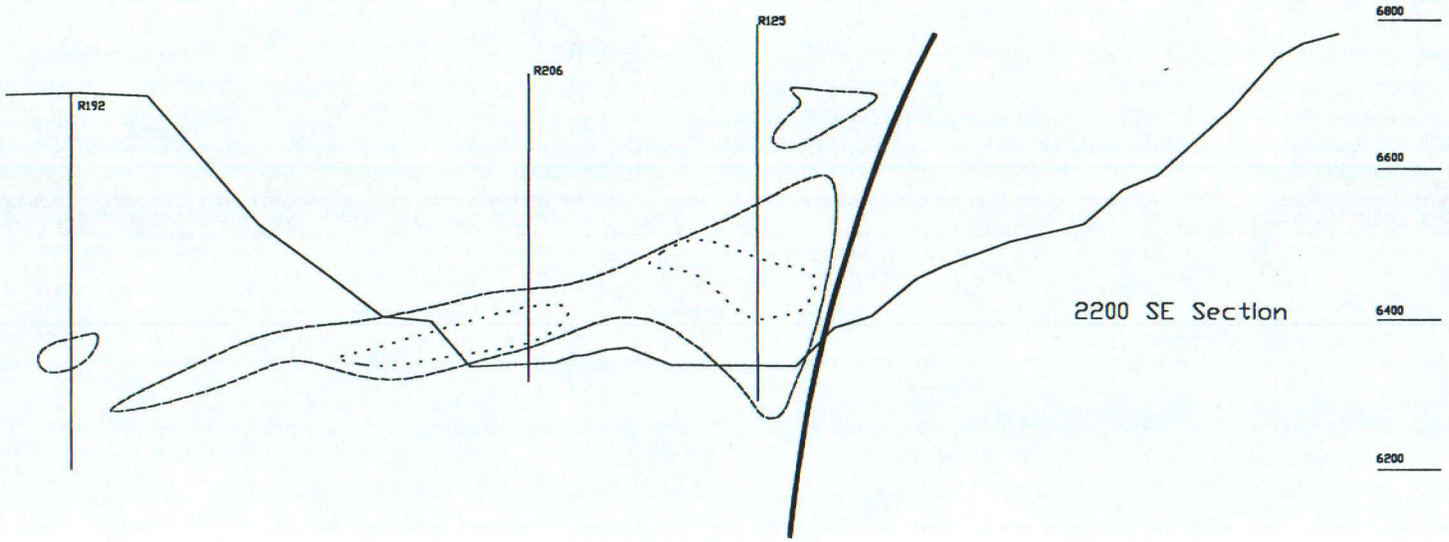

Figure 12: Source of geochemistry collected in 1981 and 1982.

	Au	Ag	As	Bi	Cd	Cu	Mo	Pb	Se	Tl	Zn
Open Pit											
mean	1.29	0.12	580.32	0.15	0.85	29.98	3.17	12.59	1.09	6.19	96.97
median	0.46	0.09	427.00	0.12	0.20	26.70	2.76	9.80	0.50	1.79	11.30
std. dev.	1.96	0.09	517.86	0.18	2.58	19.43	2.16	13.41	1.16	13.02	258.96
Underground											
mean	2.87	0.30	972.20	2.21	1.04	39.16	4.59	16.31	-------	-------	167.23
median	0.64	0.20	417.00	2.00	0.50	30.00	1.00	12.00	-------	-------	92.00
std. dev.	3.81	0.44	1660.00	1.33	1.43	70.17	6.69	21.99	-------	-------	280.05

Table 3: Comparisons of means, medians, and standard deviations between the open pit and the underground.

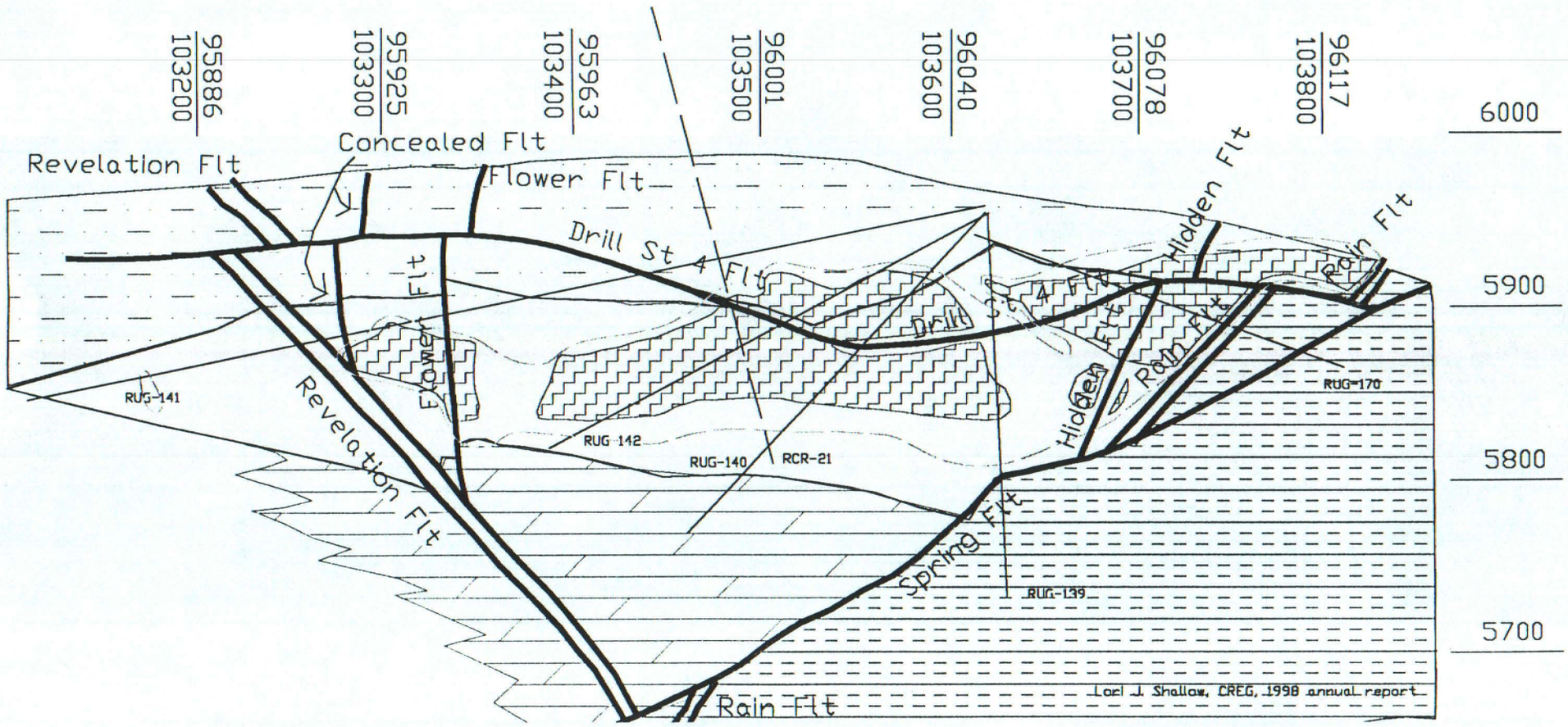

Figure 13a: Gold shapes from the geochemical samples of 1998.

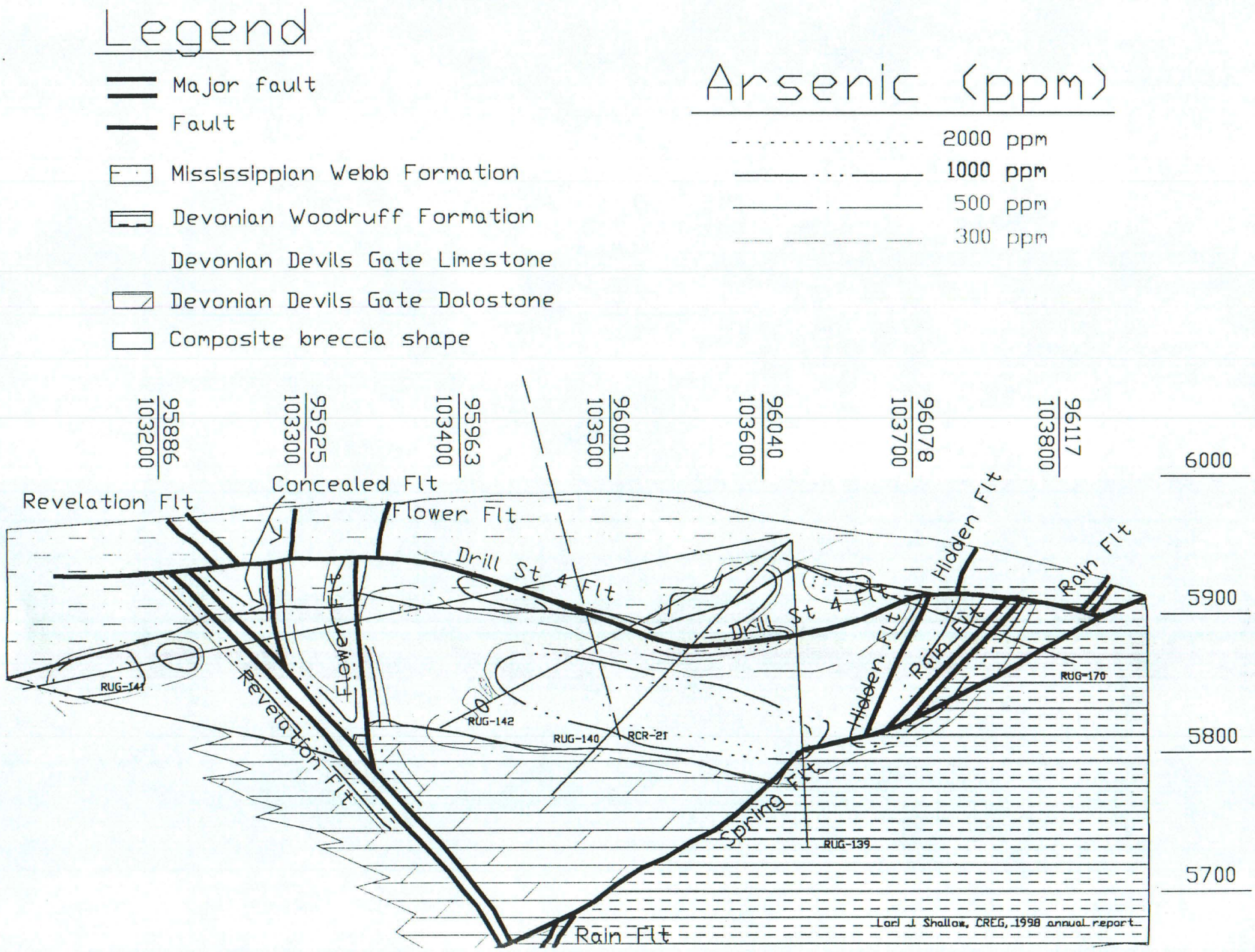

Figure 13b: As contours from the geochemical samples of 1998.

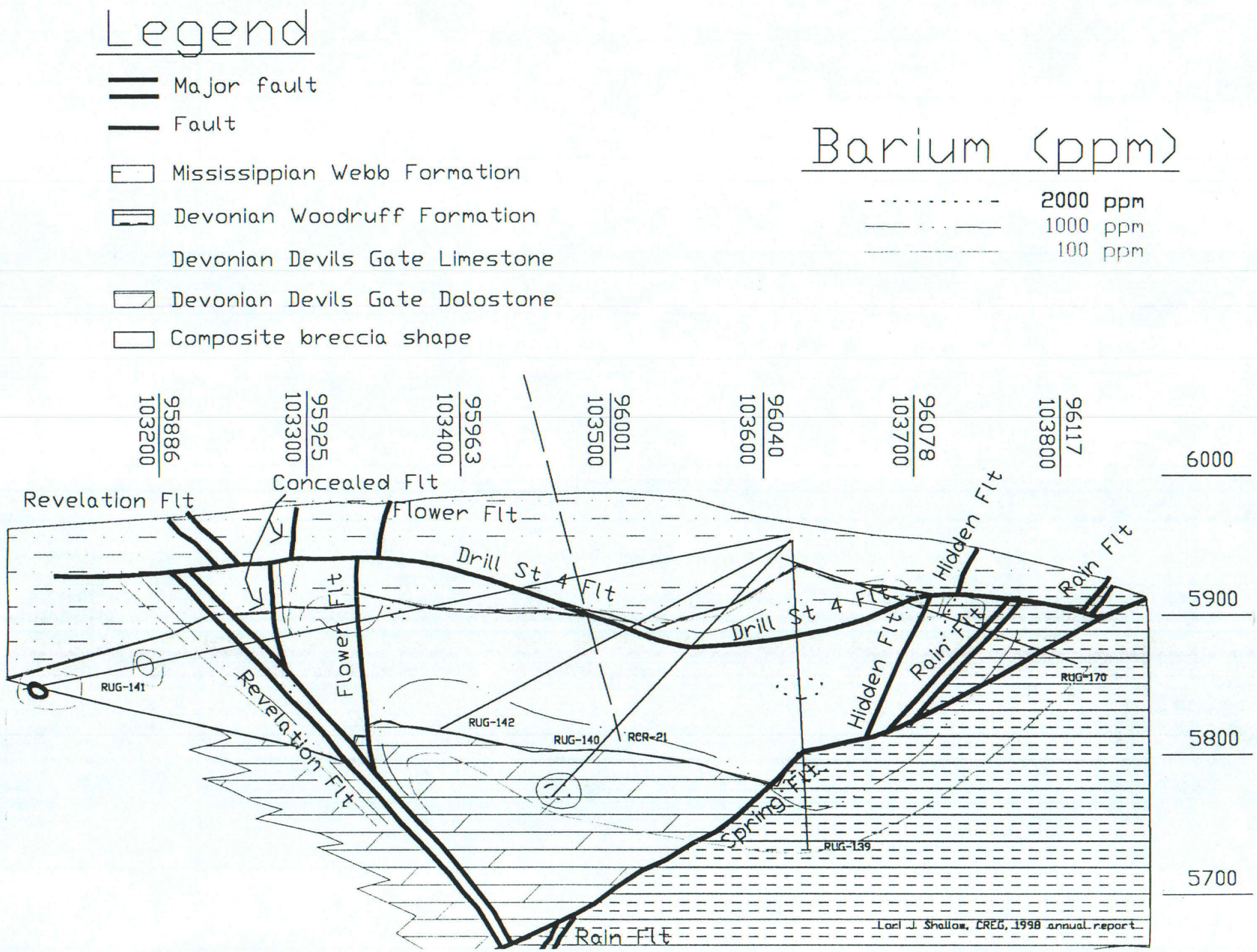

Figure 13c: Ba contours from the geochemical samples of 1998.

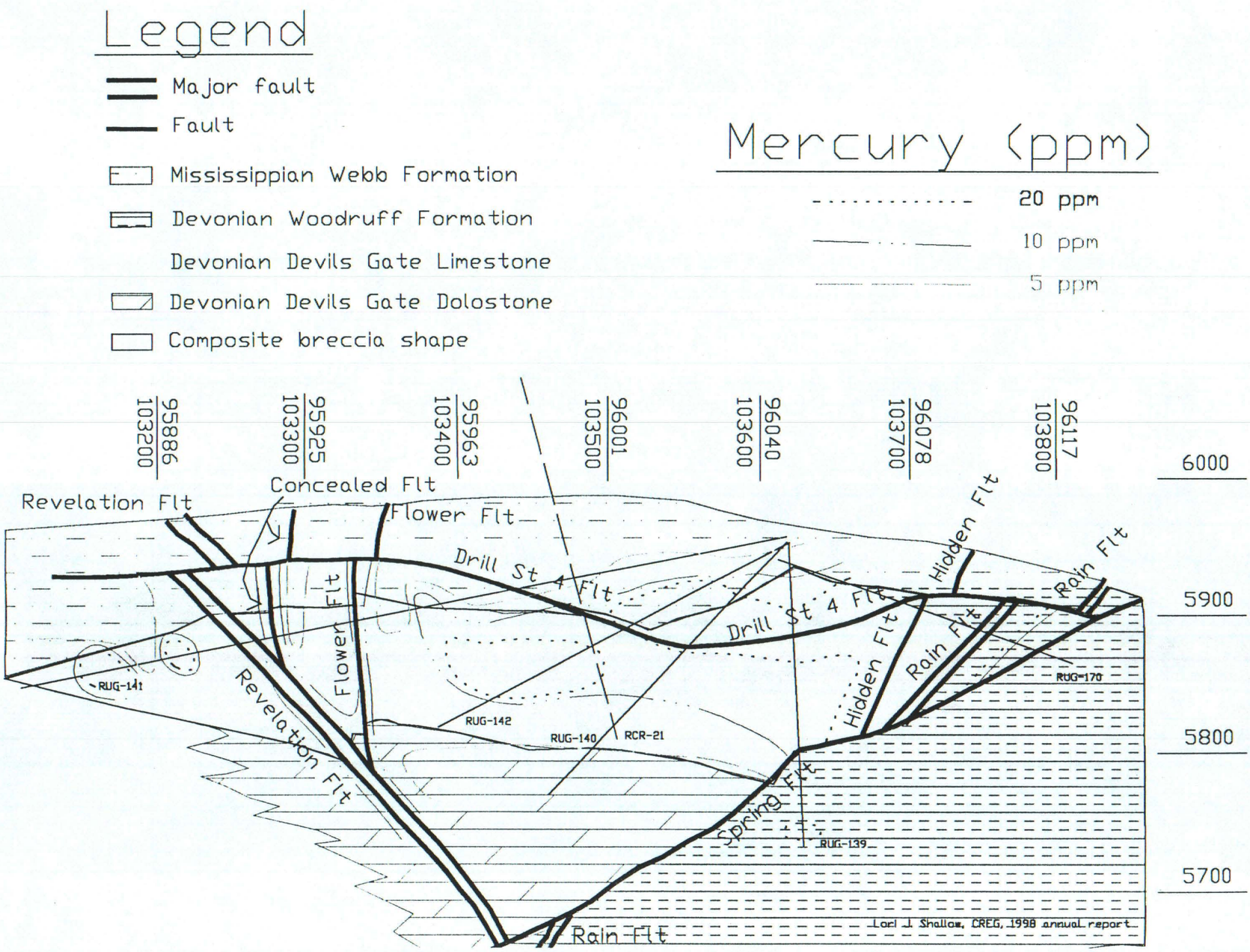

Figure 13d: Hg contours from the geochemical samples of 1998.

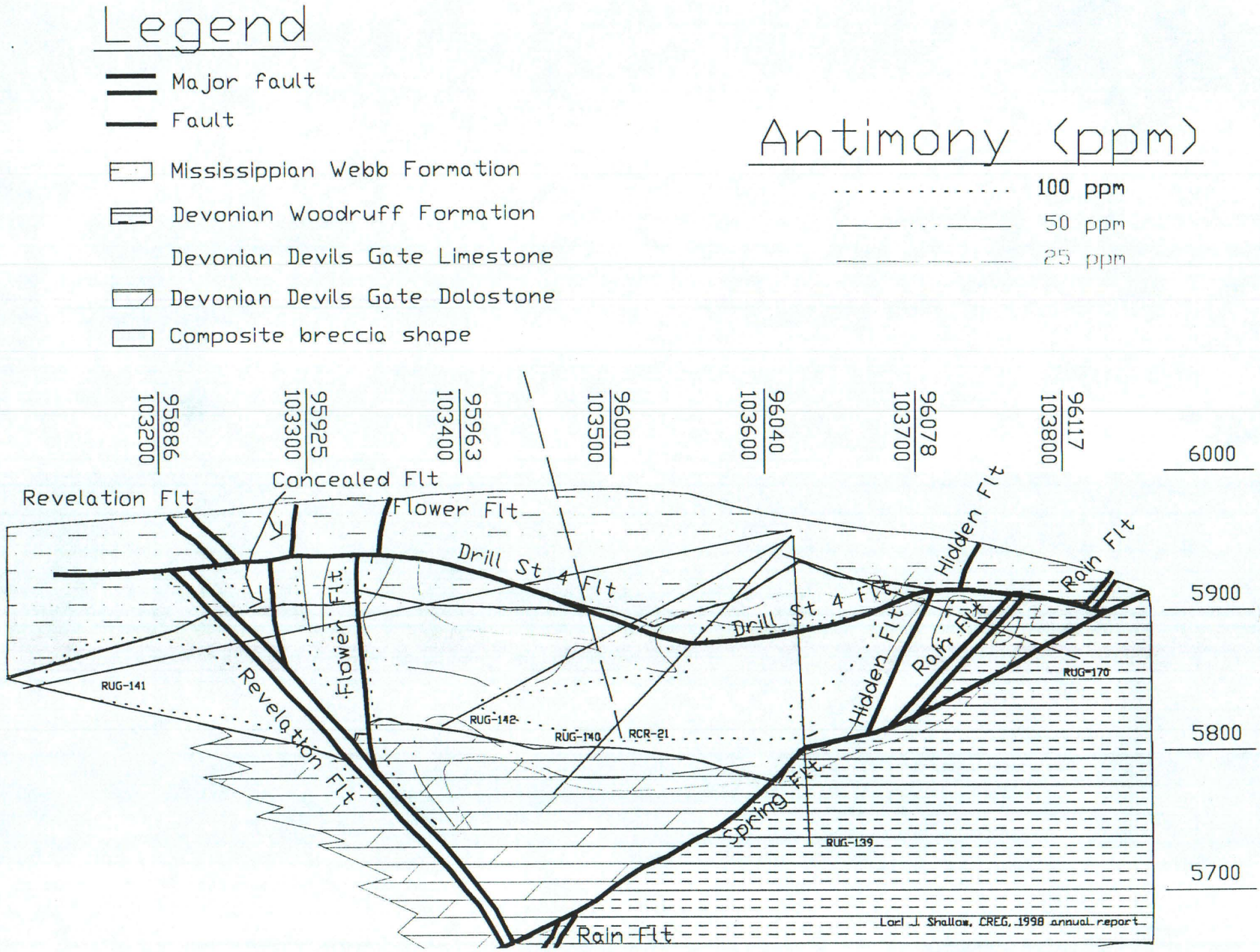

Figure 13e: Sb contours from the geochemical samples of 1998.

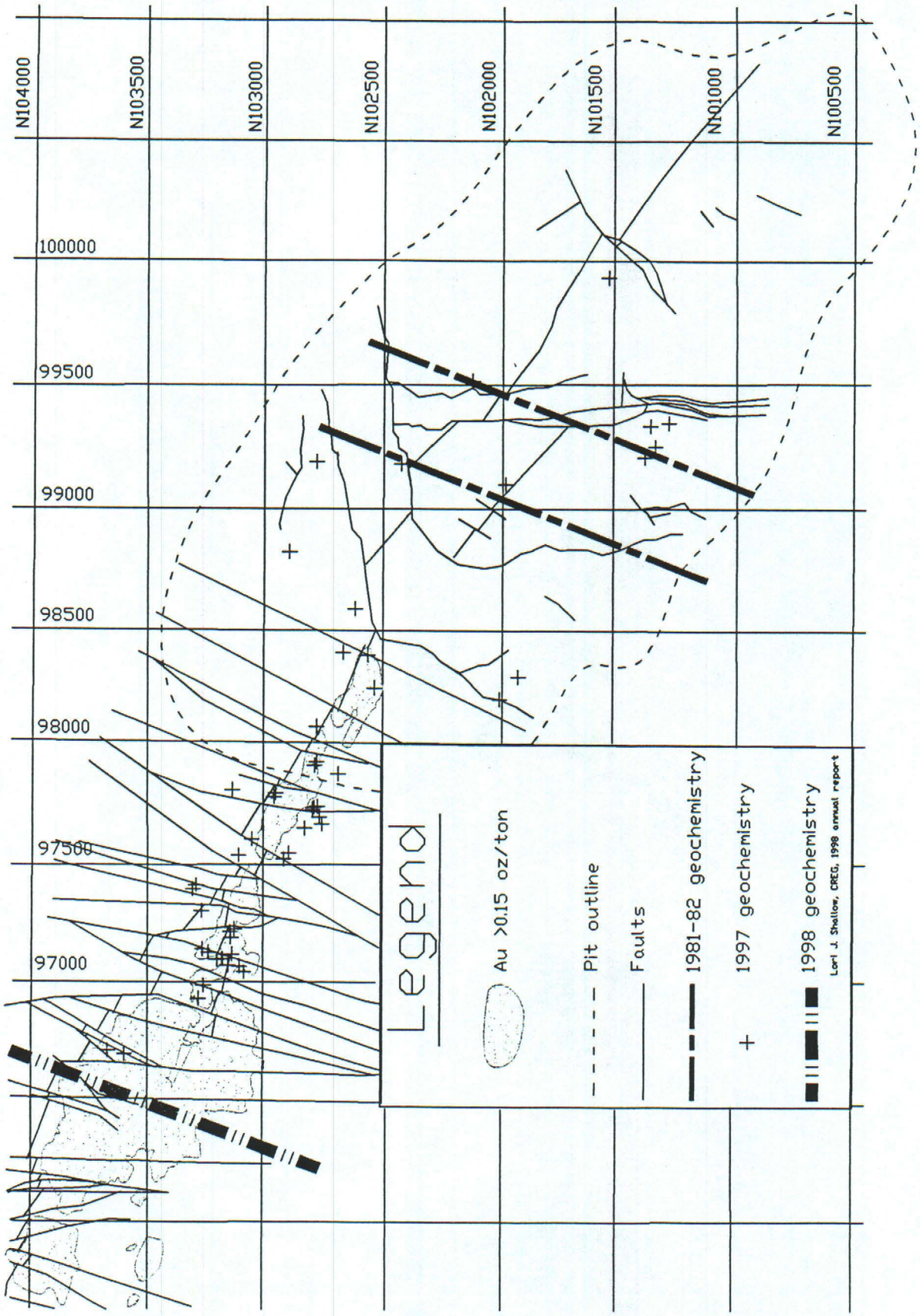

Figure 14a: Gold shapes from Newmont Gold Company (September, 1998).

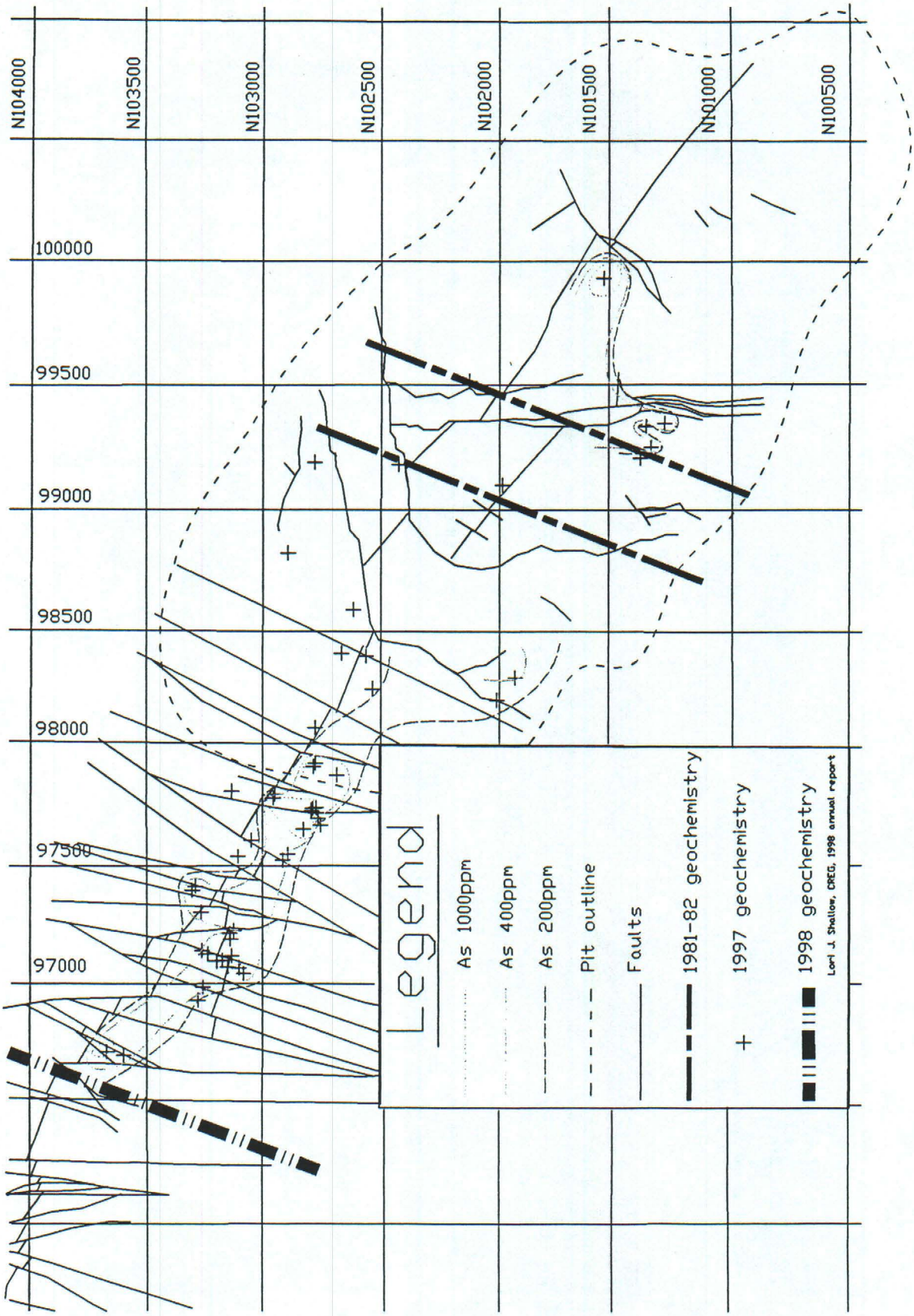

Figure 14b: As contours from the geochemical samples of 1997.

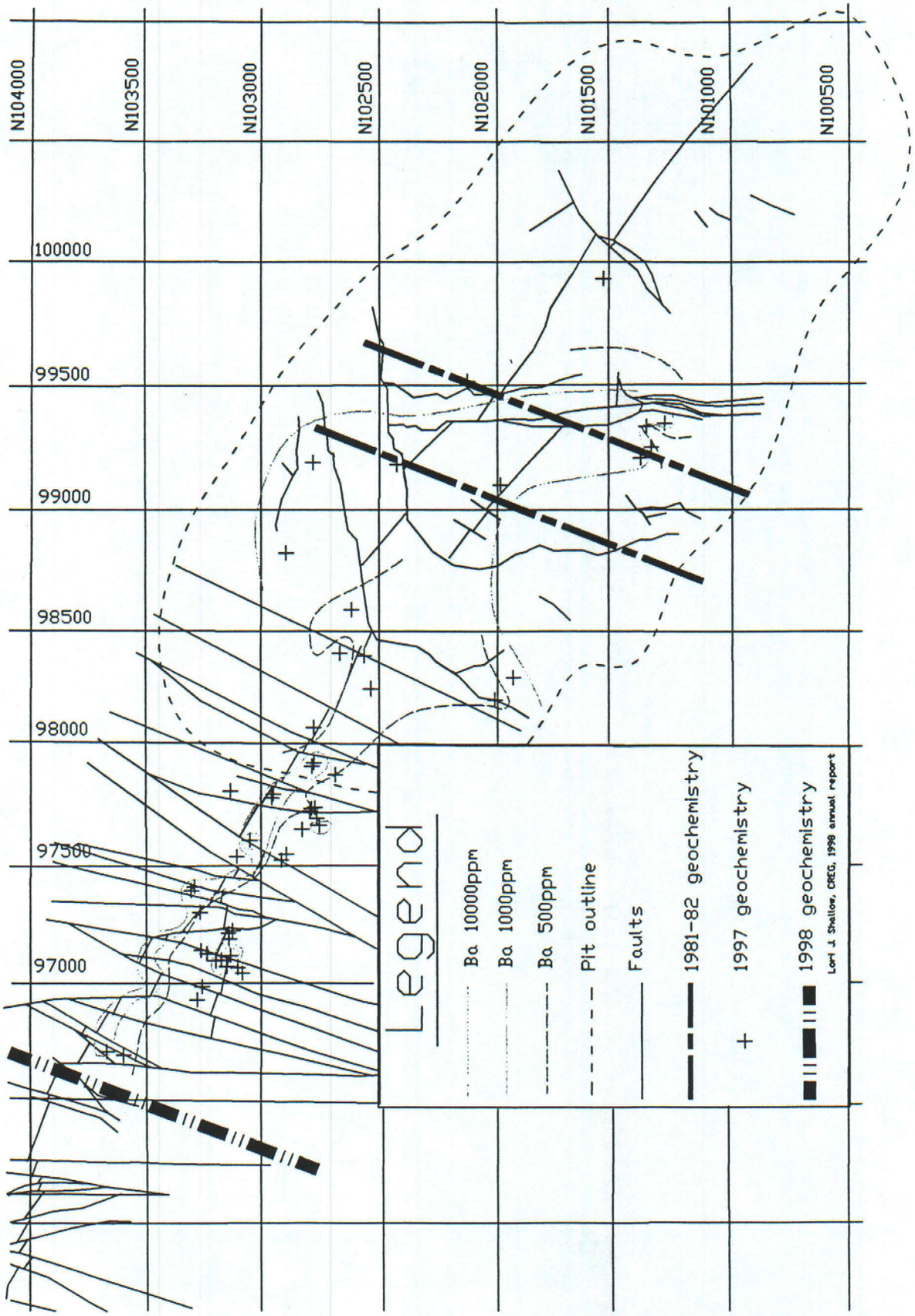

Figure 14c: Ba contours from the geochemical samples of 1997.

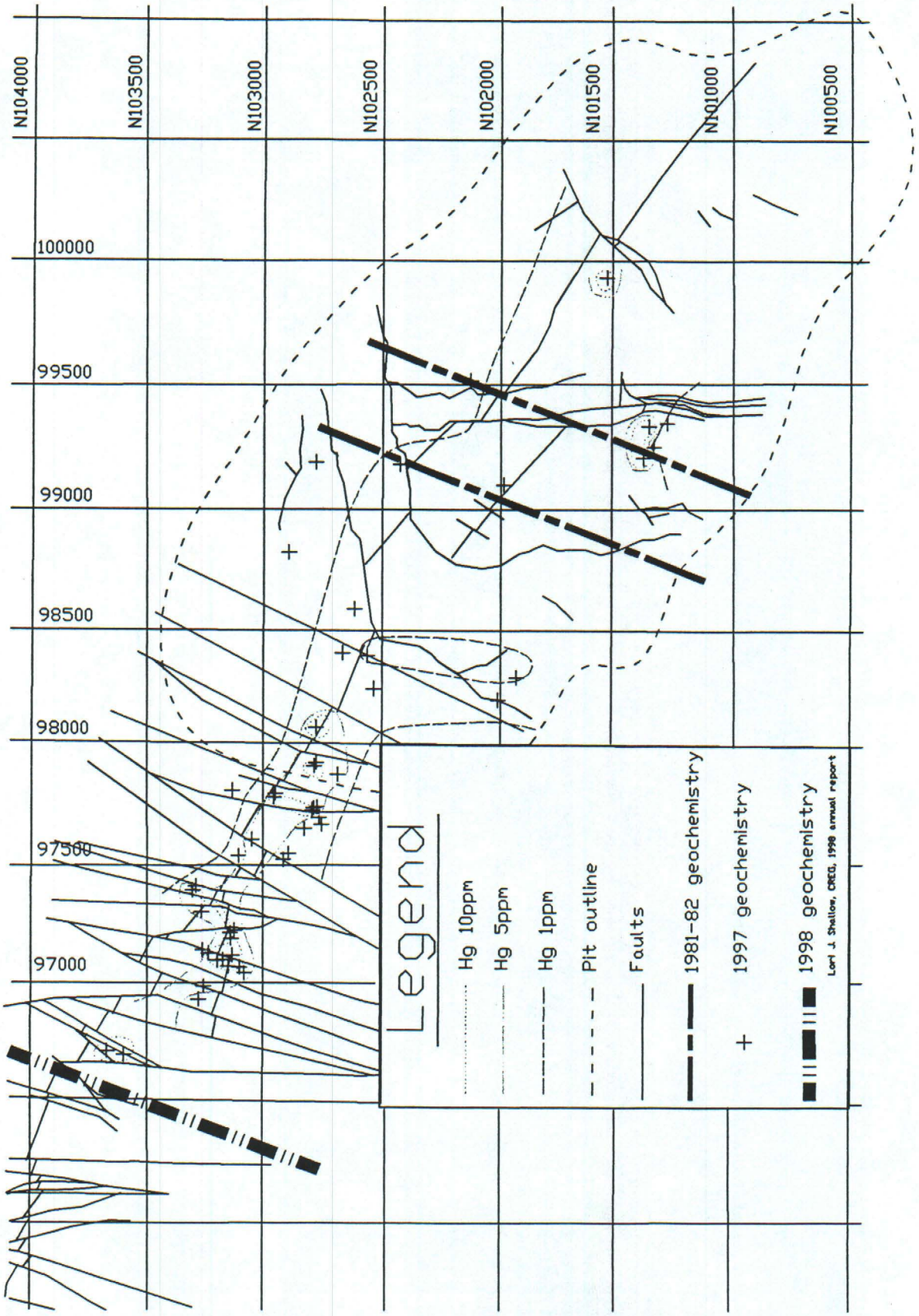

Figure 14d: Hg contours from the geochemical samples of 1997.

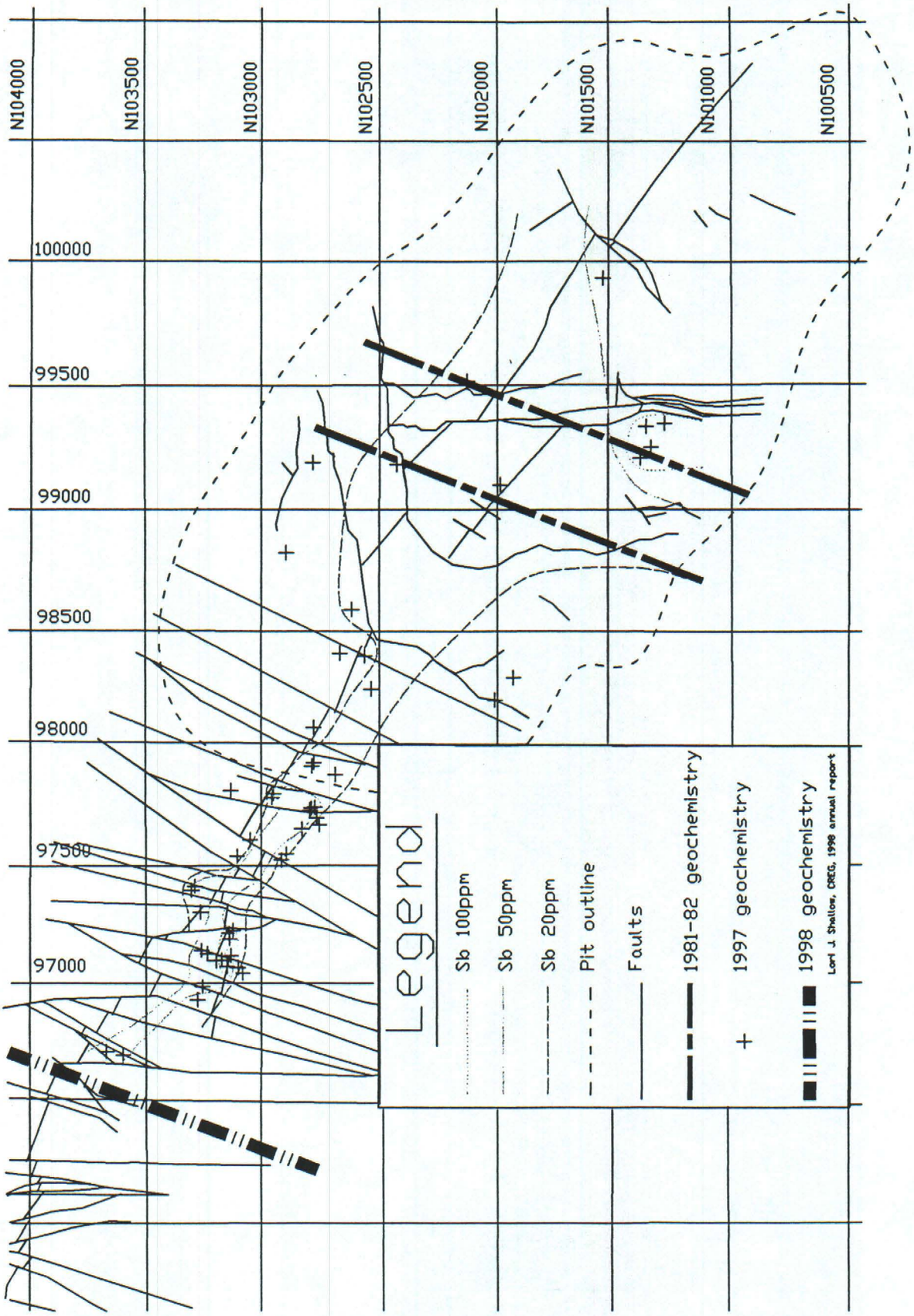

Figure 14e: Sb contours from the geochemical samples of 1997.

correlation only with cobalt. In both sets of data, antimony shows no positive correlation with any other elements.

Because the matrices from tables 4 a and b are composed from all of the units within the mine, it is likely that important mineral associations in the orebody are being masked by the other units present in the data sets. For this reason, a correlation matrix was constructed from the data collected in 1998 of the hydrothermal breccias only (Table 4c). In the hydrothermal breccia, gold shows a weak correlation with both arsenic and mercury. In addition, arsenic is weakly correlative with antimony and vanadium. Other correlative elements may reflect the supergene oxidizing fluids.

Conclusions

The Rain mine contains a complicated and distinctive orebody. Alteration types include dolomitization of the Devils Gate Limestone beneath the orebody, silicification of the host rocks and hydrothermal breccias, quartz-pyrite-barite-sphalerite veining adjacent to the orebody, and oxidation of the orebody. Gold, arsenic, antimony, mercury, and barium concentrations are elevated in the orebody and along the Rain and Rain-parallel faults. Increasing averages of gold and arsenic in the underground relative to the open pit and larger areas of gold, arsenic, antimony, and mercury concentrations where positive flower structures have developed indicate a strengthening system to the northwest. Oxide and refractory breccias are very similar with respect to both geochemistry and alteration.

Field relations indicate that the source of oxidizing fluids is supergene. In the oxide portion of the orebody, refractory pods are commonly associated with impermeable tuffisites. In the refractory portion of the orebody, oxide breccias occur most commonly adjacent to faults.

Acknowledgments

Field and analytical expenses were paid by the Ralph J. Roberts Center for Research in Economic Geology. I would also like to express appreciation to Newmont Gold Company for funding geochemical studies and for supporting other research at the Rain mine. Special thanks should go to John Read, Cindy Williams, Bruce Harlan, Warren Dunbar, and Jon Powell for their valuable input of ideas and materials. Thanks is also given Roger Metz and his crew at Maggie Creek Core Complex for preparing all of my geochemical samples and retrieving numerous boxes of core and bags of chips over the last two summers. I am grateful to the USGS for use of a trailer for the past summer and use of a truck on several occasions. Appreciation shall also be given to Kinross

	Au	Ag	Al	As	Ba	Be	Ca	Cd	Co	Cr	Cu	Fe	Hg	K	Mg	Mn	Mo	Ni	P	Pb	Sb	Sr	Tl	V	W
Au	1																								
Ag	-0.1	1																							
Al	-0.4	0.24	1																						
As	0.16	-0.07	0.22	1																					
Ba	0.1	0.16	-0.12	-0.03	1																				
Be	-0.1	0.67	0.5	-0.05	0.27	1																			
Ca	-0.2	0.05	-0.16	-0.06	0.22	0.06	1																		
Cd	-0	0.34	0.17	0.17	0.08	0.13	0.04	1																	
Co	-0.1	-0.08	0.49	0.67	-0.37	0	-0.13	0.05	1																
Cr	0.22	0.32	-0.07	-0.02	0.36	0.29	-0.26	0.18	-0.17	1															
Cu	-0.4	0.25	0.58	0.11	-0.49	0.26	-0.24	0.01	0.45	-0.2	1														
Fe	0.31	-0.14	0	0.39	-0.07	-0.11	-0.11	0.12	0.08	-0.1	-0.09	1													
Hg	0.24	0.06	0.1	0.61	-0.07	-0.05	-0.05	0.11	0.53	0.06	0.06	0.21	1												
K	-0.5	-0.17	0.54	-0.2	-0.56	-0.06	-0.22	-0.16	0.2	-0.5	0.6	-0.14	-0.2	1											
Mg	-0.1	-0.07	-0.18	-0.07	0.17	-0.04	0.79	-0.03	-0.08	-0.2	-0.24	-0.06	-0.05	-0.17	1										
Mn	-0.2	-0.05	0.04	-0.01	0.27	0.07	0.68	0.04	0.04	-0.2	-0.23	0.04	-0.08	-0.16	0.59	1									
Mo	0.26	0.48	-0.19	0.06	0.13	0.2	-0.11	0.24	-0.13	0.52	-0.11	0.09	0.09	-0.42	-0.15	-0.15	1								
Ni	-0.2	0.33	0.46	0.53	-0.07	0.21	-0.06	0.48	0.59	0.07	0.31	0.23	0.23	0.03	-0.06	0.05	0.25	1							
P	-0.2	0.66	0.57	0.18	0.18	0.62	0.08	0.5	0.08	0.2	0.2	0.07	0.13	-0.04	-0.06	0.13	0.29	0.44	1						
Pb	0.07	-0.13	-0.1	0.11	0.2	-0.1	-0.1	0.21	0.02	0.2	-0.15	0.1	0.07	-0.26	-0.06	0.02	0.04	0.14	-0.04	1					
Sb	0.16	-0.06	-0.08	0.36	0.34	-0.07	0.16	0.24	-0.16	0.16	-0.41	0.48	0.11	-0.38	0.13	0.28	0.17	0.22	0.27	0.22	1				
Sr	-0.1	0.6	0.58	0.05	0.4	0.85	0.14	0.31	0.05	0.33	0.14	-0.06	0.05	-0.13	0.02	0.18	0.2	0.29	0.7	-0.1	0.09	1			
Tl	0.08	-0.06	0.02	0.28	-0.16	-0.04	0.11	0.01	0.14	-0.1	-0.03	0.04	0.24	-0.01	0.02	0.11	-0.03	0.03	0.21	0	0.2	-0.05	1		
V	-0.2	0.81	0.42	0	0.15	0.61	-0.05	0.41	-0.01	0.34	0.31	-0.03	0.01	-0.02	-0.14	-0.07	0.47	0.44	0.68	-0.1	0.02	0.66	-0.1	1	
W	0.12	0.03	0.01	0.09	0.04	-0.02	-0.04	0	-0.06	0.2	-0.09	0.19	-0.03	-0.15	-0.03	-0.03	0.1	0.12	-0.03	0.12	0.4	-0.01	-0.04	-0.02	1
Zn	-0.1	0.33	0.54	0.18	0.28	0.52	0.16	0.57	0.23	0.19	0.05	0.12	0.01	-0.14	0.12	0.38	0.13	0.59	0.62	0.22	0.3	0.74	0.03	0.44	0.08

Table 4a: Correlation matrix for the geochemistry from 1998. Elements with little or no variation are excluded.

	AU	*AS*	*SB*	*HG*	*AG*	*AL*	*BA*	*BE*	*BI*	*CA*	*CD*	*CO*	*CR*	*CU*	*FE*	*K*	*MG*	*MN*	*MO*	*NA*	*NI*	*P*	*PB*	*SR*	*TI*	*V*	*W*	*ZN*
AU	1.00																											
AS	0.09	1.00																										
SB	0.03	0.07	1.00																									
HG	0.12	0.22	0.28	1.00																								
AG	-0.20	0.02	-0.23	-0.18	1.00																							
AL	-0.24	0.36	-0.15	-0.11	-0.05	1.00																						
BA	0.01	-0.09	-0.14	0.12	0.05	-0.30	1.00																					
BE	-0.32	-0.25	0.14	-0.27	0.25	0.23	-0.26	1.00																				
BI	0.19	0.46	-0.11	0.00	0.19	0.46	-0.01	-0.08	1.00																			
CA	-0.10	-0.10	0.19	-0.11	0.00	-0.24	-0.07	-0.10	-0.05	1.00																		
CD	-0.06	-0.17	-0.06	0.05	0.33	-0.40	0.62	-0.07	-0.11	0.12	1.00																	
CO	-0.11	**0.65**	-0.08	0.04	0.07	**0.72**	-0.10	-0.03	**0.60**	-0.08	-0.13	1.00																
CR	-0.12	0.35	-0.18	-0.08	0.47	0.44	-0.08	0.10	0.33	-0.28	-0.21	**0.53**	1.00															
CU	-0.17	-0.04	-0.17	-0.11	-0.01	0.37	-0.15	0.06	0.00	-0.10	-0.09	0.24	0.09	1.00														
FE	-0.04	0.47	0.29	0.20	-0.17	0.49	-0.33	0.20	0.28	-0.28	-0.42	**0.54**	0.38	0.16	1.00													
K	-0.20	-0.08	-0.13	-0.16	-0.23	**0.81**	-0.43	0.34	0.17	-0.23	-0.42	0.36	0.12	0.44	0.35	1.00												
MG	-0.11	-0.10	0.02	-0.12	-0.09	-0.16	-0.08	-0.11	-0.04	**0.81**	-0.04	-0.05	-0.29	-0.05	-0.22	-0.13	1.00											
MN	-0.11	-0.14	0.16	-0.14	0.07	-0.23	-0.11	-0.03	-0.08	**0.88**	0.17	-0.05	-0.19	-0.08	-0.26	-0.22	0.86	1.00										
MO	-0.12	-0.13	0.03	0.07	0.44	-0.35	0.17	0.08	-0.12	-0.01	0.37	-0.16	0.26	-0.11	-0.19	-0.40	-0.13	0.13	1.00									
NA	-0.24	-0.16	-0.27	-0.28	-0.10	**0.70**	-0.40	0.43	0.10	-0.25	-0.38	0.18	0.02	0.46	0.18	**0.85**	-0.12	-0.23	-0.33	1.00								
NI	-0.10	0.35	0.03	0.13	0.19	0.43	-0.25	0.23	0.26	-0.03	0.08	**0.72**	0.37	0.12	0.36	0.22	-0.06	0.10	0.10	0.15	1.00							
P	-0.14	-0.13	0.11	-0.12	**0.67**	-0.21	0.04	0.34	-0.07	-0.06	0.20	-0.14	**0.50**	-0.11	-0.09	-0.31	-0.19	-0.01	**0.62**	-0.28	0.01	1.00						
PB	-0.39	0.03	-0.20	-0.24	0.15	0.43	-0.22	0.43	-0.17	-0.10	-0.20	-0.01	0.19	0.23	0.00	0.42	-0.11	-0.13	-0.08	**0.52**	-0.04	0.08	1.00					
SR	-0.18	0.14	0.01	-0.20	0.24	0.03	-0.01	0.14	0.16	0.00	-0.20	0.05	0.48	-0.10	0.14	-0.09	0.07	0.03	0.00	-0.11	-0.16	0.46	0.14	1.00				
TI	-0.21	0.47	-0.17	-0.04	-0.08	**0.91**	-0.17	0.00	0.45	-0.19	-0.32	**0.80**	**0.51**	0.32	**0.52**	**0.68**	-0.11	-0.19	-0.33	0.43	0.42	-0.22	0.26	0.06	1.00			
V	-0.39	-0.07	-0.21	-0.15	0.38	0.27	-0.01	0.41	0.00	-0.22	0.01	0.09	0.44	0.13	0.03	0.20	-0.22	-0.19	0.52	0.29	0.15	0.40	0.46	0.13	0.15	1.00		
W	-0.04	0.37	-0.05	0.06	-0.01	**0.55**	0.05	-0.19	0.39	-0.05	-0.10	**0.70**	**0.54**	0.07	0.44	0.36	-0.03	-0.04	-0.12	-0.03	0.35	0.00	-0.09	0.15	**0.78**	0.05	1.00	
ZN	-0.15	-0.09	-0.02	-0.12	0.11	0.05	-0.17	0.31	-0.04	0.04	0.23	0.26	0.05	0.07	-0.03	0.08	0.02	0.20	0.24	0.13	**0.69**	0.10	-0.06	-0.17	-0.03	0.18	-0.07	1.00

Table 4b: Correlation matrix for the geochemistry from 1997.

	Au	*Ag*	*Al*	*As*	*Ba*	*Ca*	*Cd*	*Co*	*Cr*	*Cu*	*Fe*	*Hg*	*K*	*Mg*	*Mn*	*Mo*	*Ni*	*P*	*Pb*	*Sb*	*Sc*	*Sr*	*Tl*	*V*	*W*	*Zn*
Au	1																									
Ag	0.27	1																								
Al	-0.33	-0.22	1																							
As	**0.50**	0.22	0.19	1																						
Ba	-0.14	-0.11	-0.15	0.10	1																					
Ca	-0.07	-0.18	0.20	0.06	0.01	1																				
Cd	-0.02	-0.03	-0.10	-0.09	-0.27	0.03	1																			
Co	0.13	0.20	0.14	0.33	-0.48	0.11	0.08	1																		
Cr	0.39	0.06	-0.55	0.10	0.25	0.20	-0.03	-0.17	1																	
Cu	-0.36	-0.08	0.30	-0.17	-0.45	-0.09	0.25	0.42	-0.61	1																
Fe	0.26	0.14	0.11	0.49	-0.06	0.00	-0.09	-0.03	0.17	-0.03	1															
Hg	**0.50**	**0.60**	-0.27	0.31	-0.28	-0.15	0.33	0.30	0.08	0.04	-0.04	1														
K	-0.51	-0.24	**0.86**	-0.13	-0.26	0.02	-0.02	0.03	-0.55	0.43	-0.04	-0.37	1													
Mg	-0.24	-0.22	0.37	-0.09	0.20	**0.57**	-0.12	0.00	-0.07	0.05	0.06	-0.36	0.21	1												
Mn	-0.30	-0.11	0.41	0.04	-0.12	0.38	-0.05	0.27	-0.23	0.35	0.13	-0.22	0.35	0.58	1											
Mo	0.41	0.20	-0.31	0.17	-0.19	0.10	-0.09	0.18	**0.50**	-0.16	0.15	0.17	-0.30	-0.25	-0.14	1										
Ni	0.21	0.27	0.01	0.63	0.07	0.26	0.01	0.45	0.24	-0.06	0.32	0.33	-0.24	0.02	0.17	0.29	1									
P	-0.04	-0.13	**0.68**	0.22	-0.15	0.60	-0.03	0.01	-0.02	-0.18	0.21	-0.18	0.46	0.36	0.31	-0.02	0.12	1								
Pb	-0.05	-0.10	-0.24	0.06	0.10	0.31	0.27	-0.05	0.29	0.03	0.10	0.21	-0.23	0.18	-0.06	-0.02	0.20	-0.10	1							
Sb	0.28	0.06	-0.01	**0.54**	0.14	0.04	-0.15	-0.16	0.38	-0.32	**0.74**	0.00	-0.20	0.00	-0.05	0.17	0.43	0.21	0.12	1						
Sc	-0.30	-0.09	0.37	-0.04	-0.17	0.24	-0.08	0.25	-0.30	0.40	0.02	-0.19	0.38	0.49	0.96	-0.18	0.03	0.19	-0.12	-0.14	1					
Sr	-0.01	-0.01	**0.50**	0.40	0.18	0.33	0.18	-0.03	0.01	-0.19	0.23	0.00	0.21	0.38	0.14	-0.08	0.40	**0.60**	-0.01	0.24	-0.04	1				
Tl	0.16	0.13	-0.12	0.04	-0.20	0.33	-0.02	0.36	0.17	0.09	-0.12	0.12	-0.14	-0.17	-0.08	0.44	0.24	0.16	-0.11	-0.07	-0.07	-0.08	1			
V	0.16	0.10	0.45	**0.68**	0.05	0.10	0.00	0.11	-0.13	-0.04	**0.61**	0.09	0.15	0.03	0.13	0.09	0.47	0.47	-0.04	0.35	-0.01	**0.65**	0.02	1		
W	0.22	-0.07	-0.07	0.27	-0.05	-0.04	-0.06	-0.10	0.29	-0.10	**0.52**	-0.11	-0.13	0.04	-0.01	0.15	0.04	0.01	0.08	**0.77**	-0.04	-0.05	-0.05	-0.02	1	
Zn	0.02	0.11	0.06	0.39	-0.01	0.33	0.57	0.20	0.16	0.04	0.31	0.28	-0.13	0.15	0.27	0.00	0.61	0.23	0.33	0.30	0.07	0.61	-0.09	0.43	0.13	1

Table 4c: Correlation matrix for hydrothermal breccias only from 1998 geochemistry.

Gold for allowing the trailer to remain parked at their Lamoille office and for use of the facilities in the office.

References Cited

Putnam, Borden R. III and Henriques, Edmund Q.B., 1990, Geology and mineralization at the South Bullion Deposit, Pinon Range, Elko County, Nevada: *in* G.L. Raines, R.E. Lisle, R.W. Schafer, and W.H. Wilkinson, eds., Geology and Ore Deposits of the Great Basin: Geological Society of Nevada, Symposium Proceedings, Reno, pp. 713-728.

Williams, C.L., 1992, Breccia bodies of the Carlin Trend, Elko and Eureka Counties, Nevada: Classification, interpretation, and roles in ore formation: Colorado State University, unpublished M.S. thesis, 213 p.

APPENDIX 1

Modal Analyses of Arsenian Pyrite/Marcasite

Appendix 1

[A N A L Y S I S R E P O R T]
(For figure 6a)

GENERAL CONDITIONS

Result File : LORI1
File Version : 1
Background Method : Auto
Decon Method : Gaussian
Decon ChiSquared : 38.67
Analysis Date : 7-DEC-98
Microscope : SEM
Comments :

ANALYSIS CONDITIONS

Quant. Method : XPP
Calibration File : 0:LORI.1.0
Calibration Standards:
FESSTAN.1.0 S , Fe
GASTAN.1.0 Ga, As
SSTAN.1.0 S , Fe, Cu
Acquire Time : 60 secs
Normalization Factor: 100.00

SAMPLE CONDITIONS
---

kV : 15.0
Beam Current : 868.0 picoAmps
Working Distance : 25.0 mm
Tilt Angle : 0.0 Degrees
TakeOff Angle : 35.0 Degrees
Solid Angle*BeamCurrent: 6.9

Element	Line	Weight%	Cmpt	CmptWT%	Cnts/s	Atomic%
S	Ka	**47.11**	S	47.11	881.79	**61.97**
Fe	Ka	**42.96**	Fe	42.96	220.19	**32.45**
As	La	**9.93**	As	9.93	63.65	**5.59**

Appendix 1

[ANALYSIS REPORT]
(For figure 7)

GENERAL CONDITIONS

Result File : RCR25RM1
File Version : 1
Background Method : Auto
Decon Method : Gaussian
Decon ChiSquared : 8.54
Analysis Date : 17-APR-98
Microscope : SEM
Comments :

ANALYSIS CONDITIONS

Quant. Method : XPP
Calibration File : 0:JKM.42.0
Calibration Standards:

ALOSTAN.1.0	O , Al
ALSTAN.1.0	O , Mg, Al
BIOSTAN.1.0	O , Mg, Al, Si, K , Ti, Fe
CA2STAN.1.0	O , S , Ca
CASTAN.1.0	O , Si, Ca
COSTAN.1.0	Co
CRALMGSTAN.1.0	O , Mg, Al, Cr, Fe
CUSTAN.1.0	Cu
FEOSTAN.1.0	O , Fe
FESSTAN.1.0	S , Fe
GASTAN.1.0	Ga, As
KSTAN.1.0	O , Na, Al, Si, K , Fe
KSTAN.1.0	O , Na, Al, Si, K , Fe
MG1STAN.1.0	O , Mg, Si, Fe
MGOSTAN.1.0	O , Mg
MGSISTAN.1.0	O , Mg, Si, Ca
MNALSTAN.1.0	O , Al, Si, Mn, Fe
NAALSTAN.1.0	O , Na, Al, Si, Ca
SIALSTAN.1.0	O , Al, Si
TISTAN.1.0	O , Ti
W2STAN.1.0	O , Ca, W
WSTAN.1.0	W

Acquire Time : 60 secs
Normalization Factor: 100.00

SAMPLE CONDITIONS

kV : 15.0
Beam Current : 698.0 picoAmps
Working Distance : 37.0 mm
Tilt Angle : 0.0 Degrees
TakeOff Angle : 38.6 Degrees
Solid Angle*BeamCurrent: 2.0

Element	Line	Weight%	Cnts/s	Atomic%
S	Ka	**52.17**	843.02	**65.63**
Fe	Ka	**46.86**	192.45	**33.85**
As	La	**0.97**	5.24	**0.52**

Appendix 1

[A N A L Y S I S R E P O R T]
(For figure 8)

GENERAL CONDITIONS

Result File : RCR25BRM
File Version : 1
Background Method : Auto
Decon Method : Gaussian
Decon ChiSquared : 12.20
Analysis Date : 28-APR-98
Microscope : SEM
Comments :

ANALYSIS CONDITIONS

Quant. Method : XPP
Calibration File : 0:JKM.38.0
Calibration Standards:
AGSTAN.1.0 S , Ag
CDSTAN.1.0 S , Cd
FESSTAN.1.0 S , Fe
GASTAN.1.0 Ga, As
SSTAN.1.0 S , Fe, Cu
ZNSTAN.1.0 S , Zn
Acquire Time : 60 secs
Normalization Factor: 100.00

SAMPLE CONDITIONS
---

kV : 15.0
Beam Current : 721.0 picoAmps
Working Distance : 37.0 mm
Tilt Angle : 0.0 Degrees
TakeOff Angle : 38.6 Degrees
Solid Angle*BeamCurrent: 2.1

Element	Line	Weight%	Cnts/s	Atomic%
S	Ka	**52.49**	867.91	**66.02**
Fe	Ka	**45.74**	197.07	**33.03**
As	La	**1.77**	9.91	**0.95**

APPENDIX 2

Geochemical Data

Appendix 2-A

Hole_Id	From	To	AUFA	GC-AU	GC-AG	GC-AS	GC-BI	GC-CD	GC-CU	GC-HG
RAN-R-115	0	20		0.03	0.08	456	0.12	0.14	36.1	4.29
RAN-R-115	20	40		0.01	0.12	310	0.12	0.05	24.2	0.89
RAN-R-115	40	60		0.01	0.15	382	0.12	0.05	24.4	1.01
RAN-R-115	60	80		0.01	0.21	351	0.12	0.1	27.8	2.01
RAN-R-115	80	100		0.01	0.29	257	0.12	0.05	35.8	3.75
RAN-R-115	100	120		0.01	0.36	307	0.12	0.05	35.7	3.04
RAN-R-115	120	140		0.01	0.24	498	0.12	0.05	58.7	3.5
RAN-R-115	140	160		0.01	0.14	222	0.12	0.05	56.1	2.98
RAN-R-115	160	180		0.04	0.09	497	0.12	0.13	37.5	3.38
RAN-R-115	180	200		0.04	0.19	235	0.12	0.05	53.8	5.1
RAN-R-115	200	210		1.54	0.27	544	0.12	0.05	48.5	11.8
RAN-R-115	210	215	0.09	1.54	0.27	544	0.12	0.05	48.5	11.8
RAN-R-115	215	220	0.08	1.54	0.27	544	0.12	0.05	48.5	11.8
RAN-R-115	220	225	0.08	2.09	0.25	551	0.12	0.05	38	14.2
RAN-R-115	225	230	0.04	2.09	0.25	551	0.12	0.05	38	14.2
RAN-R-115	230	235	0.05	2.09	0.25	551	0.12	0.05	38	14.2
RAN-R-115	235	240	0.08	2.09	0.25	551	0.12	0.05	38	14.2
RAN-R-115	240	245	0.06	4.05	0.15	881	0.12	0.05	30.3	12.3
RAN-R-115	245	250	0.1	4.05	0.15	881	0.12	0.05	30.3	12.3
RAN-R-115	250	255	0.1	4.05	0.15	881	0.12	0.05	30.3	12.3
RAN-R-115	255	260	0.19	4.05	0.15	881	0.12	0.05	30.3	12.3
RAN-R-115	260	265	0.19	5.93	0.08	405	0.12	0.05	10	1.55
RAN-R-115	265	270	0.16	5.93	0.08	405	0.12	0.05	10	1.55
RAN-R-115	270	275	0.21	5.93	0.08	405	0.12	0.05	10	1.55
RAN-R-115	275	280	0.12	5.93	0.08	405	0.12	0.05	10	1.55
RAN-R-115	280	285	0.48	12.1	0.1	325	0.12	0.1	25.6	1.53
RAN-R-115	285	290	0.51	12.1	0.1	325	0.12	0.1	25.6	1.53
RAN-R-115	290	295	0.17	12.1	0.1	325	0.12	0.1	25.6	1.53
RAN-R-115	295	300	0.18	12.1	0.1	325	0.12	0.1	25.6	1.53
RAN-R-115	300	305	0.19	4.53	0.05	629	0.12	0.19	29.7	9.1
RAN-R-115	305	310	0.17	4.53	0.05	629	0.12	0.19	29.7	9.1
RAN-R-115	310	315	0.16	4.53	0.05	629	0.12	0.19	29.7	9.1
RAN-R-115	315	320	0.09	4.53	0.05	629	0.12	0.19	29.7	9.1
RAN-R-115	320	325	0.18	3.65	0.05	1099	0.12	0.3	26.9	14.6
RAN-R-115	325	330	0.16	3.65	0.05	1099	0.12	0.3	26.9	14.6
RAN-R-115	330	335	0.11	3.65	0.05	1099	0.12	0.3	26.9	14.6
RAN-R-115	335	340	0.03	3.65	0.05	1099	0.12	0.3	26.9	14.6
RAN-R-115	340	345	0.03	1.19	0.04	559	0.12	0.49	21.4	31.5
RAN-R-115	345	350	0.02	1.19	0.04	559	0.12	0.49	21.4	31.5
RAN-R-115	350	355	0.08	1.19	0.04	559	0.12	0.49	21.4	31.5
RAN-R-115	355	360	0.1	1.19	0.04	559	0.12	0.49	21.4	31.5
RAN-R-115	360	365	0.05	3.15	0.08	245	0.12	0.05	24.9	4.33
RAN-R-115	365	370	0.15	3.15	0.08	245	0.12	0.05	24.9	4.33
RAN-R-115	370	375	0.12	3.15	0.08	245	0.12	0.05	24.9	4.33
RAN-R-115	375	380	0.14	3.15	0.08	245	0.12	0.05	24.9	4.33
RAN-R-115	380	385	0.13	4.72	0.28	1553	0.12	1.24	26.9	26.7
RAN-R-115	385	390	0.15	4.72	0.28	1553	0.12	1.24	26.9	26.7
RAN-R-115	390	395	0.18	4.72	0.28	1553	0.12	1.24	26.9	26.7
RAN-R-115	395	400	0.17	4.72	0.28	1553	0.12	1.24	26.9	26.7
RAN-R-115	400	405	0.16	2.49	0.14	150	0.12	21.4	17.4	18.6

Appendix 2-A

Hole_Id	From	To	AUFA	GC-AU	GC-AG	GC-AS	GC-BI	GC-CD	GC-CU	GC-HG
RAN-R-115	405	410	0.12	2.49	0.14	150	0.12	21.4	17.4	18.6
RAN-R-115	410	415	0.06	2.49	0.14	150	0.12	21.4	17.4	18.6
RAN-R-115	415	420	0.05	2.49	0.14	150	0.12	21.4	17.4	18.6
RAN-R-115	420	425	0.04	0.97	0.06	163	0.12	3.69	7.69	12
RAN-R-115	425	430	0.02	0.97	0.06	163	0.12	3.69	7.69	12
RAN-R-115	430	435	0.04	0.97	0.06	163	0.12	3.69	7.69	12
RAN-R-115	435	440		0.97	0.06	163	0.12	3.69	7.69	12
RAN-R-115	440	460		0.08	0.03	74.3	0.12	1.53	3.86	5.92
RAN-R-115	460	465		0.13	0.03	105	0.12	0.75	7.63	6.27
RAN-R-115	465	470	1.00E-03	0.13	0.03	105	0.12	0.75	7.63	6.27
RAN-R-115	470	475	1.00E-03	0.13	0.03	105	0.12	0.75	7.63	6.27
RAN-R-115	475	480	1.00E-03	0.13	0.03	105	0.12	0.75	7.63	6.27
RAN-R-115	480	485	1.00E-03	0.37	0.02	122	0.12	1.29	10.2	6.78
RAN-R-115	485	490	1.00E-03	0.37	0.02	122	0.12	1.29	10.2	6.78
RAN-R-115	490	495	3.00E-03	0.37	0.02	122	0.12	1.29	10.2	6.78
RAN-R-115	495	500	0.01	0.37	0.02	122	0.12	1.29	10.2	6.78
RAN-R-115	500	505	0.01							
RAN-R-115	505	510								
RAN-R-115	510	515	0.01							
RAN-R-125	0	20		0.01	0.15	372	0.12	0.05	38.8	3.08
RAN-R-125	20	40		0.02	0.07	294	0.12	0.05	35.2	19.1
RAN-R-125	40	60		0.01	0.07	281	0.12	0.05	32.9	6.21
RAN-R-125	60	80		0.02	0.05	456	0.12	0.05	32.8	25.7
RAN-R-125	80	100		0.03	0.04	235	0.12	0.05	27.7	33.8
RAN-R-125	100	120		0.02	0.13	243	0.12	0.05	26.5	23.4
RAN-R-125	120	140		0.03	0.26	393	0.12	0.05	66.4	13.6
RAN-R-125	140	160		0.01	0.15	461	0.12	0.05	29.1	15.3
RAN-R-125	160	180		0.02	0.12	367	0.12	0.05	23.8	10.6
RAN-R-125	180	200		0.21	0.09	266	0.12	0.1	41.9	7.34
RAN-R-125	200	220		0.05	0.08	752	0.12	0.05	14.5	100
RAN-R-125	220	240		0.12	0.09	694	0.12	0.05	28.7	10.8
RAN-R-125	240	250		1.64	0.07	1142	0.12	0.3	51.5	24.5
RAN-R-125	250	255	0.04	1.64	0.07	1142	0.12	0.3	51.5	24.5
RAN-R-125	255	260		1.64	0.07	1142	0.12	0.3	51.5	24.5
RAN-R-125	260	275		1.4	0.12	972	0.12	0.88	50.3	25.8
RAN-R-125	275	280	0.02	1.4	0.12	972	0.12	0.88	50.3	25.8
RAN-R-125	280	285	0.05	0.6	0.12	1347	0.12	2.58	48.2	42.2
RAN-R-125	285	300		0.6	0.12	1347	0.12	2.58	48.2	42.2
RAN-R-125	300	310		1.51	0.1	1237	0.12	2.26	46.4	27.3
RAN-R-125	310	315	0.05	1.51	0.1	1237	0.12	2.26	46.4	27.3
RAN-R-125	315	320	0.09	1.51	0.1	1237	0.12	2.26	46.4	27.3
RAN-R-125	320	325	0.06	1.34	0.32	1293	0.12	0.76	23.8	10.4
RAN-R-125	325	330	0.03	1.34	0.32	1293	0.12	0.76	23.8	10.4
RAN-R-125	330	335	0.04	1.34	0.32	1293	0.12	0.76	23.8	10.4
RAN-R-125	335	340	0.05	1.34	0.32	1293	0.12	0.76	23.8	10.4
RAN-R-125	340	345	0.1	2.64	0.07	1495	0.12	0.4	26	40.3
RAN-R-125	345	350	0.05	2.64	0.07	1495	0.12	0.4	26	40.3
RAN-R-125	350	355	0.09	2.64	0.07	1495	0.12	0.4	26	40.3
RAN-R-125	355	360	0.08	2.64	0.07	1495	0.12	0.4	26	40.3
RAN-R-125	360	365	0.07	3.19	0.05	874	0.12	0.13	27.7	15.9

Appendix 2-A

Hole_Id	From	To	AUFA	GC-AU	GC-AG	GC-AS	GC-BI	GC-CD	GC-CU	GC-HG
RAN-R-125	365	370	0.1	3.19	0.05	874	0.12	0.13	27.7	15.9
RAN-R-125	370	375	0.17	3.19	0.05	874	0.12	0.13	27.7	15.9
RAN-R-125	375	380	0.05	3.19	0.05	874	0.12	0.13	27.7	15.9
RAN-R-125	380	385	0.38	5.08	0.05	663	0.12	0.25	25.1	4.59
RAN-R-125	385	390	0.16	5.08	0.05	663	0.12	0.25	25.1	4.59
RAN-R-125	390	395	0.05	5.08	0.05	663	0.12	0.25	25.1	4.59
RAN-R-125	395	400	0.02	5.08	0.05	663	0.12	0.25	25.1	4.59
RAN-R-125	400	405	0.02	0.46	0.03	395	0.12	0.28	13.6	4.92
RAN-R-125	405	415		0.46	0.03	395	0.12	0.28	13.6	4.92
RAN-R-125	415	420	0.02	0.46	0.03	395	0.12	0.28	13.6	4.92
RAN-R-125	420	425	0.02	0.52	0.01	603	0.12	0.47	14.2	7.64
RAN-R-125	425	440		0.52	0.01	603	0.12	0.47	14.2	7.64
RAN-R-125	440	445	0.02	0.79	0.04	523	0.12	0.77	33	7.88
RAN-R-125	445	450	0.02	0.79	0.04	523	0.12	0.77	33	7.88
RAN-R-125	450	455	0.05	0.79	0.04	523	0.12	0.77	33	7.88
RAN-R-125	455	460		0.79	0.04	523	0.12	0.77	33	7.88
RAN-R-125	460	480		0.38	0.02	580	0.12	1.23	35.8	5.98
RAN-R-125	480	500		0.3	0.07	698	0.12	1.64	57.4	9.96
RAN-R-127	0	20		0.03	0.06	462	0.12	0.48	45.3	6.83
RAN-R-127	20	40								
RAN-R-127	40	60		0.02	0.1	521	0.12	0.14	35.2	4.17
RAN-R-127	60	80		0.01	0.1	237	0.12	0.05	38.1	3.76
RAN-R-127	80	100		0.01	0.11	305	0.12	0.11	38	4.73
RAN-R-127	100	120		0.01	0.1	189	0.12	0.05	29.5	5.67
RAN-R-127	120	140		0.03	0.11	228	0.12	0.1	32	4
RAN-R-127	140	160		0.02	0.32	225	0.12	0.1	107	3.92
RAN-R-127	160	180		0.01	0.31	459	0.29	0.11	49.3	6.63
RAN-R-127	180	200		0.02	0.38	470	0.32	0.23	76.8	10.1
RAN-R-127	200	220		0.19	0.23	685	0.28	0.12	47.8	15.4
RAN-R-127	220	235		0.79	0.17	2309	0.12	0.05	31.7	18.4
RAN-R-127	235	240	0.07	0.79	0.17	2309	0.12	0.05	31.7	18.4
RAN-R-127	240	245	0.05	2.64	0.15	2400	0.12	0.25	39.7	15.9
RAN-R-127	245	250	0.07	2.64	0.15	2400	0.12	0.25	39.7	15.9
RAN-R-127	250	255	0.1	2.64	0.15	2400	0.12	0.25	39.7	15.9
RAN-R-127	255	260	0.1	2.64	0.15	2400	0.12	0.25	39.7	15.9
RAN-R-127	260	265	0.06	4.45	0.28	1837	0.12	0.18	31.9	17.5
RAN-R-127	265	270	0.15	4.45	0.28	1837	0.12	0.18	31.9	17.5
RAN-R-127	270	275	0.24	4.45	0.28	1837	0.12	0.18	31.9	17.5
RAN-R-127	275	280	0.11	4.45	0.28	1837	0.12	0.18	31.9	17.5
RAN-R-127	280	285	0.08	1.46	0.14	634	0.12	0.27	17.5	32.4
RAN-R-127	285	290	0.04	1.46	0.14	634	0.12	0.27	17.5	32.4
RAN-R-127	290	295	0.05	1.46	0.14	634	0.12	0.27	17.5	32.4
RAN-R-127	295	300	0.03	1.46	0.14	634	0.12	0.27	17.5	32.4
RAN-R-127	300	305	0.04	1.59	0.06	560	0.12	0.18	12.5	27.4
RAN-R-127	305	310	0.05	1.59	0.06	560	0.12	0.18	12.5	27.4
RAN-R-127	310	315	0.03	1.59	0.06	560	0.12	0.18	12.5	27.4
RAN-R-127	315	320	0.11	1.59	0.06	560	0.12	0.18	12.5	27.4
RAN-R-127	320	325	0.33	6.11	0.07	1223	0.12	0.17	9.33	48.5
RAN-R-127	325	330	0.18	6.11	0.07	1223	0.12	0.17	9.33	48.5
RAN-R-127	330	335	0.04	6.11	0.07	1223	0.12	0.17	9.33	48.5

Appendix 2-A

Hole_Id	From	To	AUFA	GC-AU	GC-AG	GC-AS	GC-BI	GC-CD	GC-CU	GC-HG
RAN-R-127	335	340	0.13	6.11	0.07	1223	0.12	0.17	9.33	48.5
RAN-R-127	340	345	0.05	1.86	0.08	1076	0.12	0.32	16.4	20.5
RAN-R-127	345	350	0.06	1.86	0.08	1076	0.12	0.32	16.4	20.5
RAN-R-127	350	355	0.09	1.86	0.08	1076	0.12	0.32	16.4	20.5
RAN-R-127	355	360	0.02	1.86	0.08	1076	0.12	0.32	16.4	20.5
RAN-R-127	360	365	0.16	4.38	0.06	422	0.12	0.15	14.3	12.1
RAN-R-127	365	370	0.26	4.38	0.06	422	0.12	0.15	14.3	12.1
RAN-R-127	370	375	0.04	4.38	0.06	422	0.12	0.15	14.3	12.1
RAN-R-127	375	380	0.06	4.38	0.06	422	0.12	0.15	14.3	12.1
RAN-R-127	380	385	0.05	0.93	0.09	552	0.12	0.19	39.4	22.6
RAN-R-127	385	390	0.03	0.93	0.09	552	0.12	0.19	39.4	22.6
RAN-R-127	390	395	0.02	0.93	0.09	552	0.12	0.19	39.4	22.6
RAN-R-127	395	400	0.03	0.93	0.09	552	0.12	0.19	39.4	22.6
RAN-R-127	400	405	0.04	0.63	0.06	544	0.12	0.2	15.2	7.13
RAN-R-127	405	420		0.63	0.06	544	0.12	0.2	15.2	7.13
RAN-R-127	420	440		0.41	0.05	1082	0.12	2.15	21	14
RAN-R-127	440	460		0.31	0.05	852	0.12	6.34	47.4	21.8
RAN-R-127	460	480		0.32	0.06	413	0.12	12.7	57.4	16.2
RAN-R-127	480	500		0.13	0.04	125	0.12	0.62	10.9	4.86
RAN-R-127	500	520		0.09	0.05	97.1	0.12	0.23	11.1	2.81
RAN-R-127	520	540		0.19	0.05	194	0.12	0.27	10.9	5.38
RAN-R-127	540	560		0.1	0.04	160	0.12	0.17	8.2	2.82
RAN-R-127	560	580		0.09	0.04	63.7	0.12	0.17	4.81	1.41
RAN-R-127	580	600		0.09	0.05	89.9	0.12	0.17	5.73	1.75
RAN-R-151	0	5	1.00E-03	0.01	0.09	360	0.12	0.46	58.4	2.15
RAN-R-151	5	10	1.00E-03	0.01	0.09	360	0.12	0.46	58.4	2.15
RAN-R-151	10	15	1.00E-03	0.01	0.09	360	0.12	0.46	58.4	2.15
RAN-R-151	15	20	1.00E-03	0.01	0.09	360	0.12	0.46	58.4	2.15
RAN-R-151	20	25	1.00E-03	0.01	0.02	718	0.24	0.95	58	2.14
RAN-R-151	25	30	1.00E-03	0.01	0.02	718	0.24	0.95	58	2.14
RAN-R-151	30	35	1.00E-03	0.01	0.02	718	0.24	0.95	58	2.14
RAN-R-151	35	40	1.00E-03	0.01	0.02	718	0.24	0.95	58	2.14
RAN-R-151	40	45	1.00E-03	0.07	0.04	411	0.12	0.27	36.4	26
RAN-R-151	45	50	4.00E-03	0.07	0.04	411	0.12	0.27	36.4	26
RAN-R-151	50	55	4.00E-03	0.07	0.04	411	0.12	0.27	36.4	26
RAN-R-151	55	60	4.00E-03	0.07	0.04	411	0.12	0.27	36.4	26
RAN-R-151	60	65	0.01							
RAN-R-151	65	70	0.01							
RAN-R-151	70	75	0.01							
RAN-R-151	75	80	0.01							
RAN-R-151	80	85	0.01	1.1	0.07	863	0.12	0.98	30.6	29.4
RAN-R-151	85	90	0.01	1.1	0.07	863	0.12	0.98	30.6	29.4
RAN-R-151	90	95	0.04	1.1	0.07	863	0.12	0.98	30.6	29.4
RAN-R-151	95	100	0.08	1.1	0.07	863	0.12	0.98	30.6	29.4
RAN-R-151	100	105	0.03	1.65	0.13	386	0.12	0.22	54.9	85.1
RAN-R-151	105	110	0.04	1.65	0.13	386	0.12	0.22	54.9	85.1
RAN-R-151	110	115	0.07	1.65	0.13	386	0.12	0.22	54.9	85.1
RAN-R-151	115	120	0.08	1.65	0.13	386	0.12	0.22	54.9	85.1
RAN-R-151	120	125	0.07	1.11	0.08	302	0.12	0.15	41.3	20.2
RAN-R-151	125	130	0.04	1.11	0.08	302	0.12	0.15	41.3	20.2

Appendix 2-A

Hole_Id	From	To	AUFA	GC-AU	GC-AG	GC-AS	GC-BI	GC-CD	GC-CU	GC-HG
RAN-R-151	130	135	0.02	1.11	0.08	302	0.12	0.15	41.3	20.2
RAN-R-151	135	140	0.02	1.11	0.08	302	0.12	0.15	41.3	20.2
RAN-R-151	140	145	0.02	0.71	0.09	129	0.12	0.13	17.3	70.6
RAN-R-151	145	150	0.02	0.71	0.09	129	0.12	0.13	17.3	70.6
RAN-R-151	150	155	2.00E-03	0.71	0.09	129	0.12	0.13	17.3	70.6
RAN-R-151	155	160	0.03	0.71	0.09	129	0.12	0.13	17.3	70.6
RAN-R-151	160	165	0.01	0.41	0.07	330	0.12	0.19	25.4	63.3
RAN-R-151	165	170	0.01	0.41	0.07	330	0.12	0.19	25.4	63.3
RAN-R-151	170	175	0.01	0.41	0.07	330	0.12	0.19	25.4	63.3
RAN-R-151	175	180	0.01	0.41	0.07	330	0.12	0.19	25.4	63.3
RAN-R-151	180	185	0.01	0.92	0.09	581	0.12	1.08	22.6	183
RAN-R-151	185	190	0.06	0.92	0.09	581	0.12	1.08	22.6	183
RAN-R-151	190	195	0.03	0.92	0.09	581	0.12	1.08	22.6	183
RAN-R-151	195	200	0.01	0.92	0.09	581	0.12	1.08	22.6	183
RAN-R-151	200	205	0.01	0.25	0.11	2640	0.12	1.93	15.7	40.3
RAN-R-151	205	210	0.01	0.25	0.11	2640	0.12	1.93	15.7	40.3
RAN-R-151	210	215	0.01	0.25	0.11	2640	0.12	1.93	15.7	40.3
RAN-R-151	215	220	0.01	0.25	0.11	2640	0.12	1.93	15.7	40.3
RAN-R-151	220	225	0.02	0.5	0.22	1037	0.12	0.64	50.2	36.6
RAN-R-151	225	230	0.01	0.5	0.22	1037	0.12	0.64	50.2	36.6
RAN-R-151	230	235	0.01	0.5	0.22	1037	0.12	0.64	50.2	36.6
RAN-R-151	235	240	0.03	0.5	0.22	1037	0.12	0.64	50.2	36.6
RAN-R-151	240	245	0.02	0.55	0.16	1278	0.12	0.23	22.8	45.9
RAN-R-151	245	250	0.01	0.55	0.16	1278	0.12	0.23	22.8	45.9
RAN-R-151	250	255	0.02	0.55	0.16	1278	0.12	0.23	22.8	45.9
RAN-R-151	255	260	0.02	0.55	0.16	1278	0.12	0.23	22.8	45.9
RAN-R-151	260	265	0.02	0.19	0.06	473	0.12	0.2	10.7	9.15
RAN-R-151	265	270	2.00E-03	0.19	0.06	473	0.12	0.2	10.7	9.15
RAN-R-151	270	275	2.00E-03	0.19	0.06	473	0.12	0.2	10.7	9.15
RAN-R-151	275	280	0.01	0.19	0.06	473	0.12	0.2	10.7	9.15
RAN-R-151	280	285	0.02	0.53	0.23	721	0.12	0.96	44.8	26.6
RAN-R-151	285	290	0.01	0.53	0.23	721	0.12	0.96	44.8	26.6
RAN-R-151	290	295	0.01	0.53	0.23	721	0.12	0.96	44.8	26.6
RAN-R-151	295	300	0.01	0.53	0.23	721	0.12	0.96	44.8	26.6
RAN-R-151	300	320		0.22	0.09	895	0.12	0.71	35.2	15
RAN-R-151	320	340		0.19	0.05	595	0.12	0.26	29.5	8.88
RAN-R-151	340	360		0.3	0.06	595	0.12	0.42	38	14.7
RAN-R-151	360	380		0.26	0.05	629	0.12	0.84	28.9	10.7
RAN-R-151	380	400		0.42	0.09	781	0.12	3.34	58	17.3
RAN-R-151	400	420		0.29	0.1	363	0.12	2.56	45.5	16.9
RAN-R-151	420	440		0.04	0.06	76.2	0.12	1.43	16.6	6.92
RAN-R-151	440	460		0.06	0.4	67	3.13	0.72	5.25	4.72
RAN-R-151	460	480		0.05	0.04	82.4	0.12	0.47	8.91	6.35
RAN-R-151	480	500		0.06	0.04	50.4	0.12	0.53	5.76	5.72
RAN-R-151	500	520		0.03	0.05	139	0.12	0.32	11.2	4.6
RAN-R-151	520	540		0.1	0.04	127	0.12	0.26	13.1	4.56
RAN-R-151	540	560		0.03	0.05	85.6	0.12	0.32	8.98	3.86
RAN-R-151	560	580		0.02	0.04	51.8	0.12	0.29	7.94	2.73
RAN-R-151	580	600		0.04	0.04	60.3	0.12	0.23	7.96	5.26
RAN-R-192	0	10		4.00E-03	0.12	195	0.12	0.05	34.5	3.14

Appendix 2-A

Hole_Id	From	To	AUFA	GC-AU	GC-AG	GC-AS	GC-BI	GC-CD	GC-CU	GC-HG
RAN-R-192	10	20		0.01	0.12	590	0.12	0.05	58.2	3.18
RAN-R-192	20	30		0.01	0.09	574	0.12	0.33	67.4	2.53
RAN-R-192	30	40		0.01	0.17	249	0.26	0.05	40.6	2.2
RAN-R-192	40	50		0.01	0.21	356	0.12	0.05	51.8	3.57
RAN-R-192	50	60		0.01	0.21	343	0.12	0.05	31.7	1.87
RAN-R-192	60	70		0.01	0.31	316	0.12	0.05	33	2.01
RAN-R-192	70	80		0.01	0.33	303	0.33	0.05	14.4	1.34
RAN-R-192	80	90		0.01	0.24	430	0.12	0.05	31.6	1.02
RAN-R-192	90	100		0.01	0.26	229	0.12	0.05	82.2	1.9
RAN-R-192	100	110		0.01	0.39	238	0.26	0.05	95.7	1.94
RAN-R-192	110	120		0.01	0.33	184	0.27	0.05	174	1.6
RAN-R-192	120	130		0.01	0.36	192	0.12	0.05	56.3	1.44
RAN-R-192	130	140		0.01	0.43	240	0.12	0.58	56.3	1.96
RAN-R-192	140	150		0.01	0.34	194	0.12	1.87	45.1	0.97
RAN-R-192	150	160		0.01	0.36	195	0.12	0.5	50.3	1.05
RAN-R-192	160	170		0.01	0.37	172	0.23	1.59	55	1.13
RAN-R-192	170	180		0.01	0.37	213	0.22	1.35	66.7	0.99
RAN-R-192	180	190		0.01	0.39	152	0.12	0.05	75.2	1.22
RAN-R-192	190	200		0.01	0.35	111	0.26	0.05	76.9	1.2
RAN-R-192	200	210		0.01	0.34	101	0.12	0.05	40.7	2.04
RAN-R-192	210	220		0.01	0.32	145	0.29	0.05	43.8	2.15
RAN-R-192	220	230		0.01	0.13	514	0.3	0.05	39.8	0.92
RAN-R-192	230	240		0.01	0.07	424	0.25	0.05	24.8	0.57
RAN-R-192	240	250		4.00E-03	0.1	97.2	0.34	0.05	13.2	0.69
RAN-R-192	250	260		0.01	0.11	134	0.29	0.05	17.6	2.93
RAN-R-192	260	270		4.00E-03	0.12	85.9	0.4	0.05	20.5	7.43
RAN-R-192	270	280		0.01	0.12	98	0.43	0.05	11.2	9.39
RAN-R-192	280	290		4.00E-03	0.1	124	0.38	0.05	18.1	6.09
RAN-R-192	290	300		0.01	0.11	146	0.45	0.05	15.2	4.32
RAN-R-192	300	310		0.01	0.08	286	0.34	0.05	21.3	6.47
RAN-R-192	310	320		0.01	0.13	144	0.43	0.05	15.5	11.9
RAN-R-192	320	330		0.01	0.17	179	0.12	0.05	25.8	13.2
RAN-R-192	330	340		0.01	0.14	173	0.23	0.05	22.2	1.94
RAN-R-192	340	350		0.01	0.14	112	0.33	0.05	27.5	1.86
RAN-R-192	350	360		0.01	0.12	209	0.24	0.05	23.5	1.85
RAN-R-192	360	370		0.01	0.06	135	0.29	0.05	39.3	1.48
RAN-R-192	370	380		0.01	0.31	125	0.12	0.05	103	2.22
RAN-R-192	380	390		0.01	0.05	203	0.12	0.05	13.5	4.41
RAN-R-192	390	400		0.01	0.04	151	0.12	0.05	9.25	0.6
RAN-R-192	400	410		0.03	0.05	94.5	0.12	0.05	24.5	1.66
RAN-R-192	410	420		0.04	0.05	68.6	0.12	0.05	15.6	1.5
RAN-R-192	420	430		0.15	0.22	111	0.12	0.05	39	2.81
RAN-R-192	430	440		0.28	0.05	392	0.12	7.3	57.1	2.69
RAN-R-192	440	450		0.06	0.03	89.1	0.12	1	14.7	1.18
RAN-R-192	450	460		0.01	0.02	45.2	0.12	0.05	6.38	0.97
RAN-R-192	460	470		0.01	0.01	64.2	0.12	0.05	8.67	1.93
RAN-R-192	470	480		3.00E-03	0.01	29.7	0.12	0.05	5.52	1.97
RAN-R-192	480	490		3.00E-03	0.01	16.1	0.12	0.05	7.28	1.58
RAN-R-192	490	500		1.00E-03	0.02	14.3	0.12	0.05	4.76	2.12
RAN-R-206	0	20	3.00E-04	0.01	0.12	643	0.26	0.05	36.8	0.82

Appendix 2-A

Hole_Id	From	To	AUFA	GC-AU	GC-AG	GC-AS	GC-BI	GC-CD	GC-CU	GC-HG
RAN-R-206	20	40	0	0.01	0.06	640	0.12	0.05	35.6	0.42
RAN-R-206	40	60	0	0.01	0.1	242	0.12	0.05	16.5	2.24
RAN-R-206	60	80	9.00E-04	0.01	0.05	114	0.12	0.05	7.04	1.37
RAN-R-206	80	100	3.00E-04	4.00E-03	0.06	94.4	0.12	0.05	6.07	9.07
RAN-R-206	100	120	3.00E-04	4.00E-03	0.04	124	0.12	0.05	6.04	13.6
RAN-R-206	120	140	3.00E-04	0.01	0.23	218	0.26	0.05	43.1	11.5
RAN-R-206	140	160	0	0.01	0.17	274	0.38	0.05	43.4	6.83
RAN-R-206	160	180	0	0.01	0.2	142	0.12	0.05	43.5	4.41
RAN-R-206	180	200	0	0.01	0.17	190	0.12	0.05	25.2	4.52
RAN-R-206	200	220	0	0.01	0.26	289	0.34	0.05	18.6	5.63
RAN-R-206	220	240	3.00E-04	0.01	0.12	321	0.32	0.05	13.3	4.02
RAN-R-206	240	260	3.00E-04	0.02	0.05	367	0.12	0.05	11.6	1.85
RAN-R-206	260	280	3.00E-04	0.02	0.12	293	0.12	0.05	49.8	2.36
RAN-R-206	280	295	0.01	0.49	0.06	209	0.12	0.05	28.9	2.71
RAN-R-206	295	300	0.04	0.49	0.06	209	0.12	0.05	28.9	2.71
RAN-R-206	300	305	0.04	1.65	0.1	512	0.12	0.21	14.6	25
RAN-R-206	305	310	0.05	1.65	0.1	512	0.12	0.21	14.6	25
RAN-R-206	310	315	0.07	1.65	0.1	512	0.12	0.21	14.6	25
RAN-R-206	315	320	0.08	1.65	0.1	512	0.12	0.21	14.6	25
RAN-R-206	320	325	0.06	2.55	0.07	547	0.12	1.25	11.1	42.5
RAN-R-206	325	330	0.11	2.55	0.07	547	0.12	1.25	11.1	42.5
RAN-R-206	330	335	0.08	2.55	0.07	547	0.12	1.25	11.1	42.5
RAN-R-206	335	340	0.11	2.55	0.07	547	0.12	1.25	11.1	42.5
RAN-R-206	340	345	0.09	2.01	0.04	779	0.12	0.71	13.1	12.7
RAN-R-206	345	350	0.06	2.01	0.04	779	0.12	0.71	13.1	12.7
RAN-R-206	350	355	0.08	2.01	0.04	779	0.12	0.71	13.1	12.7
RAN-R-206	355	360	0.06	2.01	0.04	779	0.12	0.71	13.1	12.7
RAN-R-206	360	365	0.02	0.34	0.01	241	0.12	4.52	55.5	14.1
RAN-R-206	365	370	0.07	0.34	0.01	241	0.12	4.52	55.5	14.1
RAN-R-206	370	380	0.01	0.34	0.01	241	0.12	4.52	55.5	14.1
RAN-R-206	380	400	1.90E-03	0.07	0.03	98.8	0.12	5.39	9.72	9.2

Appendix 2-A

Hole_Id	From	To	GC-MO	GC-PB	GC-SB	GC-SE	GC-TL	GC-ZN
RAN-R-115	20	40	2.13	12.5	5.85	0.5	7.29	11.9
RAN-R-115	40	60	2.75	13.2	6	0.5	6.17	13.3
RAN-R-115	60	80	3.02	9.63	6.54	0.5	3.14	25.6
RAN-R-115	80	100	3.96	4.65	3.77	0.5	0.88	3.87
RAN-R-115	100	120	3.78	8.19	2.63	0.5	1.62	2.97
RAN-R-115	120	140	3.62	10.2	5.9	0.5	2.04	3.24
RAN-R-115	140	160	2.5	9.61	7.64	0.5	1.56	4.45
RAN-R-115	160	180	3.22	13.6	9.08	0.5	0.641	21.2
RAN-R-115	180	200	2.58	15.6	4.6	0.5	0.554	4.99
RAN-R-115	200	220	2.9	15.2	8.47	0.5	2.77	2.17
RAN-R-115	220	240	1.96	12.7	7.24	0.5	4.99	11.3
RAN-R-115	240	260	1.57	7.97	22.6	0.5	4.38	10.8
RAN-R-115	260	280	1.06	4.23	113	0.579	1.11	10.7
RAN-R-115	280	300	3.78	4.62	154	0.512	0.25	6.49
RAN-R-115	300	320	4.71	7.39	197	0.5	1.14	10.1
RAN-R-115	320	340	4.67	11.6	204	0.523	13.1	12.2
RAN-R-115	340	360	4.16	5.44	150	0.592	3.15	33.7
RAN-R-115	360	380	3.93	15.3	135	0.5	0.25	14.2
RAN-R-115	380	400	1.38	54.9	199	0.5	69	358
RAN-R-115	400	420	0.887	16.9	71.1	0.5	6.48	2278
RAN-R-115	420	440	1.15	16.4	84.8	0.6	4.75	776
RAN-R-115	440	460	0.506	10.3	29.7	0.5	4.23	735
RAN-R-115	460	480	0.761	8.47	49.4	0.5	3.41	517
RAN-R-115	480	500	0.715	11.3	66.3	0.5	12.3	392
RAN-R-125	0	20	3.11	6.75	13.6	0.5	0.74	11
RAN-R-125	20	40	5.75	2	17.2	0.5	0.731	11.7
RAN-R-125	40	60	5.55	2.92	6.7	0.5	1.14	7.26
RAN-R-125	60	80	5.96	1.86	23.3	0.5	1.32	21.8
RAN-R-125	80	100	5.11	4.38	14.7	0.5	1.3	9.82
RAN-R-125	100	120	3.59	4.88	13.5	0.5	0.981	7.48
RAN-R-125	120	140	2.03	9.57	8.16	0.5	1.26	1.19
RAN-R-125	140	160	2.5	5.95	13.9	0.5	1.48	6.69
RAN-R-125	160	180	1.78	5.36	12.1	0.5	1.92	7.5
RAN-R-125	180	200	6.08	4.64	26.2	0.5	0.879	10.7
RAN-R-125	200	220	0.686	5.44	37.7	0.601	1.93	13.6
RAN-R-125	220	240	1.14	5.63	36	0.572	1.66	9.38
RAN-R-125	240	260	3.54	9.89	127	0.5	9.3	8.91
RAN-R-125	260	280	7.22	8.82	130	0.677	5.99	19.7
RAN-R-125	280	300	5.74	17.2	258	0.613	30.1	92.9
RAN-R-125	300	320	5.54	55.1	479	0.692	31.6	45.2
RAN-R-125	320	340	4.27	123	171	0.67	45.4	19.1
RAN-R-125	340	360	5.07	84.5	147	0.568	12.1	13.6
RAN-R-125	360	380	5.45	21	112	0.5	11.7	14.8
RAN-R-125	380	400	5.74	13.2	132	0.476	3.1	20.9
RAN-R-125	400	420	2.04	30.9	128	0.5	4.74	14.8
RAN-R-125	420	440	2.24	9.58	111	0.5	7.89	82.6
RAN-R-125	440	460	4.01	20.3	144	0.5	8.49	239
RAN-R-125	460	480	3.33	24.8	155	0.523	7.4	233
RAN-R-125	480	500	4.16	38	143	0.5	8.75	306
RAN-R-127	0	20	3.22	8.16	9.04	0.5	0.25	24.3
RAN-R-127	20	40						
RAN-R-127	40	60	3.48	9.02	8.25	0.5	0.25	7.24
RAN-R-127	60	80	3.35	9.53	6.22	0.5	0.25	3.4
RAN-R-127	80	100	6.67	2.55	18.6	0.5	0.25	13.7
RAN-R-127	100	120	5	4.3	9.13	0.5	0.25	4.38
RAN-R-127	120	140	3.46	7.7	13.5	0.5	0.25	6.09

Appendix 2-A

Hole_Id	From	To	GC-MO	GC-PB	GC-SB	GC-SE	GC-TL	GC-ZN
RAN-R-127	140	160	2.99	12.1	14.4	0.5	0.987	7.68
RAN-R-127	160	180	3.18	11.2	10.8	0.5	1.27	9.02
RAN-R-127	180	200	2.97	14	12.6	0.5	6.82	71.6
RAN-R-127	200	220	2.79	10.8	9.31	0.479	2.1	10.2
RAN-R-127	220	240	3.02	14.7	12.9	0.5	17.9	5.79
RAN-R-127	240	260	3.72	12.5	32.2	0.5	15.7	7.11
RAN-R-127	260	280	2.59	17.7	55.6	0.504	38.2	8.04
RAN-R-127	280	300	2.35	31.6	27.1	0.5	10.1	10
RAN-R-127	300	320	1.74	24.1	36.8	0.5	5.19	10.8
RAN-R-127	320	340	2.13	10	65.2	0.5	1.44	8.26
RAN-R-127	340	360	3.2	12.7	99.1	0.5	4.99	10.1
RAN-R-127	360	380	3.19	4.53	76.8	0.5	0.25	4.93
RAN-R-127	380	400	7.02	6.23	149	0.5	1	7.26
RAN-R-127	400	420	2.86	7.23	130	0.5	0.624	15.7
RAN-R-127	420	440	1.85	11.2	124	0.5	21.6	424
RAN-R-127	440	460	1.85	18.7	71.5	0.5	54.3	480
RAN-R-127	460	480	1.48	14.8	38.8	0.5	37.5	1697
RAN-R-127	480	500	0.757	8.75	15.2	0.5	4.13	333
RAN-R-127	500	520	0.794	4.19	13.7	0.5	2.03	77.9
RAN-R-127	520	540	0.868	6.07	32.4	0.5	2.54	48.6
RAN-R-127	540	560	0.834	3.6	28.7	0.5	0.685	24.9
RAN-R-127	560	580	0.575	1.55	11.1	0.5	0.79	21.3
RAN-R-127	580	600	0.67	2.54	12.2	0.5	0.992	20.1
RAN-R-151	0	20	4.1	9.01	6.16	0.5	6.37	146
RAN-R-151	20	40	3.9	9.23	5.58	0.5	0.747	165
RAN-R-151	40	60	5.66	10.6	36.2	0.5	0.25	48.8
RAN-R-151	60	80						
RAN-R-151	80	100	11.4	9.02	103	0.5	0.25	41.6
RAN-R-151	100	120	11.8	7.93	110	0.5	0.25	15.7
RAN-R-151	120	140	7.8	8.97	87.1	0.5	0.25	9.2
RAN-R-151	140	160	3.32	17.7	40.9	0.5	0.25	5.37
RAN-R-151	160	180	5.28	16.9	62.8	0.5	0.25	8.84
RAN-R-151	180	200	2.86	58	52.6	0.5	3.76	60
RAN-R-151	200	220	3.24	23.1	36.6	0.5	3.68	364
RAN-R-151	220	240	11.3	19.5	139	0.5	5.5	37
RAN-R-151	240	260	5.56	25.5	144	0.5	8.46	10.3
RAN-R-151	260	280	2.06	6.6	38.3	0.5	2.11	9.81
RAN-R-151	280	300	7.21	14.1	164	0.5	9.37	18.9
RAN-R-151	300	320	9.08	13.5	483	0.5	7.69	44.1
RAN-R-151	320	340	8.1	11.3	247	0.5	1.78	26.9
RAN-R-151	340	360	11.1	11.1	225	0.5	1.52	36.2
RAN-R-151	360	380	6.35	7.85	258	0.5	11.9	89.6
RAN-R-151	380	400	6.7	26	290	0.5	89	355
RAN-R-151	400	420	4.39	35.3	113	0.5	25	415
RAN-R-151	420	440	1.05	10.9	20	0.5	6.74	315
RAN-R-151	440	460	0.503	6.3	12.5	1.01	10.9	141
RAN-R-151	460	480	0.756	7.24	18.7	0.5	2.53	154
RAN-R-151	480	500	0.951	4.86	16.1	0.5	0.984	61.3
RAN-R-151	500	520	2.15	9.23	70	0.5	2.82	74.6
RAN-R-151	520	540	2.11	22.6	63.8	0.5	2	56.7
RAN-R-151	540	560	1.42	13.7	42.1	0.5	1.86	42
RAN-R-151	560	580	1.03	6.13	20.4	0.5	1.92	45.2
RAN-R-151	580	600	1	7.18	28.6	0.5	2.84	56.1
RAN-R-192	0	10	2.76	8.09	12.8	1.16	0.25	5
RAN-R-192	10	20	5.21	11.9	22.1	5.72	0.25	76.4
RAN-R-192	20	30	4.77	16.6	17.3	5.05	0.878	101

Appendix 2-A

Hole_Id	From	To	GC-MO	GC-PB	GC-SB	GC-SE	GC-TL	GC-ZN
RAN-R-192	30	40	3.28	15	4.17	1.76	1.18	2.67
RAN-R-192	40	50	4.76	12.6	4.99	2.38	0.968	5
RAN-R-192	50	60	3.6	8.47	6.42	3.38	0.648	5
RAN-R-192	60	70	2.77	14.8	6.44	3.46	2.76	5
RAN-R-192	70	80	2.87	16.3	5.29	0.5	2.18	5
RAN-R-192	80	90	4.51	10.6	8.98	3.15	1.06	5
RAN-R-192	90	100	2.67	8.25	5.61	0.5	1.35	5
RAN-R-192	100	110	2.46	12.4	5.89	2.09	1.84	5
RAN-R-192	110	120	2.38	12.2	3.02	1.91	1.7	5
RAN-R-192	120	130	2.37	12.2	3.04	1.88	2.34	5
RAN-R-192	130	140	2.18	10.3	4.17	2.01	2.08	1.37
RAN-R-192	140	150	2.01	11.9	3.31	1.32	1.36	11.1
RAN-R-192	150	160	2.35	13.1	3.97	2.16	1.67	19.2
RAN-R-192	160	170	2.34	14.7	4.57	1.47	1.78	21.9
RAN-R-192	170	180	2.07	13.5	5.03	2.42	1.71	21.1
RAN-R-192	180	190	2.01	15	3.33	1.46	1.39	5
RAN-R-192	190	200	2.4	14.8	4.02	2.4	1.41	7.85
RAN-R-192	200	210	2.69	15.9	3.95	3.5	1.95	5
RAN-R-192	210	220	2.49	14.2	4.32	5.1	1.29	6.99
RAN-R-192	220	230	2.96	16.2	16.5	2.08	1.7	222
RAN-R-192	230	240	3.8	8.96	25.1	2.31	1.48	162
RAN-R-192	240	250	2.37	4.55	10.1	1.32	2.08	5.38
RAN-R-192	250	260	4.17	4.14	17.4	1.26	2.02	9.38
RAN-R-192	260	270	3.33	6.4	9.43	3.36	2.1	5
RAN-R-192	270	280	2.57	5.93	2.96	3.69	2.12	5
RAN-R-192	280	290	2.1	7.01	13.9	2.36	1.98	5
RAN-R-192	290	300	2.14	7.06	21.3	2.06	2.34	6.18
RAN-R-192	300	310	2.62	11.9	70.2	1.64	2.26	37.5
RAN-R-192	310	320	2.65	9.88	17.5	2.86	2.14	5
RAN-R-192	320	330	2.44	9.9	6.02	5.28	0.57	5
RAN-R-192	330	340	2.54	10.3	14.2	3.84	0.937	5
RAN-R-192	340	350	2.55	15.9	10.4	4.17	1.54	5
RAN-R-192	350	360	2.52	10.2	20.7	5.15	1.01	1.21
RAN-R-192	360	370	1.91	14.7	5.49	3.81	1.11	1.1
RAN-R-192	370	380	1.78	9.71	3.58	4.44	0.894	5
RAN-R-192	380	390	1.73	6.34	38.8	2.02	0.783	5.63
RAN-R-192	390	400	0.665	2.7	48.6	0.5	0.79	5
RAN-R-192	400	410	0.996	8.16	65.9	2.96	0.704	5
RAN-R-192	410	420	1.39	4.68	83.7	2.3	0.834	3.74
RAN-R-192	420	430	3.12	29.7	116	2.97	1.8	62.1
RAN-R-192	430	440	4.12	36.6	224	2.48	19.3	1229
RAN-R-192	440	450	0.881	10.2	29.7	1.49	3.48	423
RAN-R-192	450	460	0.39	2.94	12.5	1.73	1.69	183
RAN-R-192	460	470	0.265	3.04	19.3	2.56	2.09	239
RAN-R-192	470	480	0.212	2.04	7.99	2.58	1.05	62.5
RAN-R-192	480	490	0.147	10.5	3.71	1.59	0.878	48.1
RAN-R-192	490	500	0.162	1.66	3.39	0.5	0.852	36.2
RAN-R-206	0	20	3.21	8.62	8.14	0.5	0.25	18.7
RAN-R-206	20	40	3.88	5.05	11.7	0.5	0.25	62.1
RAN-R-206	40	60	2.83	3.65	11.7	0.5	0.25	8.94
RAN-R-206	60	80	4.15	2.68	6.81	0.5	0.25	14.9
RAN-R-206	80	100	6.85	1.21	6.47	0.5	0.25	8.54
RAN-R-206	100	120	3.38	2.27	8.93	0.5	0.25	4.41
RAN-R-206	120	140	3.01	6.98	6.98	0.5	0.25	3.86
RAN-R-206	140	160	2.57	8.13	12.5	0.5	0.674	2.48
RAN-R-206	160	180	2.61	8.49	11.5	0.5	0.25	2.35

Appendix 2-A

Hole_Id	From	To	GC-MO	GC-PB	GC-SB	GC-SE	GC-TL	GC-ZN
RAN-R-206	180	200	2.03	8.34	8.73	0.5	2.94	4.3
RAN-R-206	200	220	1.88	12.4	9.61	0.5	6.45	9.77
RAN-R-206	220	240	1.54	10.5	12.2	0.5	4.08	7.95
RAN-R-206	240	260	0.737	3.14	13.9	0.54	1.15	8.84
RAN-R-206	260	280	0.734	4.43	20.9	0.656	1.09	6.39
RAN-R-206	280	300	1.51	3.21	120	0.498	1.04	12.2
RAN-R-206	300	320	3.89	22.9	265	0.5	4.05	56.5
RAN-R-206	320	340	3.88	6.25	396	0.581	69.1	144
RAN-R-206	340	360	4.72	4.36	733	0.5	17.2	180
RAN-R-206	360	380	1.24	3.23	144	0.5	59.8	501
RAN-R-206	380	400	0.636	2.1	50.9	0.5	32.2	276

Appendix 1-B

Sample_Id	Description	AU	AS	SB	HG	AG	AL	BA	BE	BI	CA	CD	CO	CR	CU	FE	K	MG	MN	MO	NA	NI	P	PB	SR	TI	V	W	ZN
RUF-4430	Bx 1	10	534	33	2.69	0.2	59300	610	1	10	800	0.5	4	92	25	19300	23600	1700	20	1	1400	12	810	2	248	2000	131	10	54
RUF-4431	Bx 2 ox	3.04	142	17.5	7.13	0.2	2800	10000	0.5	2	300	4	1	33	17	5300	400	100	20	1	100	9	80	2	127	100	8	10	14
RUF-4432	Tuffisite	0.17	10000	20	20.5	1.4	109000	2590	0.5	16	900	0.5	67	294	60	67300	6800	600	10	1	400	134	1850	4	735	8600	207	40	12
RUF-4433	Dw	0.02	172	5.6	0.26	0.6	55800	390	2	6	4500	0.5	25	132	73	23500	18700	3600	50	1	800	113	1880	4	99	4100	188	10	440
RUF-4434	Dw	0.025	164	13	0.88	0.8	29000	410	1.5	2	1500	3.5	29	166	78	15100	7400	1700	105	23	600	251	5460	2	66	1000	316	10	2370
RUF-4435	Bx 2 ox from Revelation flt	2.16	664	86	22.3	0.2	4400	10000	0.5	2	400	5.5	1	28	12	14200	900	100	15	1	100	7	1030	2	79	400	20	10	30
RUF-4436	Bx 2 ox	3.88	1175	230	27	0.2	11300	670	0.5	2	600	0.5	1	61	13	25100	3700	400	20	1	100	5	2300	2	232	900	42	10	24
RUF-4437	Tuffisite	0.385	516	56	19.6	0.2	112500	3180	0.5	6	2600	0.5	55	316	132	68900	38300	3800	40	1	600	121	3620	2	569	12000	230	110	30
RUF-4438	Bx 2 ox	3.61	515	110	16.9	0.2	5200	460	0.5	2	600	0.5	1	112	10	36500	3400	100	35	4	100	8	3240	2	242	700	29	10	20
RUF-4439	Bx 2 ox from FW of Phantom flt	0.665	566	71	3.13	0.2	5800	160	0.5	2	500	0.5	1	198	12	42600	5600	200	30	5	300	6	1800	2	433	600	37	10	12
RUF-4440	Bx 2 ox in Phantom flt	2.47	681	50	30.9	0.2	11300	2970	0.5	2	700	0.5	1	124	28	11100	1900	300	20	23	100	10	7440	2	270	400	73	10	12
RUF-4441	Bx 2 ox	6.2	331	20	27.2	0.2	6600	4240	0.5	2	1200	0.5	1	147	11	7900	1000	200	35	5	100	8	2480	2	297	300	39	10	24
RUF-4442	Bx 2 ox from Revalation flt	0.58	990	290	13.3	0.2	38800	140	2	2	1000	0.5	12	95	32	98300	12600	1800	45	7	700	75	2450	2	172	1500	130	10	164
RUF-4443	Bx 1	1.75	383	62	4.82	0.2	9200	340	0.5	2	800	0.5	1	76	12	24500	4900	500	25	10	100	9	2280	2	452	500	66	10	20
RUF-4444	Bx 2 ox	5.8	365	52	22.8	0.2	2700	620	0.5	2	1200	0.5	1	133	7	29900	1300	200	50	2	100	14	620	4	202	200	36	10	34
RUF-4445	tuffisite	0.04	3430	19.5	14.7	0.2	110000	3940	1	2	1600	0.5	43	285	42	47500	15200	2400	50	1	1100	143	1180	8	190	8300	228	30	154
RUF-4446	Bx 2 ref	10	2520	64	23.3	0.2	14600	420	0.5	2	3100	0.5	8	139	10	33700	3800	1000	30	1	100	99	1360	2	80	500	83	10	20
RUF-4447	Dw	0.04	483	55	6.29	0.4	20300	4880	1.5	2	1800	0.5	1	214	24	34700	3900	700	25	39	400	12	5620	8	311	700	847	10	96
RUF-4448	Rain flt	0.09	343	38	58.8	0.2	8200	10000	0.5	2	700	5	3	37	38	10500	1400	400	10	16	100	9	1660	2	100	500	335	10	34
RUF-4449	Pyrite flt	0.04	1010	31	6.64	0.2	48900	280	1.5	2	3400	0.5	15	133	53	43700	17700	3800	35	1	900	118	1430	4	239	2400	209	10	562
RUF-4450	Mw	0.01	108	14.5	3.16	0.2	57700	240	1.5	2	600	0.5	12	91	53	22700	23200	4400	25	1	1200	45	810	4	291	2900	221	10	144
RUF-4451	Bx 2 ox	0.395	120	64	5.8	0.2	2300	10000	0.5	2	100	3	1	55	7	4400	400	100	20	1	100	5	120	2	182	100	10	10	6
RUF-4452	Bx 2 ox in HW of Rain flt	0.685	647	44	27.9	0.2	2800	9440	0.5	2	100	2	1	66	6	11500	500	100	15	13	100	4	860	2	134	600	133	10	4
RUF-4453	Dw in FW of Rain flt	0.085	609	50	9.77	1.2	13100	1830	0.5	2	1000	0.5	1	238	12	16900	1000	100	15	27	200	4	10000	4	556	500	345	10	14
RUF-4454	Dw	0.05	227	21	4.43	1	19100	6170	1.5	2	5200	1.5	1	276	41	17100	800	100	25	5	200	16	10000	10	1525	700	336	10	24
RUF-4456	Mw; clay-rich	0.005	505	19	9.43	0.2	75100	460	1	2	100	0.5	25	139	745	50100	26800	4300	30	1	1400	60	480	8	187	5400	232	10	250
RUF-4457	Bx 3	0.03	409	22	5.41	0.2	54900	1920	1	2	300	0.5	1	117	35	26700	17800	3000	25	1	1100	7	1100	12	406	2900	230	10	28
RUF-4458	Bx 3	0.02	232	27	4.75	0.2	58800	2660	1	2	300	0.5	1	101	31	17800	20100	3500	25	1	1100	7	1130	14	301	3200	245	10	20
RUF-4459	Bx 1	0.195	297	24	0.15	0.2	49400	620	0.5	2	200	0.5	1	122	23	22000	18000	1500	10	1	700	2	510	8	269	4900	161	10	10
RUF-4460	Mw	0.125	117	11	2.51	0.2	59500	400	1	2	400	0.5	6	113	519	25300	23000	3200	20	1	1300	19	380	8	194	3500	170	10	16
RUF-4461	Bx 1 near flt	0.495	1255	92	2.89	0.2	18300	190	2	2	2000	0.5	1	132	18	64600	7200	400	15	1	500	5	7340	4	1045	900	107	10	26
RUF-4462	Mw in FW of EOS2 flt	0.01	214	4.6	1.55	0.2	58800	420	1	2	600	0.5	5	107	132	16500	21300	4200	30	1	1100	33	520	8	162	3300	225	10	26
RUF-4463	EOS2 flt	0.01	445	12	3.52	0.2	58800	320	1.5	2	1100	0.5	6	111	102	22700	20600	3900	30	1	1100	38	1490	8	369	2900	228	10	44
RUF-4464	Bx 1	0.115	203	32	2.05	0.2	52100	1370	0.5	2	400	0.5	1	96	15	15900	20400	2400	15	1	1000	3	580	4	389	3800	159	10	14
RUF-4465	Tuffisite	2.06	10000	58	18.3	0.2	73800	690	0.5	2	1000	0.5	34	206	66	53800	9800	1600	15	1	100	89	1330	8	292	8400	169	50	18
RUF-4466	Mw; clay-rich	1.43	6200	80	9.15	0.2	43000	330	0.5	2	800	0.5	32	110	71	36300	14200	1800	15	1	800	55	580	10	399	2200	177	10	162
RUF-4467	Bx 1	1.03	2910	56	3.52	0.2	22100	420	0.5	2	500	0.5	1	160	13	32000	7200	600	20	1	300	6	870	4	718	1700	165	10	22
RUF-4468	Mw in FW of Pyrite flt	0.03	253	32	6.99	1	53600	270	2	2	2400	0.5	8	106	54	43500	20700	4200	35	1	1100	52	1420	8	252	2900	253	10	196
RUF-4469	Mw	0.03	164	28	4.96	0.2	52800	350	2.5	2	800	0.5	9	106	43	25200	19800	3900	25	1	1100	56	1250	8	333	2700	233	10	218
RUF-4470	Mw near Dike flt	0.25	621	50	6.16	0.2	50400	440	2	2	4400	0.5	7	126	38	24600	18900	3400	30	1	800	44	3120	10	476	2500	235	10	456
RUF-4471	Mw in HW of Pyrite flt	0.015	156	24	4.14	0.2	57100	410	2	2	900	0.5	9	100	53	27700	21400	4100	30	1	1100	60	860	10	307	2900	251	10	216
RUF-4472	Mw in Pyrite flt	0.025	718	360	44.1	0.2	52100	300	1.5	2	700	0.5	11	100	50	43900	18200	3500	25	1	900	100	720	6	379	2500	231	10	412
RUF-4473	Shop flt	0.04	240	5	1.78	0.2	52100	510	0.5	2	700	0.5	7	94	95	16400	13100	1300	25	1	1000	42	1210	6	319	2600	220	10	74
RUF-4474	Mw	0.01	549	7.2	0.67	0.2	38700	1860	1.5	2	800	0.5	2	103	53	38200	11700	1900	15	2	600	24	1200	10	159	2000	175	10	92
RUF-4475	Mw	0.02	50	6.2	4.26	0.2	51500	410	1	2	600	0.5	2	106	61	16700	17000	2400	15	1	1000	23	990	12	227	3000	206	10	20
RUF-4476	Mw in HW of Rain flt	0.01	87	5.6	0.83	1.4	29200	940	1.5	2	7400	1.5	3	161	54	10600	9200	1900	25	7	600	41	5910	8	188	1300	308	10	46
RUF-4477	Dw in HW of thrust flt	0.01	32	4.6	0.33	2.2	20000	1060	1.5	2	13900	3	1	157	61	8300	4700	1100	20	10	300	45	10000	8	224	700	403	10	42
RUF-4478	Dw in Fw of thrust flt	0.01	68	7.2	0.35	2.2	15000	1210	1.5	2	33900	5	3	206	68	9800	4300	1000	175	38	400	106	10000	8	431	600	282	10	316
RUF-4479	Bx 2 ox in Fw of Sharpstone flt	0.32	873	380	2.76	0.2	36300	1180	2	2	18300	0.5	1	131	22	27000	8800	1000	30	7	400	11	10000	6	515	1400	167	10	72
RUF-4480	Bx 2 ref in Hw of Sharpstone flt	0.99	3740	190	100	0.2	8800	110	0.5	2	500	0.5	11	97	13	42300	2400	100	25	9	100	135	610	2	216	600	35	10	10
RUF-4481	Ddg; fresh	0.1	52	170	4.26	0.2	3600	1020	0.5	2	3E+05	2	6	16	8	1800	1200	49300	305	1	100	45	130	4	132	100	10	10	234
RUF-4482	Bx 2 ox in HW of Sharpstone flt	0.355	960	340	14.1	0.2	33300	520	1.5	2	47900	2	2	125	25	21500	10200	1400	180	15	100	38	4110	6	304	1300	166	10	126
RUF-4483	Ddg; dolomitized	0.035	106	38	2.44	0.2	1100	1640	0.5	2	2E+05	0.5	1	28	4	2700	500	1E+05	395	1	100	4	60	2	612	100	11	10	92
RUF-4484	Mw in Hw of Rain flt	0.065	1200	60	95.9	0.2	49500	520	1	2	3400	0.5	1	135	23	44600	17500	1800	20	4	700	23	2590	8	145	2800	196	10	62
RUF-4485	Dw in FW of Rain flt	0.01	140	26	4.67	2	24300	6200	1.5	2	3000	1	1	242	75	11400	3600	600	40	10	600	10	8020	6	624	800	246	10	32
RUF-4486	Dw between Shop flt	0.01	188	34	1.76	0.2	29500	650	0.5	2	900	0.5	1	125	25	19600	8100	800	25	1	600	6	560	4	309	1300	195	10	10
RUF-4487	Dw near Sharpstone parallel flt	0.01	246	16	16	0.2	33800	360	0.5	2	1000	0.5	1	104	51	19000	11800	1500	25	1	800	8	1300	2	168	1500	231	10	8

Lori J. Shallow, CREG, 1998 annual report

Appendix 2-C

Hole No.	Start	End	Description	Au (ppm) FA+AA	Ag (ppm)	Al (%)	As (ppm)	Ba (ppm)	Be (ppm)	Bi (ppm)	Ca (%)	Cd (ppm)	Co (ppm)	Cr (ppm)	Cu (ppm)
RUG 139	0	22	Mw	0.145	0.2	0.96	366	10	0.5	<2	0.37	0.5	8	60	49
RUG 139	22	28	Bx1	0.2	<0.2	0.6	974	20	<0.5	<2	0.16	0.5	10	44	37
RUG 139	28	42	Bx2; ox w/ red clay on fracs	7.6	0.2	0.2	490	220	<0.5	<2	0.06	<0.5	1	169	8
RUG 139	42	68.5	Bx2; ox w/ abun.bar & lim on fracs	2.46	1	0.04	98	530	<0.5	<2	0.03	2	<1	127	10
RUG 139	68.5	69	tuffisite	1.66	<0.2	0.05	312	1850	<0.5	<2	0.04	<0.5	1	143	9
RUG 139	69	95	Bx2; ox	2.81	<0.2	0.07	420	1370	<0.5	<2	0.05	<0.5	1	137	4
RUG 139	95	119	Bx2; ox; vuggy silica	4.9	<0.2	0.05	712	1550	<0.5	<2	0.06	0.5	3	183	3
RUG 139	119	130	Bx2; ox	2.21	<0.2	0.05	742	2120	<0.5	<2	0.56	<0.5	1	226	5
RUG 139	130	150	Bx2; ox	2.94	<0.2	0.48	2280	1700	<0.5	2	0.48	2.5	9	177	11
RUG 139	150	155	Spring fault w/ sheared Dw & PO4 nodules	0.73	<0.2	1.95	2080	1750	<0.5	<2	1.05	4	33	79	13
RUG 139	155	180	Dw; ox w/ shears & PO4 nodules	0.235	1.4	2.72	830	2570	1.5	<2	1.62	2.5	14	237	60
RUG 139	130	195	Dw; partially ox w/ PO4 nodules	0.14	2.2	1.81	116	1920	1.5	<2	2.85	2	1	215	62
RUG 139	195	220	Dw; carbonaceous	0.13	2.2	1	68	770	0.5	<2	3.23	8	4	151	61
RUG 140	0	20	Mw	0.615	0.2	1.09	246	30	0.5	<2	0.32	<0.5	9	45	49
RUG 140	20	60	Tectonic bx in Mw	4.25	<0.2	0.57	1060	20	<0.5	<2	0.33	<0.5	9	43	40
RUG 140	60	66	Mw	>10.00	<0.2	0.59	1410	10	<0.5	<2	0.06	1.5	8	65	41
RUG 140	66	72	Mw (Bx1?); ox	>10.00	<0.2	0.56	1210	10	<0.5	<2	0.39	<0.5	10	51	33
RUG 140	72	87	Mw	>10.00	<0.2	0.55	1185	<10	<0.5	<2	0.18	0.5	11	54	40
RUG 140	87	94	Bx2; ox	9.54	0.6	0.12	1165	750	<0.5	<2	0.04	<0.5	<1	141	12
RUG 140	94	98	Bx2; ref	7.94	<0.2	0.06	616	1160	<0.5	<2	0.08	2	<1	182	4
RUG 140	98	104	Bx2; ox	8.11	<0.2	0.18	1055	1890	<0.5	<2	0.1	0.5	<1	180	3
RUG 140	104	107	tuffisite in Flower fault	5.85	0.2	1.41	8920	20	<0.5	2	0.5	1	49	109	53
RUG 140	107	119	Bx2; mixed ox & ref	>10.00	<0.2	0.21	1180	1210	<0.5	<2	0.1	1.5	<1	180	5
RUG 140	119	130	Bx2; ox	>10.00	0.2	0.28	582	1470	<0.5	<2	0.2	<0.5	<1	127	5
RUG 140	130	134	Bx2; mixed ox & ref w/ carbon on fracs	>10.00	<0.2	0.15	318	1690	<0.5	<2	0.42	0.5	<1	116	4
RUG 140	134	162	Bx2; ox	>10.00	<0.2	0.19	2170	810	<0.5	<2	0.08	0.5	1	216	7
RUG 140	162	185	Bx3 w/ Bx2 clasts	1.22	<0.2	0.98	4980	1050	<0.5	<2	1.31	10.5	10	136	18
RUG 140	135	205	Bx3 w/ Bx2 clasts	2.81	0.6	1.05	1665	740	<0.5	<2	0.24	1.5	6	162	20
RUG 140	205	240	Ddg dol	0.42	<0.2	0.33	292	330	0.5	<2	14.65	1.5	4	36	5
RUG 140	240	250	Ddg dol w/ abundant bar	0.145	<0.2	0.11	80	2090	0.5	<2	>15.00	<0.5	1	24	3
RUG 141	0	20	Mw	0.036	0.2	1.03	158	30	0.5	<2	0.32	<0.5	8	45	55
RUG 141	20	40	Mw	0.0086	0.2	0.77	132	30	0.5	<2	0.27	<0.5	7	28	48
RUG 141	40	60	Mw w/ abun py veins	0.0034	0.2	0.74	144	60	0.5	<2	0.25	<0.5	8	25	47
RUG 141	60	80	Mw	0.0034	0.2	0.78	296	30	0.5	<2	0.27	<0.5	7	24	51

Appendix 2-C

Hole No.	Start	End	Description	Au (ppm) FA+AA	Ag (ppm)	Al (%)	As (ppm)	Ba (ppm)	Be (ppm)	Bi (ppm)	Ca (%)	Cd (ppm)	Co (ppm)	Cr (ppm)	Cu (ppm)
RUG 141	80	100	Mw	0.0069	<0.2	0.82	396	40	0.5	<2	0.25	<0.5	8	26	49
RUG 141	100	120	Mw	0.0034	0.2	0.96	356	40	0.5	<2	0.27	<0.5	9	32	49
RUG 141	120	140	Mw	0.0034	<0.2	0.79	434	40	0.5	<2	0.21	<0.5	7	56	45
RUG 141	140	146	Mw	0.0034	0.2	0.84	306	60	0.5	<2	0.22	<0.5	7	52	41
RUG 141	146	180	Mw ss w/ py replacing grains	0.0034	0.2	0.58	282	40	<0.5	<2	0.22	<0.5	6	134	27
RUG 141	180	195	Mw	0.0034	0.2	0.81	414	10	0.5	<2	0.18	<0.5	7	60	40
RUG 141	195	215	Bx w/ clay matrix	0.0034	0.2	0.62	608	20	<0.5	2	0.12	<0.5	9	62	34
RUG 141	215	240	Mw	0.0034	0.2	0.73	1005	60	0.5	<2	0.22	<0.5	8	55	42
RUG 141	240	260	Mw	0.0129	<0.2	0.72	818	40	<0.5	<2	0.2	<0.5	8	30	46
RUG 141	260	276	Mw	0.0621	<0.2	0.58	708	30	<0.5	<2	0.07	<0.5	14	30	58
RUG 141	276	209	Bx1	0.1882	<0.2	0.52	298	1480	<0.5	<2	0.02	<0.5	<1	57	33
RUG 141	290	305	Bx1	0.4453	<0.2	0.5	250	2600	<0.5	<2	0.01	<0.5	<1	61	17
RUG 141	305	315	Bx2; ref	0.4755	0.2	0.75	304	100	<0.5	<2	0.03	<0.5	6	41	28
RUG 141	315	325	Flt bx	2.9	<0.2	0.49	1230	170	<0.5	<2	0.03	<0.5	4	47	22
RUG 141	325	343	Bx2; ox	2.249	<0.2	0.18	364	570	<0.5	<2	0.03	0.5	<1	117	15
RUG 141	343	360	Flt bx	1.898	<0.2	1.06	478	1600	<0.5	<2	0.08	<0.5	<1	83	10
RUG 141	360	374	Bx2; ox	2.508	<0.2	1.07	1155	160	<0.5	<2	0.09	<0.5	<1	128	4
RUG 141	374	389	Flt bx	0.987	<0.2	1.26	2070	1450	<0.5	<2	0.26	1	1	87	9
RUG 141	389	421	Flt bx	0.1458	<0.2	0.23	376	2320	<0.5	<2	8.07	0.5	2	39	7
RUG 141	421	428	Flt bx	0.6982	<0.2	0.83	308	1300	<0.5	<2	0.63	<0.5	2	101	7
RUG 141	429	473	Bx3; ref	1.867	<0.2	0.85	1710	30	<0.5	<2	0.81	2	9	57	26
RUG 141	473	484	Bx3; ox w/ dol clasts	2.488	<0.2	0.28	808	1070	0.5	2	9.46	1	<1	25	4
RUG 141	484	497	Bx3; ref w/ clasts of dol, Bx2, & bar	1.593	<0.2	0.66	2780	20	<0.5	<2	2.18	1	6	44	17
RUG 141	497	533	Bx3; ref w/ clasts of dol, tuffisite, & rare Bx2	0.838	<0.2	0.52	1390	30	<0.5	<2	5.57	1.5	5	56	14
RUG 141	533	552	Bx3; ox w/ ls +/- tuffisite	0.199	<0.2	0.2	1135	700	<0.5	2	>15.00	0.5	1	31	6
RUG 141	552	560	Ddg ls	0.012	<0.2	0.04	268	1940	<0.5	<2	>15.00	<0.5	<1	11	3
RUG 142	0	20	Mw	0.22	0.2	0.54	110	50	0.5	<2	0.28	<0.5	8	27	45
RUG 142	20	40	Mw	>10.00	0.2	0.55	504	10	<0.5	<2	0.21	<0.5	8	35	46
RUG 142	40	65	Mw	0.67	<0.2	0.62	508	30	0.5	<2	0.26	<0.5	8	34	47
RUG 142	65	80	Mw (high grade)	>10.00	0.2	0.65	1040	30	0.5	<2	0.24	0.5	9	39	49
RUG 142	80	100	Mw	7.99	<0.2	0.28	394	<10	<0.5	6	0.04	0.5	4	72	25
RUG 142	100	129	Mw (very high grade)	>10.00	<0.2	0.59	1075	<10	<0.5	2	0.07	0.5	11	55	45
RUG 142	129	140	tuffisite (w/ grade .365-.247)	>10.00	<0.2	0.13	564	160	<0.5	2	0.01	<0.5	<1	69	8
RUG 142	140	145	Bx2; ox	5.1	0.2	0.07	84	1510	<0.5	<2	0.01	<0.5	<1	138	3

Appendix 2-C

Hole No.	Start	End	Description	Au (ppm) FA+AA	Ag (ppm)	Al (%)	As (ppm)	Ba (ppm)	Be (ppm)	Bi (ppm)	Ca (%)	Cd (ppm)	Co (ppm)	Cr (ppm)	Cu (ppm)
RUG 142	145	165	Bx2; ref	7.77	<0.2	0.04	146	1030	<0.5	<2	0.04	<0.5	<1	219	7
RUG 142	165	189	Bx2; ref	>10.00	0.2	0.28	1050	140	<0.5	<2	0.72	1.5	5	154	14
RUG 142	189	226	Bx2; ref w/ local barite rich & silicification	>10.00	0.8	0.09	1490	50	<0.5	<2	0.04	0.5	18	171	18
RUG 142	226	245	Bx2; ox	>10.00	<0.2	0.07	278	1250	<0.5	<2	0.05	<0.5	1	184	15
RUG 142	245	263	Bx3; ox w/ clay matrix & clasts of Bx2 & bar	2.08	<0.2	0.72	115	730	<0.5	2	1.93	2.5	1	101	12
RUG 142	263	275	Bx2; ref	1.61	<0.2	0.31	400	130	<0.5	<2	0.33	1.5	5	83	17
RUG 142	275	290	Bx3; ox w/ Bx2 ox & ref clasts	5.5	<0.2	0.22	730	240	<0.5	<2	0.35	1	5	202	11
RUG 170	0	30	Mw	0.24	<0.2	0.6	160	50	0.5	<2	0.34	<0.5	9	32	48
RUG 170	30	54	Tectonic bx in Mw	0.225	<0.2	0.49	580	20	0.5	<2	0.22	0.5	11	39	53
RUG 170	54	57	Bx2	0.34	<0.2	0.45	2140	10	0.5	4	0.03	0.5	7	75	29
RUG 170	57	75	Bx1	4.17	<0.2	0.22	838	50	<0.5	<2	0.04	3	4	64	28
RUG 170	75	92	Bx1	5.31	0.2	0.21	386	140	<0.5	<2	0.04	9.5	4	120	22
RUG 170	92	97	Bx2; ox (tectonic)	>10.00	0.2	0.15	486	360	<0.5	<2	0.04	<0.5	<1	91	7
RUG 170	97	110	Bx2; ref	>10.00	<0.2	0.48	1315	140	<0.5	<2	0.06	<0.5	5	75	12
RUG 170	110	112	tuffisite	0.705	<0.2	0.91	>10000	10	<0.5	<2	0.08	1.5	43	36	33
RUG 170	112	123	Bx2; ref w/ tr FeOx on fracs	9.21	<0.2	0.39	2160	50	<0.5	<2	0.04	<0.5	13	76	14
RUG 170	123	136	Bx2; ref	8.15	0.2	0.43	3250	2590	<0.5	<2	0.04	0.5	<1	108	5
RUG 170	136	139	Bx2; ox	>10.00	0.8	0.4	2960	1810	<0.5	2	0.07	0.5	3	152	6
RUG 170	139	153	Bx2; ref	>10.00	0.6	0.18	1340	1010	<0.5	<2	0.03	<0.5	2	75	5
RUG 170	153	159	Rain fault zone	4.22	<0.2	0.47	2140	30	<0.5	<2	0.11	0.5	20	54	31
RUG 170	159	181	Dw; carbonaceous	0.72	0.6	0.23	678	1370	<0.5	<2	0.06	0.5	3	177	16
RUG 170	181	200	Dw; carbonaceous	0.655	1.4	0.38	362	200	0.5	2	0.48	2.5	5	145	41
RUG 170	200	225	Dw; carbonaceous	0.235	2.4	0.54	244	240	1	<2	2.7	2.5	4	148	79
RCR 21	820	840	Mc	0.001	0.2	0.82	270	80	<0.5	<2	0.06	0.5	9	171	39
RCR 21	840	860	Mc	0.001	<0.2	0.81	364	240	<0.5	2	0.07	1.5	6	275	41
RCR 21	860	880	Mc	0.001	0.2	0.56	258	260	<0.5	<2	0.03	0.5	8	266	42
RCR 21	880	900	Mc	0.001	<0.2	0.55	250	140	<0.5	<2	0.05	0.5	10	177	35
RCR 21	900	920	Mc	0.001	0.2	0.61	146	210	0.5	<2	0.05	0.5	12	144	41
RCR 21	920	940	Mc	0.001	0.2	0.51	156	150	<0.5	<2	0.04	0.5	11	175	38
RCR 21	940	960	Mc	0.001	0.2	0.56	186	100	<0.5	<2	0.05	<0.5	9	149	32
RCR 21	960	1000	Mw	0.001	0.2	0.87	246	100	0.5	<2	0.09	<0.5	12	140	42
RCR 21	1000	1040	Mw	0.001	<0.2	0.97	304	30	0.5	<2	0.25	0.5	11	89	45
RCR 21	1040	1080	Mw	0.001	0.2	0.93	126	50	0.5	<2	0.13	0.5	10	74	48
RCR 21	1080	1120	Mw	0.001	<0.2	0.97	242	30	0.5	<2	0.23	<0.5	11	73	45

Appendix 2-C

Hole No.	Start	End	Description	Au (ppm) FA+AA	Ag (ppm)	Al (%)	As (ppm)	Ba (ppm)	Be (ppm)	Bi (ppm)	Ca (%)	Cd (ppm)	Co (ppm)	Cr (ppm)	Cu (ppm)
RCR 21	1120	1160	Mw	0.001	0.2	0.95	100	50	0.5	<2	0.23	<0.5	10	63	44
RCR 21	1160	1200	Mw	0.001	<0.2	0.83	188	60	0.5	<2	0.25	<0.5	9	76	42
RCR 21	1200	1240	Mw	0.001	0.2	0.9	212	50	0.5	<2	0.26	<0.5	9	69	47
RCR 21	1240	1280	Mw	0.001	<0.2	0.81	172	50	0.5	<2	0.24	0.5	9	69	46
RCR 21	1280	1320	Mw	0.001	<0.2	0.86	222	50	0.5	<2	0.23	<0.5	9	82	41
RCR 21	1320	1360	Mw	0.001	<0.2	0.98	228	30	0.5	<2	0.26	<0.5	10	69	45
RCR 21	1360	1400	Mw	0.001	<0.2	0.76	184	50	0.5	<2	0.26	<0.5	8	25	46
RCR 21	1400	1428	Mw	0.001	<0.2	0.64	354	40	0.5	<2	0.11	<0.5	9	27	44
RCR 21	1428	1440	Bx2; ox	0.209	<0.2	0.39	382	1430	<0.5	<2	0.01	<0.5	<1	53	14
RCR 21	1440	1460	Bx2; ox	0.096	<0.2	0.07	116	1880	<0.5	<2	0.02	<0.5	<1	142	7
RCR 21	1460	1487	Bx2; ox	0.379	0.2	0.18	478	1510	<0.5	<2	0.03	<0.5	2	153	12
RCR 21	1487	1494	tuffisite w/ high bar; ref	0.02	<0.2	1.37	5890	20	<0.5	<2	0.21	<0.5	22	84	154
RCR 21	1494	1511	Ddg dol	0.027	0.2	0.23	626	240	0.5	<2	9.64	0.5	16	48	6
RCR 21	1510	1520	Ddg dol	0.025	<0.2	0.11	436	660	<0.5	<2	3.24	0.5	3	50	6

Appendix 2-C

Hole No.	Start	End	Description	Fe (%)	Ga (ppm)	Hg (ppm)	K (%)	La (ppm)	Mg (%)	Mn (ppm)	Mo (ppm)	Na (%)	Ni (ppm)	P (ppm)	Pb (ppm)
RUG 139	0	22	Mw	2.79	<10	6	0.42	<10	0.08	30	1	<0.01	41	1310	12
RUG 139	22	28	Bx1	3.73	<10	8	0.26	<10	0.06	830	<1	<0.01	36	450	12
RUG 139	28	42	Bx2; ox w/ red clay on fracs	2.56	<10	16	0.1	<10	0.01	40	32	<0.01	14	580	14
RUG 139	42	68.5	Bx2; ox w/ abun.bar & lim on fracs	0.6	<10	67	0.01	<10	<0.01	15	4	<0.01	7	190	22
RUG 139	68.5	69	tuffisite	3.19	<10	33	<0.01	<10	<0.01	35	10	<0.01	39	600	78
RUG 139	69	95	Bx2; ox	2.5	<10	20	0.02	<10	0.01	20	4	<0.01	41	400	44
RUG 139	95	119	Bx2; ox; vuggy silica	2.32	<10	13	0.01	<10	<0.01	35	6	<0.01	45	320	13
RUG 139	119	130	Bx2; ox	1.99	<10	18	0.01	<10	0.07	40	5	<0.01	32	300	198
RUG 139	130	150	Bx2; ox	5.67	<10	13	0.05	<10	0.05	250	9	<0.01	97	2540	78
RUG 139	150	155	Spring fault w/ sheared Dw & PO4 nodules	2.67	<10	11	0.03	<10	0.06	1095	1	<0.01	125	5310	102
RUG 139	155	180	Dw; ox w/ shears & PO4 nodules	1.94	<10	7	0.15	20	0.03	635	11	<0.01	81	>10000	8
RUG 139	130	195	Dw; partially ox w/ PO4 nodules	1.27	<10	5	0.12	10	0.04	45	4	0.01	72	>10000	4
RUG 139	195	220	Dw; carbonaceous	0.89	<10	84	0.19	<10	0.05	35	15	0.01	95	>10000	4
RUG 140	0	20	Mw	2.65	<10	5	0.48	<10	0.11	30	<1	<0.01	42	930	14
RUG 140	20	60	Tectonic bx in Mw	2.65	<10	18	0.26	<10	0.13	30	<1	<0.01	33	670	6
RUG 140	60	66	Mw	3.08	<10	33	0.22	<10	0.05	20	2	<0.01	30	230	10
RUG 140	66	72	Mw (Bx1?); ox	4.78	<10	24	0.23	<10	0.24	35	3	<0.01	54	360	14
RUG 140	72	87	Mw	10.9	<10	54	0.2	<10	0.11	25	<1	<0.01	44	380	12
RUG 140	87	94	Bx2; ox	11.2	<10	24	0.03	<10	0.01	55	9	<0.01	12	780	26
RUG 140	94	98	Bx2; ref	2.51	<10	21	0.01	<10	0.01	30	1	<0.01	7	290	4
RUG 140	98	104	Bx2; ox	4.87	<10	12	0.03	<10	0.03	45	3	<0.01	14	820	16
RUG 140	104	107	tuffisite in Flower fault	8.86	<10	469	0.09	<10	0.26	70	4	<0.01	97	3950	22
RUG 140	107	119	Bx2; mixed ox & ref	5.44	<10	16	0.03	<10	0.04	60	5	<0.01	12	970	16
RUG 140	119	130	Bx2; ox	3.15	<10	12	0.02	<10	0.1	45	2	<0.01	15	1250	20
RUG 140	130	134	Bx2; mixed ox & ref w/ carbon on fracs	2.45	<10	30	0.02	<10	0.23	45	3	<0.01	20	670	8
RUG 140	134	162	Bx2; ox	10.6	<10	10	0.01	<10	0.03	70	12	<0.01	31	1050	48
RUG 140	162	185	Bx3 w/ Bx2 clasts	>15.00	10	11	0.15	10	0.1	165	12	<0.01	198	6850	42
RUG 140	135	205	Bx3 w/ Bx2 clasts	5.65	<10	5	0.03	<10	0.08	85	4	<0.01	101	1000	40
RUG 140	205	240	Ddg dol	1.48	<10	5	0.12	<10	8.21	600	<1	<0.01	31	530	10
RUG 140	240	250	Ddg dol w/ abundant bar	0.53	<10	2	0.03	<10	9.45	565	<1	0.01	13	100	<2
RUG 141	0	20	Mw	3.47	<10	4	0.45	<10	0.07	30	1	<0.01	40	1110	16
RUG 141	20	40	Mw	2.66	<10	3	0.34	<10	0.05	25	1	<0.01	36	980	14
RUG 141	40	60	Mw w/ abun py veins	1.99	<10	3	0.34	<10	0.05	30	<1	<0.01	38	870	10
RUG 141	60	80	Mw	2.6	<10	6	0.36	<10	0.06	25	<1	<0.01	40	980	14

Appendix 2-C

Hole No.	Start	End	Description	Fe (%)	Ga (ppm)	Hg (ppm)	K (%)	La (ppm)	Mg (%)	Mn (ppm)	Mo (ppm)	Na (%)	Ni (ppm)	P (ppm)	Pb (ppm)
RUG 141	80	100	Mw	2.16	<10	8	0.36	<10	0.06	60	1	<0.01	38	850	12
RUG 141	100	120	Mw	2.39	<10	8	0.42	<10	0.07	35	1	<0.01	41	960	14
RUG 141	120	140	Mw	2.02	<10	10	0.34	<10	0.05	25	1	<0.01	37	720	12
RUG 141	140	146	Mw	1.85	<10	5	0.36	<10	0.06	25	<1	<0.01	33	740	14
RUG 141	146	180	Mw ss w/ py replacing grains	1.75	<10	3	0.25	<10	0.04	25	1	<0.01	30	790	12
RUG 141	180	195	Mw	3.4	<10	4	0.35	<10	0.05	25	<1	<0.01	31	600	12
RUG 141	195	215	Bx w/ clay matrix	2.19	<10	4	0.27	<10	0.04	25	<1	<0.01	31	400	10
RUG 141	215	240	Mw	1.97	<10	6	0.32	<10	0.05	25	1	<0.01	36	750	14
RUG 141	240	260	Mw	2.14	<10	9	0.32	<10	0.04	20	1	<0.01	38	730	14
RUG 141	260	276	Mw	2.74	<10	11	0.24	<10	0.03	20	<1	<0.01	33	360	14
RUG 141	276	209	Bx1	1.96	<10	3	0.2	<10	0.03	20	<1	<0.01	3	310	8
RUG 141	290	305	Bx1	1.67	<10	<1	0.18	<10	0.03	20	1	<0.01	3	180	10
RUG 141	305	315	Bx2; ref	3.6	<10	7	0.26	<10	0.04	40	2	<0.01	19	660	4
RUG 141	315	325	Flt bx	12	<10	13	0.13	<10	0.01	95	6	<0.01	15	1200	28
RUG 141	325	343	Bx2; ox	6.58	<10	8	0.02	<10	<0.01	55	6	<0.01	7	1460	52
RUG 141	343	360	Flt bx	2.52	<10	6	0.21	10	0.01	25	<1	<0.01	5	4600	12
RUG 141	360	374	Bx2; ox	3.61	<10	3	0.44	10	0.01	20	1	<0.01	4	4880	10
RUG 141	374	389	Flt bx	10	<10	19	0.19	20	0.04	140	2	<0.01	23	4340	18
RUG 141	389	421	Flt bx	4.6	<10	5	0.08	<10	4.52	1660	<1	<0.01	18	430	20
RUG 141	421	428	Flt bx	2.49	<10	6	0.18	<10	0.11	530	2	<0.01	12	4830	10
RUG 141	429	473	Bx3; ref	2.59	<10	36	0.25	<10	0.05	45	2	<0.01	43	4200	14
RUG 141	473	484	Bx3; ox w/ dol clasts	8.37	<10	3	0.06	<10	4.93	1855	<1	<0.01	24	1900	16
RUG 141	484	497	Bx3; ref w/ clasts of dol, Bx2, & bar	3.67	<10	42	0.21	<10	0.45	620	1	0.01	30	5640	24
RUG 141	497	533	Bx3; ref w/ clasts of dol, tuffisite, & rare Bx2	2.17	<10	21	0.19	<10	2.64	205	<1	0.01	25	3780	42
RUG 141	533	552	Bx3; ox w/ ls +/- tuffisite	2.61	<10	16	0.08	<10	0.2	690	<1	<0.01	12	1100	6
RUG 141	552	560	Ddg ls	0.64	<10	8	<.0.01	<10	0.94	980	<1	<0.01	2	50	<2
RUG 142	0	20	Mw	1.85	<10	3	0.27	<10	0.04	30	1	<0.01	40	920	12
RUG 142	20	40	Mw	3.56	<10	13	0.26	<10	0.04	25	1	<0.01	37	710	16
RUG 142	40	65	Mw	2.4	<10	6	0.29	<10	0.04	45	<1	<0.01	39	880	10
RUG 142	65	80	Mw (high grade)	3.51	<10	28	0.3	<10	0.04	25	<1	<0.01	39	860	16
RUG 142	80	100	Mw	14.5	<10	25	0.13	<10	0.01	20	3	<0.01	16	150	20
RUG 142	100	129	Mw (very high grade)	11.35	<10	40	0.19	<10	0.03	35	1	<0.01	45	440	34
RUG 142	129	140	tuffisite (w/ grade .365-.247)	14.4	<10	20	0.03	<10	<0.01	80	5	<0.01	8	980	16
RUG 142	140	145	Bx2; ox	0.5	<10	6	0.01	<10	<0.01	15	7	<0.01	5	60	14

Appendix 2-C

Hole No.	Start	End	Description	Fe (%)	Ga (ppm)	Hg (ppm)	K (%)	La (ppm)	Mg (%)	Mn (ppm)	Mo (ppm)	Na (%)	Ni (ppm)	P (ppm)	Pb (ppm)
RUG 142	145	165	Bx2; ref	0.67	<10	15	0.03	<10	<0.01	20	12	<0.01	12	100	4
RUG 142	165	189	Bx2; ref	2.18	<10	25	0.05	<10	0.01	50	18	<0.01	37	3220	16
RUG 142	189	226	Bx2; ref w/ local barite rich & silicification	1.98	<10	53	0.02	<10	<0.01	15	20	<0.01	52	290	14
RUG 142	226	245	Bx2; ox	0.78	<10	54	0.01	<10	0.01	20	6	<0.01	13	170	70
RUG 142	245	263	Bx3; ox w/ clay matrix & clasts of Bx2 & bar	5.22	<10	9	0.12	<10	0.05	125	3	<0.01	31	7480	8
RUG 142	263	275	Bx2; ref	1.96	<10	16	0.12	<10	0.02	30	2	<0.01	25	1270	8
RUG 142	275	290	Bx3; ox w/ Bx2 ox & ref clasts	1.89	<10	13	0.04	<10	0.03	40	14	<0.01	33	1280	8
RUG 170	0	30	Mw	2.11	<10	5	0.29	<10	0.05	70	<1	<0.01	42	930	14
RUG 170	30	54	Tectonic bx in Mw	3.13	<10	11	0.24	<10	0.03	40	<1	<0.01	51	820	18
RUG 170	54	57	Bx2	>15.00	<10	28	0.13	<10	0.01	65	12	<0.01	67	1590	18
RUG 170	57	75	Bx1	2.98	<10	42	0.1	<10	0.01	25	4	<0.01	22	330	118
RUG 170	75	92	Bx1	1.94	<10	50	0.09	<10	<0.01	25	3	<0.01	16	530	70
RUG 170	92	97	Bx2; ox (tectonic)	2.33	<10	22	0.02	<10	<0.01	20	3	<0.01	10	350	24
RUG 170	97	110	Bx2; ref	2.95	<10	54	0.07	<10	0.01	30	3	<0.01	34	1210	28
RUG 170	110	112	tuffisite	5.39	<10	60	0.1	<10	0.03	25	1	<0.01	125	760	10
RUG 170	112	123	Bx2; ref w/ tr FeOx on fracs	2.22	<10	40	0.02	<10	<0.01	10	3	<0.01	28	680	14
RUG 170	123	136	Bx2; ref	2.81	<10	31	0.06	<10	0.01	25	5	<0.01	22	1160	16
RUG 170	136	139	Bx2; ox	7.55	<10	64	0.03	<10	<0.01	65	12	<0.01	109	1330	28
RUG 170	139	153	Bx2; ref	1.26	<10	20	0.03	<10	<0.01	15	2	<0.01	21	550	12
RUG 170	153	159	Rain fault zone	3.48	<10	31	0.14	<10	0.02	50	6	<0.01	89	1190	16
RUG 170	159	181	Dw; carbonaceous	2.55	<10	23	0.07	<10	<0.01	35	15	<0.01	54	990	10
RUG 170	181	200	Dw; carbonaceous	1.45	<10	7	0.06	<10	<0.01	20	20	<0.01	81	2860	4
RUG 170	200	225	Dw; carbonaceous	0.82	<10	4	0.08	<10	0.01	25	24	<0.01	85	>10000	6
RCR 21	820	840	Mc	2.54	<10	16	0.24	<10	0.05	65	1	<0.01	30	620	20
RCR 21	840	860	Mc	2.25	<10	13	0.2	<10	0.03	40	4	<0.01	21	920	18
RCR 21	860	880	Mc	1.66	<10	10	0.16	<10	0.02	30	3	<0.01	25	370	16
RCR 21	880	900	Mc	2.01	<10	10	0.2	<10	0.04	35	1	<0.01	31	280	8
RCR 21	900	920	Mc	1.5	<10	5	0.25	<10	0.05	35	1	<0.01	37	310	14
RCR 21	920	940	Mc	1.76	<10	4	0.19	<10	0.03	60	3	<0.01	32	350	12
RCR 21	940	960	Mc	1.49	<10	1	0.2	<10	0.04	30	1	<0.01	35	230	10
RCR 21	960	1000	Mw	1.89	<10	3	0.33	<10	0.06	50	2	<0.01	48	530	22
RCR 21	1000	1040	Mw	2.8	<10	2	0.4	<10	0.07	40	<1	<0.01	49	880	34
RCR 21	1040	1080	Mw	2.27	<10	1	0.37	<10	0.07	85	3	<0.01	53	550	26
RCR 21	1080	1120	Mw	2.8	<10	<1	0.4	<10	0.07	105	3	<0.01	48	870	12

Appendix 2-C

Hole No.	Start	End	Description	Fe (%)	Ga (ppm)	Hg (ppm)	K (%)	La (ppm)	Mg (%)	Mn (ppm)	Mo (ppm)	Na (%)	Ni (ppm)	P (ppm)	Pb (ppm)
RCR 21	1120	1160	Mw	2.37	<10	1	0.4	<10	0.07	135	2	<0.01	44	820	22
RCR 21	1160	1200	Mw	2.87	<10	1	0.36	<10	0.09	350	1	<0.01	47	880	14
RCR 21	1200	1240	Mw	2.48	<10	<1	0.4	<10	0.07	60	2	<0.01	44	840	14
RCR 21	1240	1280	Mw	2.53	<10	2	0.36	<10	0.06	160	1	<0.01	42	790	20
RCR 21	1280	1320	Mw	2.35	<10	1	0.38	<10	0.06	80	3	<0.01	37	810	12
RCR 21	1320	1360	Mw	2.92	<10	2	0.42	<10	0.07	90	2	<0.01	42	890	28
RCR 21	1360	1400	Mw	2.39	<10	1	0.37	<10	0.07	300	1	<0.01	34	850	12
RCR 21	1400	1428	Mw	3.72	<10	7	0.31	<10	0.04	60	<1	<0.01	30	440	10
RCR 21	1428	1440	Bx2; ox	1.95	<10	10	0.18	<10	0.02	30	<1	<0.01	3	250	16
RCR 21	1440	1460	Bx2; ox	0.36	<10	4	0.02	<10	<0.01	10	6	<0.01	5	50	4
RCR 21	1460	1487	Bx2; ox	2.22	<10	13	0.03	<10	<0.01	25	8	<0.01	44	480	20
RCR 21	1487	1494	tuffisite w/ high bar; ref	4.63	<10	34	0.17	10	0.05	35	3	<0.01	70	3270	44
RCR 21	1494	1511	Ddg dol	2.22	<10	3	0.06	<10	5.6	1105	<1	<0.01	85	1460	20
RCR 21	1510	1520	Ddg dol	1.97	<10	4	0.03	<10	2.01	140	<1	<0.01	24	340	52

Appendix 2-C

Hole No.	Start	End	Description	Sb (ppm)	Sc (ppm)	Sr (ppm)	Ti (%)	Tl (ppm)	U (ppm)	V (ppm)	W (ppm)	Zn (ppm)
RUG 139	0	22	Mw	6	3	20	<0.01	<10	<10	59	<10	108
RUG 139	22	28	Bx1	4	3	21	<0.01	<10	<10	34	<10	178
RUG 139	28	42	Bx2; ox w/ red clay on fracs	42	<1	46	<0.01	<10	<10	38	<10	28
RUG 139	42	68.5	Bx2; ox w/ abun.bar & lim on fracs	18	<1	62	<0.01	<10	<10	14	<10	248
RUG 139	68.5	69	tuffisite	170	3	43	0.02	<10	<10	24	<10	88
RUG 139	69	95	Bx2; ox	134	<1	37	<0.01	<10	<10	24	10	90
RUG 139	95	119	Bx2; ox; vuggy silica	170	<1	43	<0.01	<10	<10	15	<10	88
RUG 139	119	130	Bx2; ox	80	<1	26	<0.01	<10	<10	16	<10	90
RUG 139	130	150	Bx2; ox	136	1	168	<0.01	<10	<10	82	<10	790
RUG 139	150	155	Spring fault w/ sheared Dw & PO4 nodules	64	2	189	<0.01	<10	10	40	<10	1290
RUG 139	155	180	Dw; ox w/ shears & PO4 nodules	26	2	1320	<0.01	<10	30	357	<10	1900
RUG 139	130	195	Dw; partially ox w/ PO4 nodules	12	1	661	<0.01	<10	<10	334	<10	546
RUG 139	195	220	Dw; carbonaceous	6	1	437	<0.01	<10	<10	358	<10	632
RUG 140	0	20	Mw	2	4	16	<0.01	<10	<10	57	<10	74
RUG 140	20	60	Tectonic bx in Mw	8	2	11	<0.01	10	<10	31	<10	72
RUG 140	60	66	Mw	10	<1	15	<0.01	30	<10	25	<10	100
RUG 140	66	72	Mw (Bx1?); ox	12	<1	19	<0.01	30	<10	24	<10	40
RUG 140	72	87	Mw	14	<1	9	<0.01	30	<10	25	<10	50
RUG 140	87	94	Bx2; ox	118	<1	36	<0.01	<10	<10	68	<10	62
RUG 140	94	98	Bx2; ref	50	<1	41	<0.01	<10	<10	22	<10	252
RUG 140	98	104	Bx2; ox	92	<1	47	<0.01	10	<10	38	10	110
RUG 140	104	107	tuffisite in Flower fault	142	3	149	<0.01	40	<10	53	<10	138
RUG 140	107	119	Bx2; mixed ox & ref	102	<1	70	<0.01	10	<10	26	<10	166
RUG 140	119	130	Bx2; ox	80	<1	119	<0.01	10	<10	39	<10	88
RUG 140	130	134	Bx2; mixed ox & ref w/ carbon on fracs	48	<1	86	<0.01	10	<10	33	<10	72
RUG 140	134	162	Bx2; ox	526	<1	41	<0.01	<10	<10	34	30	250
RUG 140	162	185	Bx3 w/ Bx2 clasts	498	6	154	<0.01	10	<10	185	10	1095
RUG 140	135	205	Bx3 w/ Bx2 clasts	190	<1	86	<0.01	<10	<10	55	30	404
RUG 140	205	240	Ddg dol	54	1	98	<0.01	10	<10	13	<10	230
RUG 140	240	250	Ddg dol w/ abundant bar	14	<1	102	<0.01	10	<10	9	<10	150
RUG 141	0	20	Mw	6	3	19	<0.01	<10	<10	56	<10	78
RUG 141	20	40	Mw	2	3	27	<0.01	<10	<10	49	<10	84
RUG 141	40	60	Mw w/ abun py veins	<2	3	30	<0.01	<10	<10	44	<10	132
RUG 141	60	80	Mw	2	3	24	<0.01	<10	<10	49	<10	76

Appendix 2-C

Hole No.	Start	End	Description	Sb (ppm)	Sc (ppm)	Sr (ppm)	Ti (%)	Tl (ppm)	U (ppm)	V (ppm)	W (ppm)	Zn (ppm)
RUG 141	80	100	Mw	2	3	22	<0.01	<10	<10	51	<10	132
RUG 141	100	120	Mw	<2	3	23	<0.01	<10	<10	57	<10	108
RUG 141	120	140	Mw	<2	2	18	<0.01	<10	<10	47	<10	108
RUG 141	140	146	Mw	<2	2	18	<0.01	<10	<10	49	<10	74
RUG 141	146	180	Mw ss w/ py replacing grains	<2	1	13	<0.01	<10	<10	37	<10	58
RUG 141	180	195	Mw	2	1	23	<0.01	<10	<10	39	<10	94
RUG 141	195	215	Bx w/ clay matrix	2	1	10	<0.01	<10	<10	29	<10	78
RUG 141	215	240	Mw	<2	1	20	<0.01	<10	<10	40	<10	96
RUG 141	240	260	Mw	<2	1	32	<0.01	10	<10	35	<10	98
RUG 141	260	276	Mw	<2	1	38	<0.01	10	<10	18	<10	66
RUG 141	276	209	Bx1	40	<1	55	<0.01	<10	<10	27	<10	8
RUG 141	290	305	Bx1	30	<1	33	<0.01	<10	<10	27	<10	6
RUG 141	305	315	Bx2; ref	14	<1	56	<0.01	<10	<10	37	<10	30
RUG 141	315	325	Flt bx	80	<1	34	<0.01	<10	<10	36	10	40
RUG 141	325	343	Bx2; ox	170	<1	30	<0.01	<10	<10	56	<10	94
RUG 141	343	360	Flt bx	80	<1	149	<0.01	<10	<10	48	<10	20
RUG 141	360	374	Bx2; ox	118	1	105	<0.01	10	<10	55	<10	26
RUG 141	374	389	Flt bx	486	1	272	<0.01	<10	<10	126	<10	368
RUG 141	389	421	Flt bx	156	3	54	<0.01	10	<10	15	<10	118
RUG 141	421	428	Flt bx	72	2	91	<0.01	<10	<10	40	<10	192
RUG 141	429	473	Bx3; ref	118	1	33	<0.01	70	<10	38	<10	238
RUG 141	473	484	Bx3; ox w/ dol clasts	378	1	54	<0.01	10	<10	14	<10	426
RUG 141	484	497	Bx3; ref w/ clasts of dol, Bx2, & bar	254	1	29	<0.01	160	<10	26	<10	302
RUG 141	497	533	Bx3; ref w/ clasts of dol, tuffisite, & rare Bx2	166	1	63	<0.01	70	<10	25	<10	424
RUG 141	533	552	Bx3; ox w/ ls +/- tuffisite	130	1	93	<0.01	30	<10	12	10	110
RUG 141	552	560	Ddg ls	78	1	140	<0.01	20	<10	8	<10	44
RUG 142	0	20	Mw	2	3	12	<0.01	<10	<10	30	<10	96
RUG 142	20	40	Mw	2	2	9	<0.01	<10	<10	28	<10	124
RUG 142	40	65	Mw	2	3	9	<0.01	<10	<10	38	<10	74
RUG 142	65	80	Mw (high grade)	6	1	14	<0.01	20	<10	37	<10	100
RUG 142	80	100	Mw	<2	<1	1	<0.01	<10	<10	14	<10	88
RUG 142	100	129	Mw (very high grade)	20	1	9	<0.01	30	<10	21	<10	204
RUG 142	129	140	tuffisite (w/ grade .365-.247)	22	<1	11	<0.01	<10	<10	70	<10	32
RUG 142	140	145	Bx2; ox	8	<1	16	<0.01	<10	<10	4	<10	2

Appendix 2-C

Hole No.	Start	End	Description	Sb (ppm)	Sc (ppm)	Sr (ppm)	Ti (%)	Tl (ppm)	U (ppm)	V (ppm)	W (ppm)	Zn (ppm)
RUG 142	145	165	Bx2; ref	8	<1	14	<0.01	<10	<10	14	<10	20
RUG 142	165	189	Bx2; ref	64	<1	45	<0.01	40	<10	40	<10	118
RUG 142	189	226	Bx2; ref w/ local barite rich & silicification	24	<1	17	<0.01	30	<10	28	<10	38
RUG 142	226	245	Bx2; ox	44	<1	15	<0.01	<10	<10	9	<10	44
RUG 142	245	263	Bx3; ox w/ clay matrix & clasts of Bx2 & bar	190	1	64	<0.01	<10	<10	44	<10	350
RUG 142	263	275	Bx2; ref	98	<1	44	<0.01	<10	<10	20	<10	160
RUG 142	275	290	Bx3; ox w/ Bx2 ox & ref clasts	48	<1	36	<0.01	10	<10	34	<10	136
RUG 170	0	30	Mw	<2	3	10	<0.01	<10	<10	32	<10	62
RUG 170	30	54	Tectonic bx in Mw	2	3	12	<0.01	<10	<10	34	<10	230
RUG 170	54	57	Bx2	40	2	9	<0.01	<10	<10	51	10	218
RUG 170	57	75	Bx1	20	<1	23	<0.01	<10	<10	30	<10	274
RUG 170	75	92	Bx1	18	<1	70	<0.01	<10	<10	36	<10	442
RUG 170	92	97	Bx2; ox (tectonic)	30	<1	34	<0.01	<10	<10	27	<10	40
RUG 170	97	110	Bx2; ref	80	<1	71	<0.01	<10	<10	60	<10	114
RUG 170	110	112	tuffisite	26	2	42	<0.01	20	<10	28	<10	156
RUG 170	112	123	Bx2; ref w/ tr FeOx on fracs	44	<1	21	<0.01	10	<10	37	<10	42
RUG 170	123	136	Bx2; ref	120	<1	100	<0.01	<10	<10	74	<10	124
RUG 170	136	139	Bx2; ox	318	<1	87	<0.01	<10	<10	77	<10	368
RUG 170	139	153	Bx2; ref	36	<1	31	<0.01	<10	<10	34	<10	58
RUG 170	153	159	Rain fault zone	48	1	34	<0.01	30	<10	26	<10	92
RUG 170	159	181	Dw; carbonaceous	56	1	53	<0.01	<10	<10	302	<10	118
RUG 170	181	200	Dw; carbonaceous	18	2	98	<0.01	<10	<10	415	<10	114
RUG 170	200	225	Dw; carbonaceous	8	1	227	<0.01	<10	<10	288	<10	202
RCR 21	820	840	Mc	<2	2	71	<0.01	<10	<10	71	<10	58
RCR 21	840	860	Mc	2	1	124	<0.01	<10	<10	82	<10	52
RCR 21	860	880	Mc	<2	1	60	<0.01	<10	<10	53	<10	74
RCR 21	880	900	Mc	<2	1	38	<0.01	<10	<10	56	<10	90
RCR 21	900	920	Mc	<2	2	47	<0.01	<10	<10	52	<10	166
RCR 21	920	940	Mc	<2	1	40	<0.01	<10	<10	48	<10	78
RCR 21	940	960	Mc	<2	1	31	<0.01	<10	<10	41	<10	138
RCR 21	960	1000	Mw	2	3	55	<0.01	<10	<10	59	<10	280
RCR 21	1000	1040	Mw	2	3	30	<0.01	<10	<10	56	<10	156
RCR 21	1040	1080	Mw	<2	3	61	<0.01	<10	<10	57	<10	208
RCR 21	1080	1120	Mw	2	3	30	<0.01	<10	<10	64	<10	162

Appendix 2-C

Hole No.	Start	End	Description	Sb (ppm)	Sc (ppm)	Sr (ppm)	Ti (%)	Tl (ppm)	U (ppm)	V (ppm)	W (ppm)	Zn (ppm)
RCR 21	1120	1160	Mw	<2	3	28	<0.01	<10	<10	56	<10	152
RCR 21	1160	1200	Mw	<2	3	21	<0.01	<10	<10	50	<10	146
RCR 21	1200	1240	Mw	<2	3	22	<0.01	<10	<10	52	<10	166
RCR 21	1240	1280	Mw	<2	3	22	<0.01	<10	<10	48	<10	156
RCR 21	1280	1320	Mw	2	3	23	<0.01	<10	<10	53	<10	114
RCR 21	1320	1360	Mw	<2	3	22	<0.01	<10	<10	60	<10	128
RCR 21	1360	1400	Mw	2	3	19	<0.01	<10	<10	41	<10	78
RCR 21	1400	1428	Mw	2	2	14	<0.01	<10	<10	28	<10	58
RCR 21	1428	1440	Bx2; ox	18	<1	24	<0.01	<10	<10	38	<10	22
RCR 21	1440	1460	Bx2; ox	8	<1	19	<0.01	<10	<10	27	<10	10
RCR 21	1460	1487	Bx2; ox	100	<1	60	<0.01	30	<10	44	<10	84
RCR 21	1487	1494	tuffisite w/ high bar; ref	76	16	83	<0.01	20	<10	67	<10	240
RCR 21	1494	1511	Ddg dol	68	1	79	<0.01	10	<10	14	<10	796
RCR 21	1510	1520	Ddg dol	158	<1	128	<0.01	<10	<10	12	<10	244